UNIVERSITY OF CALIFORNIA

Los Angeles

Emerging Techniques in Coastal Water Quality in the US and Belize:

Remote Sensing and Metagenomics

A dissertation submitted in partial satisfaction of the

requirements for the degree Doctor of Philosophy

in Civil Engineering

by

Ileana Callejas

2023

ABSTRACT OF THE DISSERTATION

Emerging Techniques in Coastal Water Quality in the US and Belize:

Remote Sensing and Metagenomics

by

Ileana Callejas

Doctor of Philosophy in Civil Engineering

University of California, Los Angeles, 2023

Professor Jennifer Ayla Jay, Chair

Water quality monitoring is essential for the wellbeing of humans, animals, and the environment. Monitoring coastal water quality is critical for the sustainable management and development of coastal resources as over one-third of the human population live in coastal areas. The health of our coasts, oceans, and cities highly depends on our changing climate and anthropogenic activities. Creating robust solutions to climate change and achieving coastal resilience requires interdisciplinary research by leveraging various datasets and techniques. The water quality monitoring techniques encompassed by this body of work aim to leverage satellite remote sensing to monitor water clarity and sea surface temperature for coral health and the second are a suite of microbiological techniques to monitor antibiotic resistance. The first two studies utilize remote sensing imagery to monitor water clarity and sea surface temperature (SST) in

coastal Belize. The third and fourth studies use culture, amplification, and sequencing techniques to elucidate levels of antibiotic resistance genes (ARGs) and antibiotic resistant bacteria (ARB) in two major cities—Los Angeles, CA, USA and Belize City, Belize. The final chapter captures the impact remote sensing modules and a course-based undergraduate research experience (CURE) can have on the confidence and self-efficacy of STEM and non-STEM students.

The first chapter investigates water clarity changes using Aqua MODIS imagery during the COVID-19 anthropause. Here satellite derived Kd(490) (proxy for water clarity), marine traffic data, and climate model data were used to uncover significant improvements in water clarity during 2020 compared to the baseline period from 2002-2019 in areas with typically heavy marine traffic.

In the second chapter, a Google Earth Engine and RStudio based toolkit is devised to combine Aqua MODIS-derived Kd(490) and SST into a coral vulnerability index for marine protected areas (MPAs) in Belize. Using the coral vulnerability index, Belizean MPAs were ranked based on the number of heat stress days and index scores to draw attention to MPAs that may need more intervention.

Chapter three elucidates the impacts of land use and water reclamation plants on ARGs and ARB in the Los Angeles River watershed. The developed sampling sites were 2-3 orders of magnitude higher ARG concentrations compared to beaches and undeveloped areas.

The fourth chapter uses multiple microbiology techniques to measure ARG and ARB levels in the Belize River, coastal lagoon, and Belize Barrier Reef. Belize City, in particular the sewage treatment lagoons and fish market, were found to contribute most to the resitome.

The final chapter allowed students the opportunity to learn remote sensing to investigate environmental change and was found to increase their understanding of remote sensing and coding.

The dissertation of Ileana Callejas is approved.

Shaily Mahendra

Sanjay K. Mohanty

Adriane C. Jones

Christine M. Lee

Jennifer Ayla Jay, Committee Chair

University of California, Los Angeles

2023

Table of Contents

List of Acronyms

Antibiotic resistant bacteria	ARB
Antimicrobial resistance	AMR
Antibiotic resistance genes	ARGs
Belize Barrier Reef Reserve System	BBRRS
The Coronavirus disease 2019	COVID-19
Course-based undergraduate research experiences	CUREs
Coastal Zone Management Authority and Institute	CZMAI
Digital droplet polymerase chain reaction	ddPCR
Degree heating weeks	DHW
Dissolved oxygen	DO
Extended-spectrum beta-lactamase	ESBL
Fecal indicator bacteria	FIB
Gross domestic product	GDP
Google Earth Engine	GEE
Horizontal gene transfer	HGT
High traffic areas	HTAs
Integrated Coastal Zone Management Plan	ICZMP
Diffuse attenuation coefficient of downwelling irradiance at 490 nm	Kd(490)
Los Angeles River	LAR
Low traffic areas	LTAs
Million gallons per day	MGD
Mobile genetic elements	MGEs
Moderate resolution imaging spectroradiometer	MODIS
Marine protected areas	MPA
Optical Reef and Coastal Area Assessment	ORCAA
Quantitative polymerase chain reaction	qPCR
Resistome risk	RR
Sustainable Development Goal	SDG
State of emergency	SoE
Sea surface temperature	SST
Science, technology, engineering, and math	STEM
United Nations	UN
The United Nations Educational, Scientific and Cultural Organization	UNESCO
Underrepresented minorities	URM
Vertical gene transfer	VGT
Water reclamation plants	WRPs
Wastewater treatment plants	WWTPs

List of Figures

List of Tables

Acknowledgements

I'd like to thank my amazing advisor Dr. Jennifer Jay for her support throughout most of my time at UCLA. Without her guidance and care, this work would not have been possible. I would like to thank my committee members, Dr. Shaily Mahendra and Dr. Sanjay Mohanty, for peaking and shaping my interests within environmental microbiology and environmental engineering. I thank Dr. Christine Lee for being a great mentor and enabling so much of this work. I thank Dr. Adriane Jones for all of her guidance in research and teaching.

I would like to thank all current and previous Jay lab members during my time at UCLA: Dr. Marisol Cira, Karina Jimenez, Yuwei Kong, Renate Boronowsky, Katie Osborn, Zanobia Ibrahim-Watkins, Dr. Wayne Hung, Dr. Megyn Rugh, Dr. Victoria Whitener, and Dr. Cristina Echeverria. I've had a great experience working alongside them and have learned from each of them. I also want to thank the undergraduate students that assisted in this work with special thanks to Taylor Cason.

Lastly, I want to thank my God, my family, my fiancé, friends, and His Church. I thank God for being my one constant in this tumultuous time and always being faithful, even when I wasn't and during the uncertainty that came with the COVID-19 pandemic. I want to thank my parents Miguel De Dios and Irma Ortega for supporting me and my siblings Emely and Kevin Callejas. I want to thank Bryan Galdamez for supporting me throughout my academic journey. I thank my friend Onja Davidson Raoelison for being an inspiration and always being a light. I am grateful for all of my brothers and sisters in Christ at the UCLA 4Corners Fellowship and Shepherd Church in Porter Ranch, Ca.

Chapter one is a modified version of a published study "Effect of COVID-19 Anthropause on Water Clarity in the Belize Coastal Lagoon" (doi:10.3389/FMARS.2021.648522) currently in

Frontiers in Marine Science. This study was co-authored by Christine Lee, Deepak Mishra, Stacey Felgate, Claire Evans, Abel Carrias, Andria Rosado, Robert Griffin, Emil Cherrington, Mariam Ayad, Megha Rudresh, Benjamin Page, and Jennifer Jay. This work was supported by the NASA RRNES (Grant #80NSSC20K1746) and NASA ROSES A.8 (cooperative agreement number #80NSSC19K0200), UCLA's Center for Diverse Leadership in Science, and the Joan Doren Family Foundation. This work was performed in part at the Jet Propulsion Laboratory, California Institute of Technology, under contract with the National Aeronautics and Space Administration.

Chapter two is a modified version of a published study entitled "A GEE toolkit for water quality monitoring from 2002 to 2022 in support of SDG 14 and coral health in marine protected areas in Belize" (doi:10.3389/frsen.2022.1020184) in *Frontiers in Remote Sensing*. This study was co-authored by Katie Osborn, Christine Lee, Deepak Mishra, Nicole Auil Gomez, Abel Carrias, Emil Cherrington, Robert Griffin, Andria Rosado, Samir Rosado, and Jennifer Jay. This work was supported by the NASA RRNES (Grant #80NSSC20K1746) and NASA ROSES A.8 (cooperative agreement number #80NSSC19K0200), UCLA's Center for Diverse Leadership in Science, the Joan Doren Family Foundation, NSF NRT: Graduate Traineeship in Integrated Urban Solutions for Food, Energy, and Water Management-DGE-1735325, and the California NanoSystems Institute. This work was performed in part at the Jet Propulsion Laboratory, California Institute of Technology, under contract with the National Aeronautics and Space Administration.

Chapters three, four, and five are in preparation for publication. The third chapter is co-authored by Yuwei Kong, Wei-Cheng Hung, Marisol Cira, Taylor Cason, Aaron Masikip, Akshyae Singh, Adriane Jones, and Jennifer Jay. Chapter four is co-authored by Karina Jimenez, Marisol Cira, Katie Osborn, Mariam Ayad, Bryan Galdamez, Kai Patel, Christine Lee, Nicole Auil Gomez, Myles Phillips, Emil Cherrington, Robert Griffin, Samir Rosado, Andria Rosado, Deepak Mishra, and Jennifer Jay. Chapter five is co-authored by Liana Huang, Marisol Cira, Benjamin Croze, Christine Lee, Taylor Cason, Elizabeth Schiffler, Carlin Soos, Paul Stainier, Zichan Wang, Shanna Shaked, Moana McClellan, Wei-Cheng Hung, and Jennifer Jay

VITA

EDUCATION

University of California, Los Angeles (UCLA)	Expected June 2023
Ph.D. Candidate in Environmental Engineering	
University of California, Los Angeles	June 2019
M.S. in Environmental and Water Resources Engineering	
University of California, Los Angeles	
B.S. in Environmental Science (Minor: Environmental Engineering)	June 2018

EXPERIENCE

Instructor, Biological Sciences, Mount Saint Mary's University	2022-Present
Graduate Student Researcher, Civil and Environmental Engineering, UCLA	2018-Present
Intern, Water & Ecosystems Group, NASA Jet Propulsion Laboratory (JPL)	2020-2022
Intern, Earth and Environmental Sciences, Lawrence Berkeley National Laboratory	2019
Undergrad Student Researcher, Civil and Environmental Engineering, UCLA	2017-2018
Intern, Metropolitan Water District of Southern California	2018
Intern, Watershed Protection Division, Bureau of Sanitation, City of Los Angeles	2017
Public Programs Intern, Heal the Bay	2016

PEER-REVIEWED PUBLICATIONS

- **Callejas, I. A.**, Osborn, K., Lee, C. M., Mishra, D. R., Gomez, N. A., Carrias, A., et al. (2022). A GEE Toolkit for water quality monitoring from 2002-2022 in support of SDG 14 and coral health in Marine Protected Areas in Belize. *Front. Remote Sens.*, 1–13. doi:10.3389/frsen.2022.1020184.
- **Callejas, I.** (2022). Monitoring coastal water quality with satellite data. *Nature Reviews Earth & Environment*, 3(September), 556. doi:10.1038/s43017-022-00337-1.
- Martín-Arias, V., Evans, C., Griffin, R., Cherrington, E. A., Lee, C. M., Mishra, D. R., Gomez, N. A., Rosado, A., **Callejas, I. A.**, Jay, J. A., & Rosado, S. (2022). Modeled Impacts of LULC and Climate Change Predictions on the Hydrologic Regime in Belize. *Frontiers in Environmental Science*, 10(April), 1–16. doi:10.3389/fenvs.2022.848085.
- Alves, R. J. E., **Callejas, I. A.**, Marschmann, G. L., Mooshammer, M., Singh, H. W., Whitney, B., Torn, M. S., & Brodie, E. L. (2021). Kinetic Properties of Microbial Exoenzymes Vary With Soil Depth but Have Similar Temperature Sensitivities Through the Soil Profile. *Frontiers in Microbiology*, 12(November), 1–23.doi:10.3389/fmicb.2021.735282.
- **Callejas, I. A.**, Lee, C. M., Mishra, D. R., Felgate, S. L., Evans, C., Carrias, A., Rosado, A., Griffin, R., Cherrington, E. A., Ayad, M., Rudresh, M., Page, B. P., & Jay, J. A. (2021). Effect of COVID-19 Anthropause on Water Clarity in the Belize Coastal Lagoon. *Frontiers in Marine Science*, 8, 490. doi:10.3389/FMARS.2021.648522.
- Cira, M., Echeverria-Palencia, C. M., **Callejas, I.**, Jimenez, K., Herrera, R., Hung, W.-C., Colima, N., Schmidt, A., & Jay, J. A. (2021). Commercially available garden products as important sources of antibiotic resistance genes—a survey. *Environmental Science and Pollution Research*, 1–8. doi:10.1007/s11356-021-13333-7.

PRESENTATIONS

- **Callejas, I. A.**, Hung, W., Cira, M., Cason, T., Masikip, A., Singh, A., Jones, A. C., & Jay, J. A., "The Influence of Land Use and Water Reclamation Plants on Fecal Indicator Bacteria and Antibiotic Resistance in the Los Angeles River Watershed," *AGU Fall Meeting*, Fall 2022.
- **Callejas, I. A.**, Osborn, K., Lee, C. M., Mishra, D. R., Auil Gomez, N., Carrias, A., Cherrington, E., Griffin, R., Rosado, A., Rosado, S., & Jay, J. A., "A Toolkit for Water Quality Monitoring from 2002-2022 in Support of Sustainable Development Goal 14 and Coral Health in Marine Protected Areas in Belize," *AGU Fall Meeting*, Fall 2022.
- **Callejas, I. A.**, Lee, C. M., Mishra, D. R., Felgate, S. L., Evans, C., Carrias, A., Rosado, A., Griffin, R., Cherrington, E. A., Ayad, M., Rudresh, M., Page, B. P., Cassano, K. S., & Jay, J. A., "Remote sensing of water quality in coastal Belize: Implications for coastal zone management and informing Sustainable Development Goals," *AGU Fall Meeting*, Fall 2021.
- Rudresh, M., Mishra, D. R., Wheelock, C., Phillips, M., **Callejas, I. A.**, Lee, C. M., Griffin, R., Cherrington, E. A., & Rosado, S., "Monitoring Changes in Water Quality in the Belize Barrier Reef Coastal Lagoon During COVID-19," *AGU Fall Meeting*, Fall 2021.
- Alves, R. J. E., **Callejas, I. A.**, Marschmann, G., Mooshammer, M., Singh, H. W., Whitney, B., Torn, M. S., and Brodie, B., "Kinetic Properties of Microbial Exoenzymes Vary With Soil Depth but Have Similar Temperature Sensitivities Through the Soil Profile," *AGU Fall Meeting*, Fall 2020.
- Cira, M., **Callejas, I.**, Echeverria-Palencia, C., and Jay, J. A., "Commercially Available Garden Products as Potential Sources of Antibiotic Resistance Genes," *ACS National Conference,* Summer 2019.

HONORS AND AWARDS

International Institute Fieldwork Fellowship, UCLA	2022
GradSWE@UCLA Support Scholarship	2022
Graduate Traineeship:Integrated Urban Solutions for Food, Energy, and Water Systems	2021
Charles F. Scott Fellowship, UCLA	2020
Center for Diverse Leadership in Science (CDLS) Early Career Fellow, UCLA	2019
Competitive Edge Fellowship, UCLA	2019
Graduate Degrees for Minorities in Engineering and Science (GEM) Fellowship	2019
Eugene V. Cota-Robles Fellowship, UCLA	2019
Graduate Opportunity Fellowship Program (GOFP), UCLA	2018

TEACHING & GRADING EXPERIENCE

Instructor, Microbiology Laboratory, Mount Saint Mary's University	2022-2023
Teaching Assistant, Chemical Fate and Transport in Aquatic Environments, UCLA	2022
Teaching Assistant, Introduction to Sustainable Architecture and Community Planning, UCLA	2020
Grader, Environmental Politics and Governance, UCLA	2019-2020
Grader, Chemical Fate and Transport in Aquatic Environments, UCLA	2019
Teaching Assistant, Environmental Aquatic Inorganic Chemistry, UCLA	2019
Seminar Co-Director, Sustainability Talks, UCLA	2017

JOURNAL CONTRIBUTIONS

Reviewed for Frontiers in Remote Sensing

Chapter 1: Effect of Covid-19 Anthropause on Water Clarity in The Belize Coastal Lagoon

1. Introduction

The Central American nation of Belize is home to the Belize Barrier Reef Reserve System, the largest barrier reef system in the northern hemisphere and a World Heritage Site[1–3]. Belize's reef system is approximately 250 km in length, 963 km^2 in area, and is located 0.5-80 km offshore between Mexico and Guatemala's borders[4–6]. This reef system contains hundreds of reef patches which developed during the Holocene[4,7]. Belize's coral reefs support high levels of biodiversity[8], and provide essential ecosystem services such as coastal protection and fisheries[9], and important economic revenue as tourism is a primary contributor to the economy[10]. Since 1998, the main use for Belize's reefs has been identified as tourism and thus the nation must continuously monitor tourism impacts in order to prevent the degradation of the reefs and preserve Belize's competitiveness in ecotourism markets[11,12].

The Coronavirus disease 2019 (COVID-19) pandemic caused shifts in the environment and climate due to global lockdowns resulting in a reduction of social and economic activities[13,14]. On March 23, 2020, a mandatory quarantine was placed on Ambergris Caye within Belize followed by a countrywide state of emergency (SoE) declared on March 30, 2020[15,16]. To limit the spread of COVID-19, Belize closed their borders to international travelers by closing land borders and its international airport[17]. On October 1, 2020, the reopening phase of Belize's international airport began while expecting 140 travelers on its first day[18].

Tourism has declined on a global scale, which can have devastating impacts on local and regional economies. Other observed impacts include a reduction of anthropogenic footprint on natural ecosystems[13]. Remote sensing datasets are especially well-positioned to assess these changes by providing a mechanism to observe larger scale responses to these declines in human activity, often referred to as the “anthropause”[19]. This is especially important in data-scare regions such as Belize. For example, Landsat-8, Sentinel-2, Sentinel-3, and moderate resolution imaging spectroradiometer (MODIS) have been used to evaluate changes in air quality emissions[20–22], water clarity[23–25], and coastal/ocean productivity[26–28]. A variety of satellites have been used for impact assessment such as Landsat-8[29–31], PlanetScope[32], Sentinel-2[33,34], Sentinel-3[29,35], and MODIS (Gaiser et al., *in press*). Multiple studies report reductions in air, water, and noise pollution due to global lockdown orders. Within the hydrosphere, rivers[30,34,36], lakes[31], lagoons[32,33], and coastal regions[35,37] experienced improvements in water quality with decreases in turbidity, pollution, and pathogens. Improvements in water quality were attributed to reductions in industrial discharges, boat traffic, and public interactions in general. These anthropogenic activities tend to increase water column turbidity and sediment resuspension in the near-shore environments and diminish water quality in the lagoon. Here, we hypothesize that the COVID-19 lockdowns and the subsequent decline in tourism and marine traffic will improve the water clarity in the Belizean coast, namely near major ports and tourist regions.

To test the hypothesis, we used satellite datasets, model produced runoff and precipitation outputs, and marine traffic data conjunctively to investigate the impacts of the COVID-19 pandemic on coastal water quality in Belize. Using the vertical diffuse attenuation coefficient [Kd(490)] as the primary indicator of water quality, we compared the monthly variations in water clarity in 2020 to that observed from 2002 to 2019.

2. Methods

2.1 Study Area and High and Low Marine Traffic Areas

Belize is located between Mexico and Guatemala with approximately 280 km of coastline. The climate is tropical with high humidity occurring from June to October. Belize is also on the western side of “Hurricane Alley” with tropical storms and hurricanes appearing from June to

November[38]. Most of Belize's major cities, towns, tourist centers, and residential properties are located along the coast. The Belizean coastal lagoon is classified as a Case-1 waters like other Caribbean coastal waters[39–42] as well as being oligotrophic in nature[43,44]. In addition, multiple studies operate under the knowledge and understanding of these water being oligotrophic[45–48] which is necessary for the development and flourishing of corals[48,49]. The Belizean coast hosts multiple diverse ecosystems including coral reefs, mangroves, and seagrasses[50–54] which not only attract tourists but also play an integral role in mitigating coastal erosion and impacts from tropical storms[55]. Though these ecosystems contribute millions of United States dollars to Belize's economy[55], industries such as tourism, fisheries, real estate, and agriculture stand to threaten the very ecosystems that allow them to operate[52]. Tourism season in Belize takes place during in dry, winter months from November to April[56].

Belize's Integrated Coastal Zone Management Plan (ICZMP) divides its coast into nine regions based on biological, geographical, economic, and administrative characteristics[57]. Six of these nine regions were characterized as high and low traffic areas (HTAs and LTAs, respectively) based on a 2019 marine traffic density map assumed to depict typical traffic patterns prior to COVID-related lockdowns (**Figure 1-1**). The four HTAs comprise the Central Region which includes Belize City (A), South Northern Region which includes Dangriga (B), part of South Central Region containing Placenia, Big Creek, and Harvest Caye (C), and the Southern Region containing Punta Gorda and Barranco (D). The two LTAs are to the north, at Ambergris Caye (E), and Caye Caulker (F).

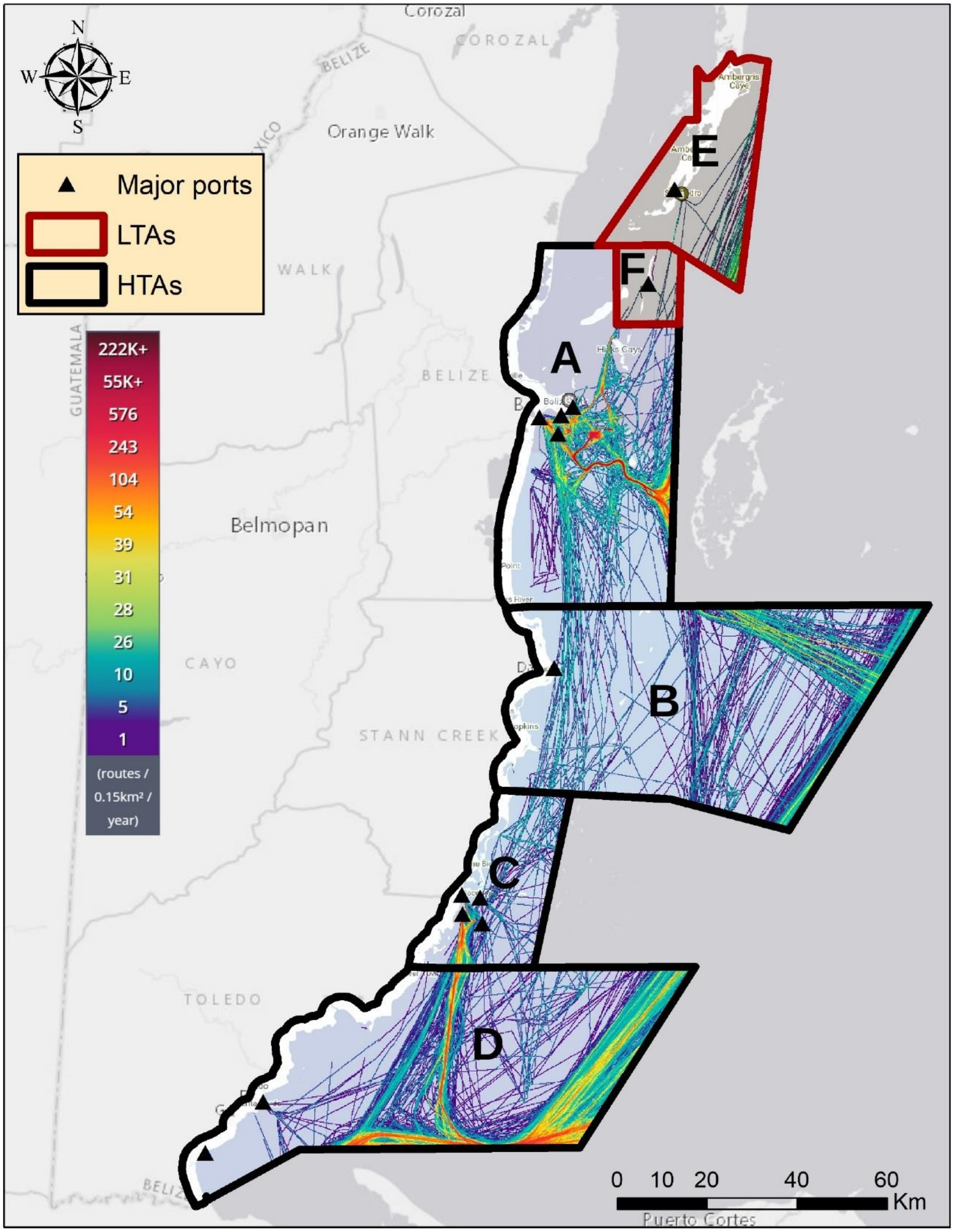

Figure 1-1. Belize Coastal Zones, Major Ports, and Marine Traffic Density. Six coastal areas were used in this study: (A) Central Region, (B) South Northern Region, (C) South Central Region, (D) Southern Region, (E) Ambergris Caye, and (F) Caye Caulker. Areas (A–D) are denoted as high traffic areas (HTAs) and E & F as low traffic areas (LTAs). Each zone is filled with 2019 marine traffic density maps where the color of each line corresponds to the number of routes/0.15 km^2/year.

2.2 High Traffic Areas

Belize City is the largest city within the Belize District (17.5046° N, 88.1962° W) and is home to the nation's principal port[58]. The Port of Belize Limited is located on the south side of Belize City and is responsible for containerized and break bulk cargo[59]. Other major port facilities in Belize City include Puma Energy Bahamas SA for bulk fuel import, Fort Street Tourism Village, a water taxi terminal operated by the Belize Border Management Agency (BMA), Radisson Fort George, and Old Belize port.

Dangriga is a town in southern Belize and the capital of Stann Creek District (16.9696° N, 88.2315° W). Though the Commerce Bight port 1.5 miles south of Dangriga is currently not operational[60], Dangriga is known as "the cultural capital of Belize" and is a popular tourist location[61].

Placencia is located on the Placencia Peninsula (16.5212° N, 88.3713° W) on the southeast coast of Belize within the Stann Creek District and is rapidly growing in tourism[56,62]. Just south of the Stann Creek District in the Toledo District is the Port of Big Creek, the nation's second major port[63], responsible for banana exports, crude oil tank farming, and sugar storage[64]. South of both Big Creek and Placencia and a mile off the coast is Harvest Caye, a private island developed for tourism by a Miami-based Norwegian Cruise Line[56]. Belize City and Placencia are two major coastal cities which have experienced coral growth declines[5] and mangrove clearings[50].

Punta Gorda (16.0989° N, 88.8095° W) and Barranco (16.0011° N, 88.9186° W) are both towns located in the southernmost region of Belize located in the Toledo District. Punta Gorda is the capital of the Toledo District and is home to the Punta Gorda Port[65]. The Port of Barranco is a very small port in the town of Barranco[66].

2.3 Low Traffic Areas

San Pedro is a town in the southern part of Ambergris Caye in the Belize District in northern Belize (17.9214° N, 87.9611° W). There is a water taxi terminal with six berths located in San Pedro under the Belize BMA[67].

Caye Caulker is a small island off the coast of Belize (17.7612° N, 88.0277° W) accessible by water taxis and small planes[68].

2.4 Satellite Images

The average vertical diffuse attenuation coefficient for downwelling irradiance at 490 nm, Kd(490), was calculated in Google Earth Engine (GEE) from images collected from MODIS onboard the Aqua satellite. The images processed in GEE started from June 4, 2002 to July 31, 2020. The rest of the images for 2020 were downloaded from https://oceancolor.gsfc.nasa.gov/ and ingested into GEE. All images were Level-3 daily images with a spatial resolution of 4 km and Kd(490) was calculated using the NASA operational algorithm[69]. The algorithm is a fourth-order polynomial between blue and green remote sensing reflectances (Rrs) and Kd(490). The algorithm is based on two high quality bio-optical global datasets, the SeaWiFS Bio-Optical Archive and Storage System (SeaBASS) and the NASA bio-Optical Marine Algorithm Data (NOMAD) archives. Though the datasets encompass a broad range of water types and locations, certain oceanic regions remain underrepresented.

The NASA operational algorithm is as follows for the MODIS sensor:

$$Kd(490) = 10^{(-0.8813-2.0584x+2.5878x^2-3.4885x^3-1.5061x^4)} + 0.0166$$

where $x = \log_{10}\frac{Rrs(488)}{Rrs(547)}$. Beside numerous open ocean applications, MODIS-derived Kd(490) products have also been used in turbid coastal water[70], for coastal river plume characterization during high flow[71], and turbidity impacts on coral health[72,73]. Caribbean coastal waters are generally considered as Case-1 waters because thriving seagrass and reef habitats help reduce water column turbidity[40,41]. The NASA operational algorithm for Kd(490) has also been used specifically in coastal Caribbean regions[71,74,75]. A function was created to calculate Kd(490) for each image and the newly calculated band was appended to the image collection. Monthly averages for Kd(490) were calculated for the coast of Belize using a mean reducer for LTAs and HTAs and compared between 2020 and the baseline period. The number of pixels included in each monthly calculation was obtained through the count reducer which computes the number of non-null inputs. Percent difference maps of Kd(490) were also created in GEE by filtering the images for each respective month of the year, taking the average for the years of 2002–2019 and 2020, and mapping the percent difference between the two time frames. A decrease in Kd(490) indicates a decline in water clarity, generally associated with degradation in water quality, whereas an increase in Kd(490) indicates an increase in water clarity, associated with an improvement.

2.5 Marine Traffic Data

Marine traffic data were obtained from the company MarineTraffic (marinetraffic.com) for ports and anchorages in Belize from January 2020 to November 2020 (**Figure 1-2**). The data uses both Automated Identification System (AIS) data and data from satellite receivers. The data includes arrival and departure data for ports in Belize City, Belize City anchorage, Old Belize, Radisson Fort George, Placencia, Big Creek, Big Creek anchorage, Harvest Caye, San Pedro, and Caye Caulker. The company also detects port calls from Dangriga, Punta Gorda, and Barranco ports, but in 2020 there were no port calls detected through AIS or satellite data for these ports.

2.6 Runoff and Precipitation Models

Monthly time-averaged precipitation and runoff were calculated over Belize using NASA's Modern-Era Retrospective analysis for Research and Applications, Version 2 (MERRA-2) model from June 2002 to October 2020. MERRA-2 is a global atmospheric reanalysis produced by NASA's Global Modeling and Assimilation Office[76]. For precipitation, the "total surface precipitation" variable was used (M2TMNXFLX v5.12.4) and for runoff, the "overland runoff including throughflow" variable was used (M2TMNXLND v5.12.4). The model outputs were extracted from NASA Giovanni (https://giovanni.gsfc.nasa.gov/giovanni/).

2.7 Statistical Analysis

For each month of the year where data were available, data for each location for years 2002–2019 and for the year 2020 were grouped and tested for normality using histograms created in R[77]. In no cases were both the previous years and 2020 found to be normal, so the Wilcoxon unpaired test was used to test the null hypothesis that there was no difference between 2020 and previous years. We computed means and standard deviation for both time periods.

3. Results

At the start of 2020 prior to the Belize SoE COVID shutdown, the Kd(490) was consistently similar to that observed for previous years, with no significant differences observed for any location (**Figure 1-2**). However, the monthly Kd(490) maps show notable decreases in Kd(490) along the Belizean coast at HTAs following the initial lockdown orders in place on March 23, 2020 compared to the 2002-2019 average (**Figure 1-3A**). Following the SOE in April, 2020 data showed a lower K_d (indicating increased water clarity) compared to previous years in (most) HTAs, but not the LTAs. For example, for HTA-D, which includes Placencia, the average Kd(490) from 2002 to 2019 for the month of April was 0.068 m–1 (SD 0.002), while for 2020 the value was 0.057 m–1 (SD 0.001). In May of 2020, HTA-A, which includes Belize's most popular port, shows a K_d of 0.051 m–1 (SD 0.008) in 2020, compared to 0.090 m–1 (SD 0.008) for the years 2002–2019. See **Table 1-1** for the p-values for hypothesis testing for the difference between 2020 and previous years. While LTAs showed some differences in means, these tended to be smaller, and statistically significant differences were only observed at HTAs. For both HTAs and LTAs for the months of June and July, none of the observed differences in means were significant, possibly due to the tourism season ending so no major differences in marine traffic would be expected.

Figure 1-3A shows the percent difference of Kd(490) between 2020 and previous years. A greater fraction of the coastal waters shows a decrease (blue) compared to previous years for the months of April through October. In November 2020, Kd(490) increases (brown) drastically across the entire coast. This increase coincides with a record-breaking hurricane season where Belize experienced impacts of Hurricanes Nana, Eta, Iota, and Tropical Storm Cristobal[78]. **Figures 1-3B,C** show the precipitation and runoff for 2002 through 2020 of Belize. While month to month 2020 was not an atypical year for precipitation through the month of October, both precipitation and runoff were dramatically elevated for the month of November (**Figures 1-3B,C**).

Because Kd(490) incorporates both inorganic and organic components within the water column, we tested for correlations between in situ chlorophyll-a and MODIS-derived Kd(490). Using a dataset from 2018 and 2019, we saw no significant correlation between chlorophyll-a and Kd(490) after calculating the Spearman's rank order correlation coefficient following tests for normality using Q–Q plots and histograms (Spearman's rho = 0.34).

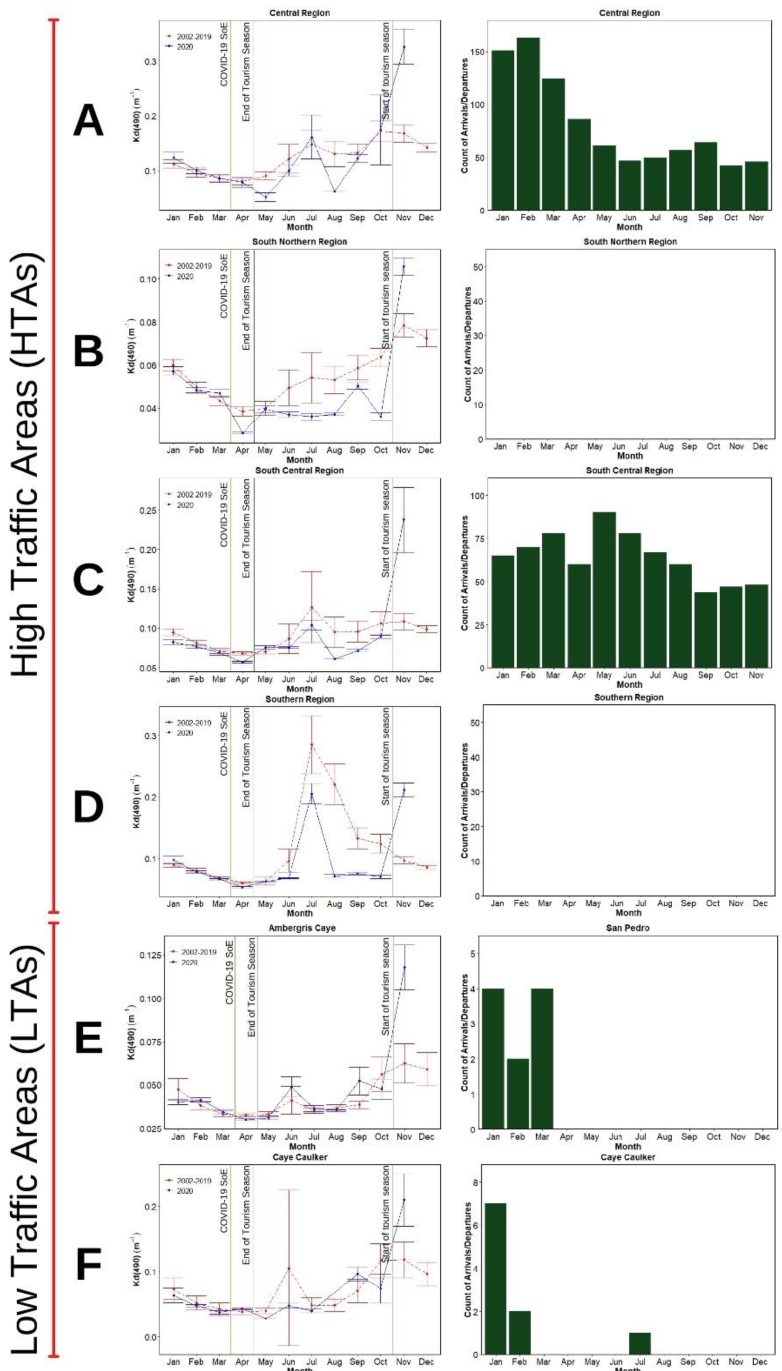

Figure 1-2. Kd(490) Time Series Plots and 2020 Total Port Counts. The first vertical column of figures are plots of monthly Kd(490) values and standard deviations for the 2020 and 2002–2019 time periods. The orange vertical line marks the time of the COVID-19 SoE in Belize. The green lines represent the beginning and end of the tourist season in Belize. The second column of figures are total port counts for each month for 2020. Some ports did not have any port calls in 2020 through AIS or satellite data. Each lettered row of plots corresponds to the areas in *Figure 1*. (A) Central Region, (B) South Northern Region, (C) South Central Region, (D) Southern Region, (E) Ambergris Caye, and (F) Caye Caulker.

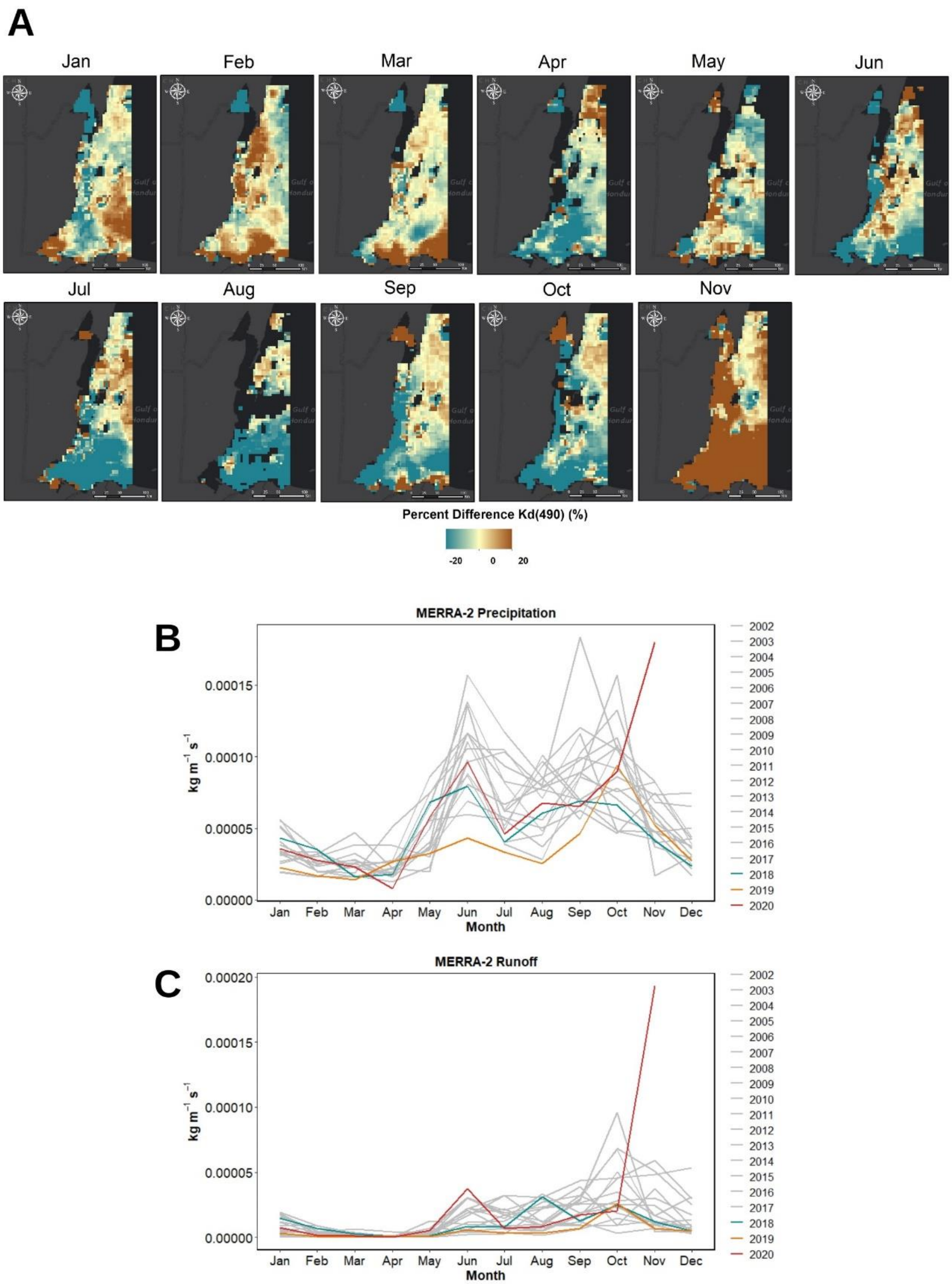

Figure 1-3. Percent Difference Kd(490) Maps and MERRA-2 Model Outputs. (A) Monthly percent difference maps comparing 2020 Kd(490) values against those of the 2002–2019 (baseline) time period. (B) MERRA-2 precipitation output for the country of Belize from 2002 to 2020 in kg m^{-1} s^{-1}. (C) MERRA-2 runoff output for Belize from 2002 to 2020 in kg m^{-1} s^{-1}.

Table 1-1. Wilcoxon test p-values for each month between Kd(490) values in 2020 versus 2002–2019 baseline for all regions.

Site	Coastal Region	HTA/LTA	Wilcoxon Test p-values										
			Jan	Feb	Mar	Apr	May	Jun	Jul	Aug	Sep	Oct	Nov
A	Central Region	HTA	0.679	0.374	0.987	0.705	0.029*	0.895	0.651	0.269	0.982	0.067	0.006*
B	South Northern Region	HTA	0.806	0.866	0.164	0.018*	0.429	0.988	0.479	0.250	0.83	0.006*	0.033*
C	South Central Region	HTA	0.082	0.250	0.230	0.046*	0.165	0.359	-	0.113	0.004*	0.496	<0.001*
D	Southern Region	HTA	0.600	0.968	0.423	0.483	0.063	0.403	0.852	0.044*	0.009*	0.003*	<0.001*
E	Ambergris Caye	LTA	0.131	0.021*	0.504	0.313	0.382	-	0.590	0.787	0.591	0.419	0.002*
F	Caye Caulker	LTA	0.567	0.353	0.481	-	-	-	-	-	0.162	0.178	0.009*

4. Discussion

This preliminary study shows that MODIS Kd(490) data can be used to better understand spatiotemporal changes in water quality impacts associated with environmental disturbances. This is particularly important in locations where in situ data are limited and healthy ecosystems are essential to the local economy. Belize relies on robust tourist traffic to support the economy, and water clarity is critical for coral reef health[79]. Marine traffic due to both commerce and tourism have the potential to result in decreased water clarity through an increase in suspended solids. In addition, marine traffic is also shown to increase nutrient depositions which spurs phytoplankton growth[80]. For this site, chlorophyll-a and Kd(490) were not significantly associated, suggesting that Kd(490) is mainly attributed to sediment resuspension rather than algal particles. Nonetheless, the possible contribution of chlorophyll-a to MODIS Kd(490) at the study site needs further investigation, and future data collection should attempt to deconvolute their signals.

The COVID-19 shutdown in 2020, along with the availability of satellite data with an extended recorded (2002–2019), presented an opportunity to understand the impacts of tourism on water quality and subsequent effects on coral reef health in a data-scarce region. As shown in this work, the COVID-19 shutdown resulted in increased water clarity in areas along the Belizean coast with typically high marine traffic, while water clarity was similar in areas with typically low marine traffic during the tourism season. This finding, along with knowledge of the relationships between water clarity and reef health, provides insight on the role of commerce and tourism on the long-term sustainability of the northern hemisphere's largest barrier reef system. Additionally, this finding is similar to other studies that investigated COVID-19 impacts on turbidity, suspended particulate matter (SPM), and total suspended matter (TSM). Studies in India show a 15.9% decrease in SPM in a lake[31], a significant reduction in the usual pre-monsoon phytoplankton content in coastal waters[81], water quality index increase of 37% in the Yamuna River[30], and reductions in turbidity in the Ganga River[34] all with notable changes in April 2020. A couple of studies of the Venice Lagoon, which has high water traffic, found decreases of TSM[32] and increases in water clarity[33] during their lockdowns in March and April 2020.

One expected outcome of this study is a further collaboration with colleagues at the Coastal Zone Management Authority Institute, who is committed to the protection and sustainable management of coastal resources and the ICZMP. The ICZMP is an evidence-based set of policy recommendations that enable an improved understanding of how land management might impact coastal and marine resources[82].

This work also observes substantial water clarity changes, e.g., anomalous coastal plumes, following the active hurricane season in 2020, an observation enabled by high-frequency, freely available satellite data such as MODIS. Hurricane events in November 2020 coincided with a significant decrease in water clarity compared with November during the baseline period[83,84]. Future work should include evaluating the changing climatology of hurricane events on corresponding plumes into the marine environment. Furthermore, it is critical that future work considers in situ datasets that would allow improved tuning of remote sensing based estimates of water quality as well as improved characterization of plume constituents. It has been observed that these Belize coastal plumes can be comprised of a variety of constituents, including sediments, agricultural runoff, and sewage[85–88], with Soto et al. (2009) observing a consistent year-to-year river plume occurrences with coral ecosystems[89]. Though classified as oligotrophic, river plumes can often cause Caribbean waters to become mesotrophic[49,90]. In Belize, New River is known to cause a decline in water quality affecting surrounding corals due to poor farming practices and deforestation[91,92]. Corals in particular are highly sensitive to changing conditions and it is expected that agricultural runoff and water temperature increases may contribute to their declines[5].

5. Conclusion

Remote sensing can be used to evaluate these coupled events and their spatial and temporal effects on coastal waters. This study observes an improvement in water clarity during COVID-19 shutdowns in Belize, followed by a decline in water clarity following an atypical, active hurricane season. Use of remote sensing is especially important for coastal waters, as populations rise and population density and development along the coasts continue to increase[93–95]. Remote sensing of water quality holds great promise to improve detection of changes in water quality and ecosystem health in data-scarce locations impacted by development, tourism, or climate change, and may represent an asset for nations and entities seeking to set and advance toward the UN Sustainable Development Goals[96] (https://sdgs.un.org/goals/goal14). This study in particular is closely linked with SDG 14.1 (life in water). Satellite data can be used to extend ground-based monitoring programs to increase the temporal and spatial density of data. Future research will involve the use of match-ups between in situ and satellite data to further investigate long-term relationships between in situ water quality parameters such as chlorophyll-a and TSM and isolate any signal related to COVID-19 lockdowns.

6. References

1. UNESCO. *World Heritage Committee; 20th; Convention concerning the Protection of the World Cultural and Natural Heritage; report; 1997*. (1996).
2. Cherrington, E. SERVIR - Forest Cover and Deforestation in Belize: 1980-2010 -

servir_bz_forest_cover_1980-2010.pdf. 1980–2010 (2010).

3. Cherrington, E. A. *et al.* Use of public Earth observation data for tracking progress in sustainable management of coastal forest ecosystems in Belize, Central America. *Remote Sens. Environ.* **245**, (2020).

4. Gischler, E. & Hudson, J. H. Holocene development of the Belize Barrier Reef. *Sediment. Geol.* **164**, 223–236 (2004).

5. Baumann, J. H. *et al.* Nearshore coral growth declining on the Mesoamerican Barrier Reef System. *Glob. Chang. Biol.* **25**, 3932–3945 (2019).

6. Claudino-Sales, V. Belize Barrier Reef System, Belize. in *Coastal Research Library* vol. 28 451–456 (Springer, 2019).

7. Eckert, R. J., Studivan, M. S. & Voss, J. D. Populations of the coral species Montastraea cavernosa on the Belize Barrier Reef lack vertical connectivity. *Sci. Rep.* **9**, 1–11 (2019).

8. Young, C. A. Belize's Ecosystems: Threats and Challenges to Conservation in Belize. *Trop. Conserv. Sci.* **1**, 18–33 (2008).

9. Hoegh-Guldberg, O. *et al.* Coral reefs under rapid climate change and ocean acidification. *Science (New York, N.Y.)* vol. 318 1737–1742 (2007).

10. Murray, R. A governance analysis of three MPAs in Belize: Conservation objectives compromised by tourism development priorities? *Mar. Policy* 104243 (2020) doi:10.1016/j.marpol.2020.104243.

11. Gibson, J., McField, M. & Wells, S. Coral reef management in Belize: An approach through integrated coastal zone management. *Ocean Coast. Manag.* **39**, 229–244 (1998).

12. Diedrich, A. The impacts of tourism on coral reef conservation awareness and support in coastal communities in Belize. *Coral Reefs* **26**, 985–996 (2007).

13. Bar, H. COVID-19 lockdown: animal life, ecosystem and atmospheric environment. *Environ. Dev. Sustain.* (2020) doi:10.1007/s10668-020-01002-7.

14. Rume, T. & Islam, S. M. D. U. Environmental effects of COVID-19 pandemic and potential strategies of sustainability. *Heliyon* vol. 6 e04965 (2020).

15. United Nations. Coronavirus Disease – COVID 19 Situation Note No . 4. 1–6 https://reliefweb.int/sites/reliefweb.int/files/resources/COVID 19 Situation Report No 4 BELIZE Final.pdf (2020).

16. Government of Belize Press Office. State of Emergency Declared for Ambergris Caye. (2020).

17. Government of Belize Press Office. COVID-19 – Alert Regarding Border Closures. https://www.pressoffice.gov.bz/covid-19-alert-regarding-border-closures/ (2020).

18. Government of Belize Press Office. The Philip Goldson International Airport Successfully Reopens. 1–2 https://www.pressoffice.gov.bz/the-philip-goldson-international-airport-successfully-reopens/ (2020).

19. Rutz, C. *et al.* COVID-19 lockdown allows researchers to quantify the effects of human activity on wildlife. *Nat. Ecol. Evol.* **4**, 1156–1159 (2020).

20. Wang, J. & Christopher, S. A. Intercomparison between satellite‐derived aerosol optical thickness and PM<subscr>2.5</subscr> mass: Implications for air quality studies. *Res. Lett* **30**, 2095 (2003).

21. Gupta, P. *et al.* Satellite remote sensing of particulate matter and air quality assessment over global cities. *Atmos. Environ.* **40**, 5880–5892 (2006).

22. Mishra, R. K., Agarwal, A. & Shukla, A. Predicting Ground Level PM $_{2.5}$ Concentration Over Delhi Using Landsat 8 Satellite Data. *Int. J. Remote Sens.* **42**, 827–838 (2021).

23. Barnes, B. B. *et al.* MODIS-derived spatiotemporal water clarity patterns in optically shallow Florida Keys waters: A new approach to remove bottom contamination. *Remote Sens. Environ.* **134**, 377–391 (2013).

24. Zheng, Z. *et al.* Remote sensing of diffuse attenuation coefficient patterns from Landsat 8 OLI imagery of turbid inland waters: A case study of Dongting Lake. *Sci. Total Environ.* **573**, 39–54 (2016).

25. Kuhn, C. *et al.* Performance of Landsat-8 and Sentinel-2 surface reflectance products for river remote sensing retrievals of chlorophyll-a and turbidity. *Remote Sens. Environ.* **224**, 104–118 (2019).

26. Ho, J. C., Stumpf, R. P., Bridgeman, T. B. & Michalak, A. M. Using Landsat to extend the historical record of lacustrine phytoplankton blooms: A Lake Erie case study. *Remote Sens. Environ.* **191**, 273–285 (2017).

27. Astuti, I. S., Mishra, D. R., Mishra, S. & Schaeffer, B. Spatio-temporal dynamics of inherent optical properties in oligotrophic northern Gulf of Mexico estuaries. *Cont. Shelf Res.* **166**, 92–107 (2018).

28. Caballero, I., Fernández, R., Escalante, O. M., Mamán, L. & Navarro, G. New capabilities of Sentinel-2A/B satellites combined with in situ data for monitoring small harmful algal blooms in complex coastal waters. *Sci. Rep.* **10**, 1–14 (2020).

29. Nanda, D., Mishra, D. R. & Swain, D. COVID-19 lockdowns induced land surface temperature variability in mega urban agglomerations in India. *Environ. Sci. Process. Impacts* (2020) doi:10.1039/D0EM00358A.

30. Patel, P. P., Mondal, S. & Ghosh, K. G. Some respite for India's dirtiest river? Examining the Yamuna's water quality at Delhi during the COVID-19 lockdown period. *Sci. Total Environ.* **744**, 140851 (2020).

31. Yunus, A. P., Masago, Y. & Hijioka, Y. COVID-19 and surface water quality: Improved lake water quality during the lockdown. *Sci. Total Environ.* **731**, 139012 (2020).

32. Niroumand-Jadidi, M., Bovolo, F., Bruzzone, L. & Gege, P. Physics-based bathymetry and water quality retrieval using planetscope imagery: Impacts of 2020 COVID-19 lockdown and 2019 extreme flood in the Venice lagoon. *Remote Sens.* **12**, 2381 (2020).

33. Braga, F., Scarpa, G. M., Brando, V. E., Manfè, G. & Zaggia, L. COVID-19 lockdown measures reveal human impact on water transparency in the Venice Lagoon. *Sci. Total Environ.* **736**, (2020).

34. Garg, V., Aggarwal, S. P. & Chauhan, P. Changes in turbidity along Ganga River using Sentinel-2 satellite data during lockdown associated with COVID-19. *Geomatics, Nat. Hazards Risk* **11**, 1175–1195 (2020).

35. Cherif, E. K., Vodopivec, M., Mejjad, N., Esteves, J. C. G. & Simonoviˇ, S. COVID-19 Pandemic Consequences on Coastal Water. *Water* (2020).

36. Dutta, V., Dubey, D. & Kumar, S. Cleaning the River Ganga: Impact of lockdown on water quality and future implications on river rejuvenation strategies. *Sci. Total Environ.* **743**, 140756 (2020).

37. Mishra, D., Mishra, S. & Mishra, D. R. Normalized difference chlorophyll index: A novel model for remote estimation of chlorophyll-a concentration in turbid productive waters. *Remote Sens. Environ.* **117**, 394–406 (2012).

38. Morales-Vela, B., Olivera-Gómez, D., Reynolds, J. E. & Rathbun, G. B. Distribution and habitat use by manatees (Trichechus manatus manatus) in Belize and Chetumal Bay, Mexico. *Biol. Conserv.* **95**, 67–75 (2000).

39. Alvain, S., Moulin, C., Dandonneau, Y. & Bréon, F. M. Remote sensing of phytoplankton groups in case 1 waters from global SeaWiFS imagery. *Deep. Res. Part I Oceanogr. Res. Pap.* **52**, 1989–2004 (2005).

40. Mishra, D. R., Narumalani, S., Rundquist, D. & Lawson, M. High-resolution ocean color remote sensing of benthic habitats: A case study at the Roatan Island, Honduras. *IEEE Trans. Geosci. Remote Sens.* **43**, 1592–1603 (2005).

41. Mishra, D. R., Narumalani, S., Rundquist, D., Lawson, M. & Perk, R. Enhancing the detection and classification of coral reef and associated benthic habitats: A hyperspectral remote sensing approach. *J. Geophys. Res.* **112**, C08014 (2007).

42. Shi, W. & Wang, M. Characterization of global ocean turbidity from Moderate Resolution Imaging Spectroradiometer ocean color observations. *J. Geophys. Res.* **115**, C11022 (2010).

43. Gómez, R. A. Spectral Reflectance Analysis of the Caribbean Sea. *Geofis. Int.* **53**, 385–398 (2014).

44. Mélin, F. & Vantrepotte, V. How optically diverse is the coastal ocean? *Remote Sens. Environ.* **160**, 235–251 (2015).

45. Mendoza, W. G. *et al.* Developmental strategy for effective sampling to detect possible nutrient fluxes in oligotrophic coastal reef waters in the Caribbean. *J. Oper. Oceanogr.* **2**, 35–47 (2009).

46. Contreras-Silva, A. I. *et al.* A meta-analysis to assess long-term spatiotemporal changes of benthic coral and macroalgae cover in the Mexican Caribbean. *Sci. Rep.* **10**, 1–12 (2020).

47. Correa-Ramirez, M., Rodriguez-Santana, Á., Ricaurte-Villota, C. & Paramo, J. The

Southern Caribbean upwelling system off Colombia: Water masses and mixing processes. *Deep. Res. Part I Oceanogr. Res. Pap.* **155**, 103145 (2020).

48. Guimarais, M. *et al.* The conservational state of coastal ecosystems on the mexican caribbean coast: Environmental guidelines for their management. *Sustain.* **13**, 1–25 (2021).

49. Warne, A. G., Webb, R. M. T. & Larsen, M. C. Water, Sediment, and Nutrient Discharge Characteristics of Rivers in Puerto Rico, and their Potential Influence on Coral Reefs. *U.S. Geol. Surv. Sci. Investig. Rep. 2005-5206* 58 (2005).

50. Cherrington, E. A. *et al.* Identification of Threatened and Resilient Mangroves in the Belize Barrier Reef System. *Development* (2010).

51. Baumann, J. H. *et al.* Temperature regimes impact coral assemblages along environmental gradients on lagoonal reefs in Belize. *PLoS One* **11**, 1–19 (2016).

52. Verutes, G. M. *et al.* Integrated planning that safeguards ecosystems and balances multiple objectives in coastal Belize. *Int. J. Biodivers. Sci. Ecosyst. Serv. Manag.* **13**, 1–17 (2017).

53. Sweetman, B. M., Cissell, J. R., Rhine, S. & Steinberg, M. K. Land Cover Changes on Ambergris Caye, Belize: A Case Study of Unregulated Tourism Development. *Prof. Geogr.* **71**, 123–134 (2019).

54. Helmuth, B. *et al.* High resolution spatiotemporal patterns of seawater temperatures across the Belize Mesoamerican Barrier Reef. *Sci. Data* **7**, 1–6 (2020).

55. Cooper, E., Burke, L. & Bood, N. Coastal capital: Economic contribution of coral reefs and mangroves to Belize. *World Resour. Institute, Washington, DC.* 53 (2009).

56. Renaud, L. Cruise Tourism Threatens to Drive Land Speculation and Displacement in Belize. *NACLA Rep. Am.* **52**, 442–447 (2020).

57. The Coastal Zone Management Authority and Institute (CZMAI). Coastal Planning & Monitoring Program Unit - Belize Coastal Zone Management. https://www.coastalzonebelize.org/coastal-planning-monitoring-program-unit/.

58. Belize City Council. About Belize City. https://web.archive.org/web/20140723140609/http://belizecitycouncil.org/about-belize-city.

59. Belize Port Authority. Port Facilities. https://www.portauthority.bz/port-facilities/.

60. Belize Port Authority. Commerce Bight. https://www.portauthority.bz/port-facilities/commerce-bight/.

61. Belize.com. Stann Creek Belize – Home Of Culture Capital Dangriga. https://belize.com/stann-creek/.

62. Wells, E. C. *et al.* The impacts of tourism development on perceptions and practices of sustainable wastewater management on the Placencia Peninsula, Belize. *J. Clean. Prod.* **111**, 430–441 (2014).

63. 7 News Belize. Big Business At Big Creek Port.

http://www.7newsbelize.com/sstory.php?nid=34664.

64. Port of Big Creek. Port of Big Creek. http://www.portofbigcreek.com/#smoothscroll-facts-module.

65. Belize Port Authority. Punta Gorda Port. https://www.portauthority.bz/port-facilities/punta-gorda-port/.

66. FleetMon. Port of Barranco, Belize - Arrivals, schedule and weather forecast. https://www.fleetmon.com/ports/barranco_bzbar_14265/?language=en.

67. Belize Port Authority. San Pedro Terminal. https://www.portauthority.bz/port-facilities/san-pedro-terminal/.

68. CayeCaulker.org. Belize Travels, Lodging, Diving, Guides, Mayan Tours, Fishing, Hotels and Resorts, Paradise for Scuba, Vacation, Beaches Relaxing, Fishing Tourism, Vacations, Adventures. https://cayecaulker.org/.

69. Werdell, P. J. & Bailey, S. W. An improved in-situ bio-optical data set for ocean color algorithm development and satellite data product validation. *Remote Sens. Environ.* **98**, 122–140 (2005).

70. Tomlinson, M. C., Stumpf, R. P. & Vogel, R. L. Approximation of diffuse attenuation, K_d, for MODIS high-resolution bands. *Remote Sens. Lett.* **10**, 178–185 (2019).

71. López, R., López, J. M., Morell, J., Corredor, J. E. & Del Castillo, C. E. Influence of the Orinoco River on the primary production of eastern Caribbean surface waters. *J. Geophys. Res. Ocean.* **118**, 4617–4632 (2013).

72. Freitas, L. M., Oliveira, M. de D. M., Leão, Z. M. A. N. & Kikuchi, R. K. P. Effects of turbidity and depth on the bioconstruction of the Abrolhos reefs. *Coral Reefs* **38**, 241–253 (2019).

73. Martínez-Castillo, V., Paola Rodríguez-Troncoso, A., Reyes-Bonilla, H., Aguilar-Cruz, C. A. & Rangel-Dávalos, C. Reproduction of the endangered endemic saffron coral to the Gulf of California Porites sverdrupi (Anthozoa: Scleractinia): implications for its long-term maintenance. *Helgol. Mar. Res.* **74**, (2020).

74. García-Sais, J. R., Williams, S. M. & Amirrezvani, A. Mortality, recovery, and community shifts of scleractinian corals in Puerto Rico one decade after the 2005 regional bleaching event. *PeerJ* **2017**, e3611 (2017).

75. Vega Sequeda, J. C., Zea, S. & Bernal, G. Efectos De Eventos Oceánicos Extremos En Formaciones Coralinas De Islas Del Rosario, Caribe Colombiano. *CICIMAR Oceánides* **32**, 25 (2017).

76. NASA Global Modeling and Assimilation Office. MERRA-2. https://gmao.gsfc.nasa.gov/reanalysis/MERRA-2/.

77. R Core Team. R: A language and environment for statistical computing. *R Foundation for Statistical Computing* https://www.r-project.org/ (2020).

78. Amandala Newspaper. Record-breaking 2020 Hurricane Season ends today.

https://amandala.com.bz/news/record-breaking-2020-hurricane-season-ends-today/ (2020).

79. De´ath, G. & Fabricius, K. Water quality as a regional driver of coral biodiversity and macroalgae on the Great Barrier Reef. *Ecol. Appl.* **20**, 840–850 (2010).

80. Zhang, C. *et al.* Impact of air emissions from shipping on marine phytoplankton growth. *Sci. Total Environ.* **769**, 145488 (2021).

81. Mishra, D. R. *et al.* Decline in Phytoplankton Biomass along Indian Coastal Waters due to COVID-19 Lockdown. *Remote Sens.* **12**, 2584 (2020).

82. Coastal Zone Management Authority and Institute (CZMAI). Belize Integrated Coastal Zone Management Plan: The Vision for our Coast (ICZMP). *Minsitry Agric. For. Fish. Environ. Sustain. Dev.* 265 (2016).

83. Aronson, R. B., Precht, W. F., Macintyre, I. G. & Murdoch, T. J. T. Coral bleach-out in Belize. *Nature* **405**, 36 (2000).

84. Haines, S. Managing expectations: articulating expertise in climate services for agriculture in Belize. *Clim. Change* **157**, 43–59 (2019).

85. Maidens, J. & Burke, L. Belize Coastal Threat Atlas. *World Resour. Inst.* 20 (2005).

86. Macintyre, I. G., Toscano, M. A., Feller, I. C. & Faust, M. A. Decimating Mangrove Forests for Commercial Development in the Pelican Cays, Belize: Long-Term Ecological Loss for Short-Term Gain? *Smithson. Contrib. Mar. Sci.* 281–290 (2009).

87. Emrich, K., Martinez-Colon, M. & Alegria, H. Is untreated sewage impacting coral reefs of Caye Caulker, Belize? *J. Foraminifer. Res.* **47**, 20–33 (2017).

88. Wells, C. E. *et al.* Wastewater technopolitics on the southern coast of Belize. *Econ. Anthropol.* **6**, 277–290 (2019).

89. Soto, I. *et al.* Physical connectivity in the Mesoamerican Barrier Reef System inferred from 9 years of ocean color observations. *Coral Reefs* **28**, 415–425 (2009).

90. Torregroza-Espinosa, A. C., Restrepo, J. C., Escobar, J., Pierini, J. & Newton, A. Spatial and temporal variability of temperature, salinity and chlorophyll-a in the Magdalena River mouth, Caribbean Sea. *J. South Am. Earth Sci.* **105**, 102978 (2021).

91. Espinoza-Avalos, J., Islebe, G. A. & Hernandez-Arana, H. A. *El sistema ecológico de la bahía de Chetumal / Corozal: costa occidental del Mar Caribe*. (ECOSUR, 2009).

92. Reyes, T. *et al.* Five Years in Bacalar Chico Marine Reserve : an evaluation of reef health and reserve effectiveness between. **44**, 105 (2019).

93. Martínez, M. L. *et al.* The coasts of our world: Ecological, economic and social importance. *Ecol. Econ.* **63**, 254–272 (2007).

94. Glavovic, B. C. Coasts. in *International Encyclopedia of Geography: People, the Earth, Environment and Technology* 1–25 (John Wiley & Sons, Ltd, 2017). doi:10.1002/9781118786352.wbieg0817.

95. Elliott, M. *et al.* A Synthesis: What Is the Future for Coasts, Estuaries, Deltas and Other

Transitional Habitats in 2050 and Beyond? in *Coasts and Estuaries: The Future* 1–28 (Elsevier, 2019). doi:10.1016/B978-0-12-814003-1.00001-0.

96. United Nations. Goal 14 - Conserve and sustainably use the oceans, seas and marine resources for sustainable development. https://sdgs.un.org/goals/goal14.

Chapter 2: A GEE Toolkit for water quality monitoring from 2002-2022 in support of SDG 14 and coral health in Marine Protected Areas in Belize

1. Introduction

Coral reefs have substantial cultural, economic, and environmental value[1–3]. These reefs provide a host of ecosystem services through tourism, biodiversity, fisheries, and coastal protection[4]. Coral reefs are estimated to have an asset value of approximately $1 trillion dollars, goods and services valued at over $375 billion dollars per year, with benefits reaching around 500 million people in at least 90 nations[5]. International efforts must continue to conserve these unique habitats, in light of climate change. The 2030 United Nations Agenda for Sustainable Development set forth 17 Sustainable Development Goals (SDGs) which include the most recent international goals for the sustainability and protection of oceans[1,6], succeeding the 2015 Millennium Development Goals. SDG 14 entitled “Life Below Water,” most closely outlines targets and indicators for the protection of coral reefs[7]. In particular, SDG indicators 14.1.1a, 14.2.1, 14.3.1, and 14.5.1 relate directly to the health of coral reefs and surrounding water, as well as coverage of marine protected areas[8]. Descriptions of these indicators can be found in **Supplementary Table 1**. In 2021, the United Nations Environment Programme (UNEP) published an updated manual on measuring various indicators of SDG 14[9]. This manual provides a comprehensive guide to implementing indicators via a subsection of monitoring parameters and methods under each indicator. However, for many parameters, such as water and habitat quality, ecosystem health, microalgal growth, and management effectiveness of protected areas, the UNEP states that these measurements should be taken when “national capacity to do so exists,” but does not provide any available data or methods on the parameter[9]. Therefore, there is a need for further research addressing feasible tactics for measuring these SDG 14 indicators on a national scale. The health of coral reefs may also affect the other 16 SDGs through direct benefits to the economy, indirect benefits to society, and general governance[10]. For example, SDG 12 entitled “Responsible Consumption and Production,” includes the consumption of ecosystem services such as tourism and fishing, which are both directly impacted by the health of coral reefs. SDG 8 entitled “Decent Work and Economic Growth” includes job incomes and economic sectors also relying on tourism and fishing. SDG 2, “Zero Hunger,” is impacted by communities that rely on fish catch, which in turn relies on coral reef health. Obura’s paper assesses the interactions between coral reefs and each SDG, determining that at least 11 of the 17 SDGs are potentially or strongly affected by coral reefs[10].

Earth observation data has been vital for assessing coral reef health and coverage[2,3,7]. Two important water quality parameters to monitor for coral reef health include sea surface temperature (SST) and turbidity[3]. SST is important to measure since anomalous warm temperatures can lead to coral bleaching, coral disease, coral death, loss of coral cover, and shifts in biodiversity[2,5,11,12]. Aqua MODIS SST imagery has been used for coral reefs monitoring[13,14]. Daily SST remote sensing products are used in nowcast prediction methods such as calculating HotSpot, Degree Heating Weeks, and ReefTemp[3]. In the literature, Degree Heating Weeks (DHW) is often used for assessing heat stress on coral. The NOAA Coral Reef Watch DHW product is widely used[11,15–17], but some studies have utilized Aqua MODIS SST to calculate DHW as well[18,19].

Water clarity or a measure of the diffuse attenuation coefficient is also important to map since corals depend on light penetration to grow[2] among other water quality parameters such as turbidity, nutrients, and sedimentation[20]. Kd(490) products are used as a proxy for water clarity[21–23]. The use of water clarity is important to use in addition to thermal stress data, especially in places such as Belize, where thermally induced bleaching events may play a lesser role compared to anthropogenic causes[15]. The Aqua MODIS Kd(490) product using the NASA operational algorithm has been used in global reefs[17,24], Brazil[13,22,25], and Colombian Caribbean[26]. DWH and Kd(490) have been used in combination for coral health[13,27].

Although literature on remote sensing applications for water quality monitoring is prevalent, there is a lack of research specifically using SST and Kd(490) to measure progress toward SDG 14 indicators. A systematic literature review of papers mentioning terms related to remote sensing, water quality monitoring, SDGs, Kd(490), and SST showed results for only six published papers (**Supplementary Table 2**). Of the six papers, only four were relevant to the criteria after closer analysis. In one of these studies, in situ samples validated Sentinel-2 MSI satellite data showing decreased water quality in Vembanad Lake, India, after the demolition of four high rise buildings on the shore of the lake[28]. This study measures sea surface temperature along with other variables such as salinity, DO, and pH. It also emphasizes that its use of lake water quality monitoring has potential to support SDGs 3, 6, 10, and 14. However, no specific indicators are mentioned and SDGs are only mentioned briefly in the paper. Additionally, this paper focuses on the involvement of the public in water monitoring rather than advancing remote sensing applications. Another study used ArcGIS 10.3.1 to map the spatial distribution of in-situ groundwater quality in Thatta, Sindh, in support of SDG 6. The study collected samples from pumps within the district that were then analyzed for parameters such as pH and turbidity[29]. Variation for each parameter was then interpolated using the "Kriging" tool to visualize water quality indicators throughout the entire district. Although this study used spatial variation to monitor groundwater, no satellite data were used, and SDGs were only mentioned briefly once. A third study targeting Vembanad Lake compared in situ water quality measurements collected from scientists with samples and observations determined by citizens through a mobile application[28].

The study suggests that the future use of community derived data could be used to validate satellite data, and emphasizes its potential for contribution to SDG indicator 6.3.2, "proportion of bodies of water with good ambient water quality." A final study proposed a framework involving geo-spatial maps created via remote sensing data and GIS techniques to compare water quality parameters in 13 districts of the Uttarakhand state in India in support of SDG 6[30]. Satellite data were applied to machine learning methods such as the random forest model in support of a water quality index. Turbidity was among the water quality parameters observed in this study, and SDG 6 was mentioned briefly as a potential use for the water quality index proposed. None of the studies in the criteria-based literature search specifically targeted monitoring of both SST and Kd(490) through satellite data in support of particular SDG 14 parameters. Therefore, further research on the use remote sensing water quality indices in support of specific SDG parameters is necessary for the expansion of accessible water quality monitoring.

Monitoring coral health through the synthesis of SST and Kd(490) data can directly address indicator 14.1.1 (a), Index of coastal eutrophication, since coral decline is often a direct result of eutrophication[31]. This index can also address indicator 14.2.1, Proportion of countries using ecosystem-based approaches to managing marine areas, as it provides an accessible way of monitoring both water quality and ecosystem health that can be applied to other water systems. Additionally, because acidification reduces the skeletal density of corals and makes them more prone to deterioration, this index could also be used to validate ocean acidification, in relation with SDG indicator 14.3.1, Average marine acidity (pH) measured at agreed suite of representative sampling station[32]. Specifically, increasing SST increases the rate of benthic respiration while lowering the ratio of productivity to respiration, therefore increasing the rate of $CaCO_3$ sediment dissolution and leading to a lower ocean pH[33]. Indicator 14.5.1, coverage of protected areas in relation to marine areas, can also be benefitted by a SST and Kd(490) index, as the remote assessment of coral health would allow less accessible and larger areas to be monitored. Therefore, this study provides an important, accessible workflow model for supplementing monitoring of water quality and coral reef habitat in support of at least four indicators of SDG 14 in data scarce areas.

In this study, we created a straightforward workflow based on Google Earth Engine (GEE), RStudio, and Aqua MODIS-derived SST, DHW, and Kd(490) from 2002 to early 2022 and applied it to Marine Protected Areas (MPAs) in Belize. Region-specific thresholds were used for both SST and Kd(490) data to indicate stress days for all MPAs. A coral vulnerability index was created based on SST and Kd(490) to indicate MPAs that have experienced both turbidity and temperature stress in the last 20 years. Statistical analysis was also performed on the warmest months in Belize and visualized as maps.

2. Data and methods

The overall workflow and accompanying code for each step is outlined in **Figure 2-1**.

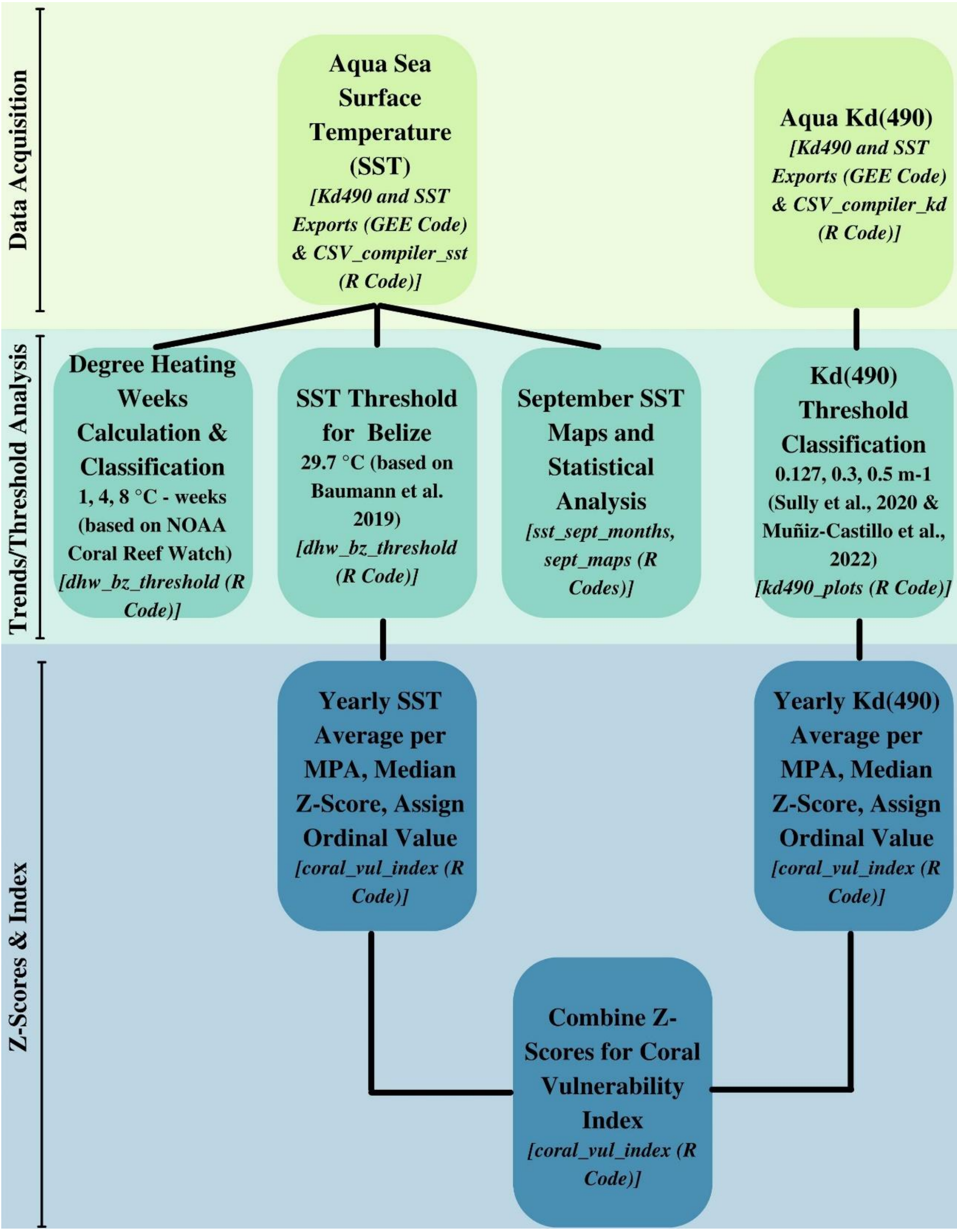

Figure 2-1. Schematic of workflow indicating data sources, processing steps, and final indices.

2.1 Study sites

Belize is a country located in Central America and home to the Belize Barrier Reef Reserve System (BBRRS). The BBRRS is the second largest barrier reef in the world and was inscribed as a UNESCO World Heritage Site in 1996[34,35]. The reef system is around 250 km in length between Mexico and Guatemala. The distance between the reefs and the mainland ranges between 0.5 and 80 km[35]. The reef system contains reef patches, faros, fringing reefs, cays, and atolls[36,37]. Marine species within the reef include fish, manatees, invertebrates, and multiple species of sea turtles[38–40]. The coral reef needs clear water and consistent temperature regimes to thrive[12,41]. Global climate change[42], pollution[41,43], mining and dredging[44], marine transportation[45], algal blooms[46], and overfishing stand to threaten the reef ecosystems of the BBRRS[47]. Recreational tourism is also seen as a threat to the reef system[48] which accounts for over 40% of the nation's GDP[49].

MPAs are managed marine environments with the purpose of conserving biodiversity[50]. MPAs in Belize were established in the early 1980s beginning with the Half Moon Caye National Monument. Later through community lobbying, more areas were added to the MPA network, such as the Hol Chan Marine Reserve in 1987[37]. Eventually an integrated approach was necessary to account for land-based pollution from outside the bounds of the MPAs that threatened the health of the reef[37]. Cox et al. (2017) showed that the MPA network alone had not been enough to promote the restoration of reefs in Belize[51]. In this study, we analyzed 24 MPAs spanning the Belizean coastal lagoon as of 2020, comprising a total area of around 5,000 km^2, as shown in **Figure 2-2**. Each MPA contains a variety of habitat designations, including fishing and spawning, general use, mangrove, marine and coral reefs, preservation, and special management, with some study areas becoming MPAs as early as 1982 and others as recently as 2020.

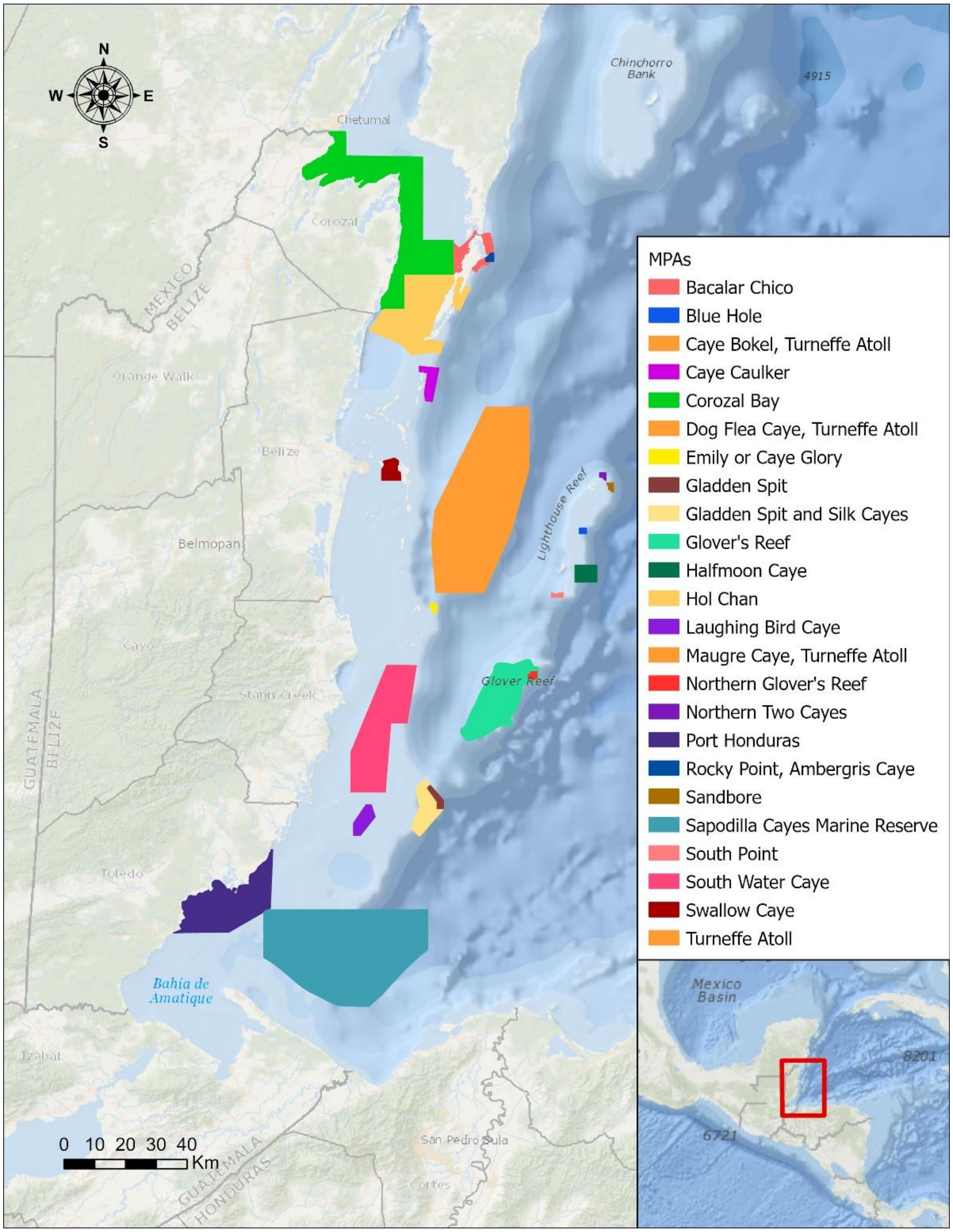

Figure 2-2. Map of Belize showing the 24 Marine Protected Areas (MPAs) created with the goal of conserving biodiversity. A variety of habitat designations are present, including fishing and spawning, general use, mangrove, marine and coral reefs, preservation, and special management.

2.2 Satellite Imagery

Images from the Moderate Resolution Imaging Spectroradiometer (MODIS) on the Aqua satellite were accessed through GEE. Images included in the study are Level-3 daily data with a 4 km resolution spanning from 4 July 2002 to 28 February 2022. These images were used to calculate water clarity and sea surface temperature (SST), a combination of water quality parameters used to assess coral health[13].

The average vertical diffuse attenuation coefficient for downwelling irradiance at 490 nm, Kd(490), was used as a proxy for water clarity. The NASA operational algorithm was used to calculate Kd(490)[52], as we used in our previous study of water clarity in Belizean coastal waters[45]. This Kd(490) product has been used for coral health in Brazil[13,22,25], for an analysis of global corals[24], and corals in the Colombian Caribbean[26].

Daily SST averages for each MPA were calculated using Aqua MODIS imagery. The MODIS SST product is commonly used to assess temperature stress on corals and impacts of SST anomalies. In addition, degree heating weeks (DHW) were calculated for all MPAs using the Aqua MODIS SST images. DHW is a common unit of measure to understand long-term thermal stress on corals[12,15,16]. DHW calculates accumulated thermal stress over a 12-week (84 days) period. Units are in °C—weeks, where 1°C—weeks is a week of SST over the maximum monthly mean. Instead of using a maximum monthly mean, a region specific threshold for coral bleaching in Belize (29.7°C) was used instead[15,53]. The region specific threshold was originally calculated for Channel Cay based on a 15 years record of NOAA/NASA AVHRR (Advanced Very High Resolution Radiometer) Oceans Pathfinder data[53]. Using this method, the DHW for a day is calculated over the 12-week running window including that day. The difference between the daily SST and Belizean threshold was calculated and retained for summation whenever the difference was greater or equal to 1°C, where it was then multiplied by 1/7 for the units to be in weeks. The factor of 1/7 is necessary since the development of coral bleaching occurs in the order of weeks[54].

DHW was calculated using the dbcaDHW package (https://github.com/dbca-wa/dbcaDHW/) in RStudio through the following formula:

$$DHW_i = \sum_{n=i-83}^{i} \left(\frac{SST_n - 29.7°C}{7}\right), where\ (SST_n - 29.7°C) \geq 1°C$$

2.3 Water clarity and sea surface temperature stress classifications

A literature review on Kd(490) thresholds and SST was conducted to find appropriate stress limits for corals in Belize and the Caribbean. A global coral study found that a Kd(490) value of 0.127 m^{-1} is too turbid for coral growth from performing a nonlinear least squares regression on the turbidity gradient within the inner Great Barrier Reef[24]. For Kd(490), "turbid" months were classified based on a coral reef diversity study[27] in the Mesoamerican Reef at 0.30 m^{-1}. Very turbid water was defined as Kd(490) values above 0.50 m^{-1} based on a Caribbean study that used this value to indicate Kd(490) anomalies[55]. The following was used for Kd(490) value classifications: 0–0.127 m^{-1} "Little/No Stress," 0.127–0.3 m^{-1} "Turbidity Stress," 0.3–0.5 m^{-1} "Turbid Month," 0.5 m^{-1}+ "Very Turbid." The following are the DHW classifications: 0–1°C—weeks "Little/No Stress," 1–4°C—weeks "Temperature stress," 4–8°C—weeks "Bleaching Risk," 8°C—weeks + "Mortality Risk." Stress days are calculated as days where SST is greater than 29.7°C and Kd(490) is greater than 0.127 m^{-1}.

2.4 Coral vulnerability index

Indices are often created in order to assess coral health[56,57] as well as overall habitat protection[58]. Z-scores have also been used previously to normalize data for corals[59,60]. Here the SST and Kd(490) data were normalized and combined to create a coral vulnerability index which was calculated for each MPA[60,61]. First, the z-score for each parameter was calculated for all MPAs through the following formula:

$$z = \frac{(x - \mu)}{\sigma}$$

Here x is the mean per MPA per year, μ is the mean across all MPAs per year, and σ is the standard deviation across all MPAs per year. The median z-score was calculated for each MPA from all years. The median z-scores were then assigned an ordinal value from 1 to 6 based on the general distribution of parameters[61]. The two variables were assumed to have equal weight and were added for each MPA in order to compute the coral vulnerability index from 2 to 12, where higher values indicate a higher vulnerability due to high SST and Kd(490). The following are the assigned values for the corresponding median z-score range: $z > 0.4$ to “6,” $z = 0.2–0.4$ to “5,” $z = 0–0.2$ to “4,” $z = −0.2–0$ to “3,” $z = −0.4$ to $−0.2$ to “2,” and $z < −0.4$ to “1.”

2.5 Statistical analysis

All subsequent visualization and calculations were performed in RStudio[62]. To account for dependence between SST temperature values, or how dependent each day’s SST was on the SST of the prior day, the lme4 package was used in R to fit the September SST dataset into a linear mixed effect model[63]. Linear fixed effect models can be favorable over linear regression in downscaling climate variables[64], and have been successfully used by other studies analyzing climate trends such as warming sea temperatures[65], decreasing sea ice cover[66], and declining carbon sinks in the Amazon[67].

3. Results

DHW was categorized based on the potential for accumulated temperature stress to impact corals. **Figure 2-3A** depicts SST and DHW where they were both plotted from 2002 to 2022 for select MPAs. Ten MPAs had most of their DHW measurements in the “Little/No Stress” category and occasionally have incidence with more severe risk. Around one-third of the MPAs had incidences of DHW values in the “Bleaching Risk” category and the remaining one-fourth had

DHW values in the “Mortality Risk” classification. Port Honduras had the highest incidences of DHW values in the “Mortality Risk” category at 10% of all calculable DHW. In almost all MPAs, an increase in severity in DHW is found following 2016. For SST, seasonality is visible with September being the warmest month across all MPAs (**Supplementary Figure 1**). Higher SSTs are particularly shown in 2008, 2017, and 2020 (**Figure 2-4**). Box plots and linear regression of the September SSTs show increases with time (**Supplementary Figure 2**).

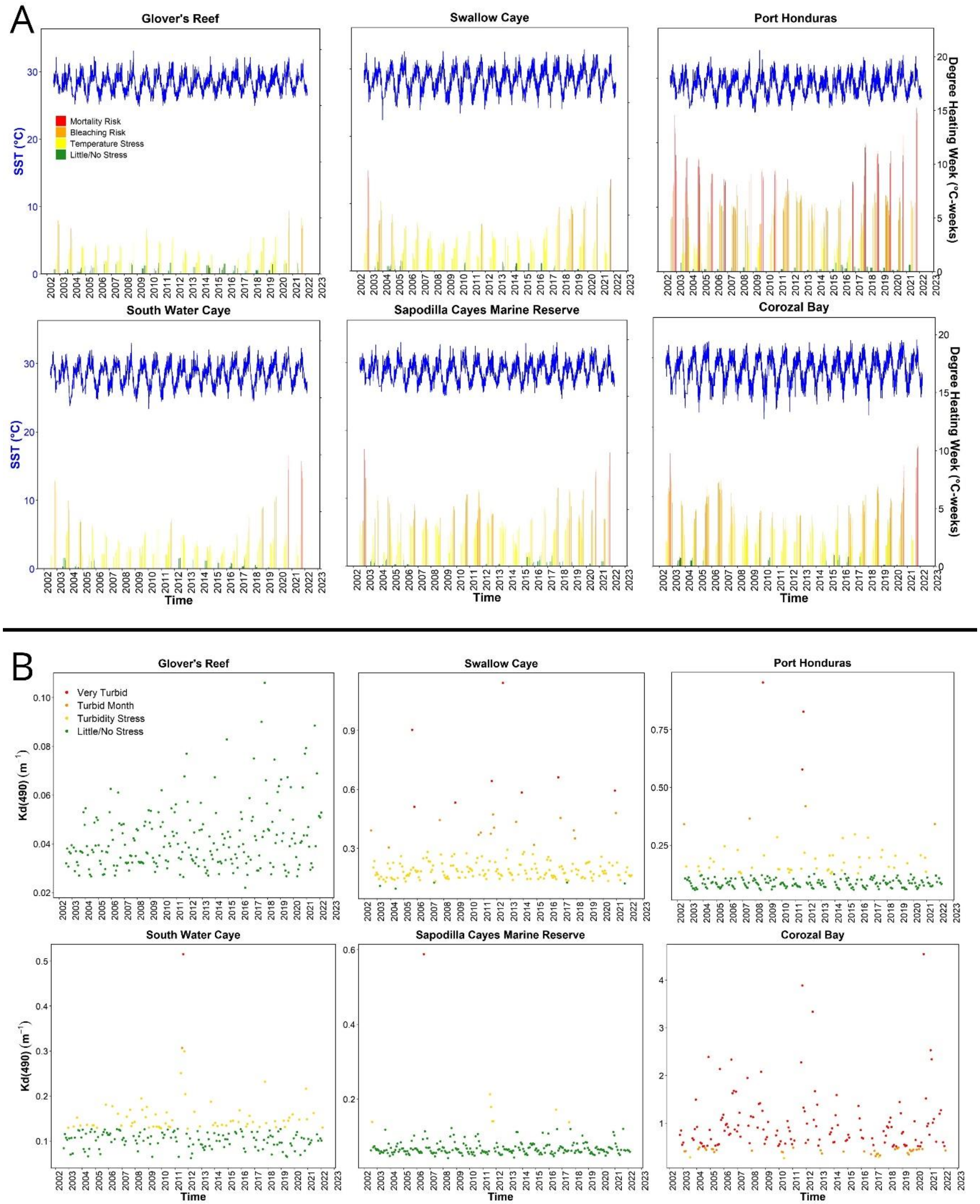

Figure 2-3. Sea surface temperature, degree heating weeks, and Kd(490) for select MPAs from 2002 to 2022. (A) Depicts SST and DHW weeks for six marine protected areas (Glover's Reef, Swallow Caye, Port Honduras, South Water Caye, Sapodilla Cayes Marine Reserve, and Corozal Bay). (B) Shows Kd(490) values for the same MPAs from 2002 to 2022.

Similarly to DHW, Kd(490) values were categorized based on thresholds and plotted as shown in **Supplementary Figure 3** for all MPAs. Select plots of MPAs are in **Figure 2-3B**. In general, most MPA did not have water clarity stress, and few had consistently high values. Corozal Bay displays significantly higher Kd(490) values compared to all MPAs with most of their classifications as "Very Turbid" for the Caribbean region. Swallow Caye also had most of the Kd(490) values within the "Turbidity Stress" classification or higher and only a handful of days where average Kd(490) would have little stress on corals. Port Honduras and South Water Caye both display seasonal trends with their Kd(490) values where higher classifications of stress occur during Belize's wet season. Other MPAs such as Laughing Bird Caye and Sapodilla Cayes Marine Reserve display seasonal trends in Kd(490) values, but all within the "Little/No Stress" category.

Using a z-score approach, sites were characterized for heat, turbidity, and a coral vulnerability index combining the two. **Supplementary Table 3** lists the median z-scores and indices for SST and Kd(490) separately and the combined coral vulnerability index. Port Honduras and Sapodilla Cayes Marine Reserve have the highest SST index values while Swallow Caye and Corozal Bay have the highest Kd(490) index values. When the variables are combined for the overall index, Port Honduras is the most vulnerable, followed by Swallow Caye and Sapodilla Cayes Marine Reserve. Swallow Caye, Corozal Bay, Port Honduras, and South Water Caye had higher Kd(490) indices. Port Honduras, Sapodilla Cayes Marine Reserve, Glover's Reef, Laughing Bird Caye, Hol Chan, Gladden Spit, and Gladden Spit and Silk Cayes had higher SST indices.

In accord with a linear fixed effect model (see Section 2.5), all 24 MPAs were assigned as random effects while year was assigned as a fixed effect in order to assess the temporal and regional effects on SST changes. Results depicted in **Supplementary Tables 4, 5** show a highly significant SST increase over time ($p < 0.0001$) for the month of September and all data.

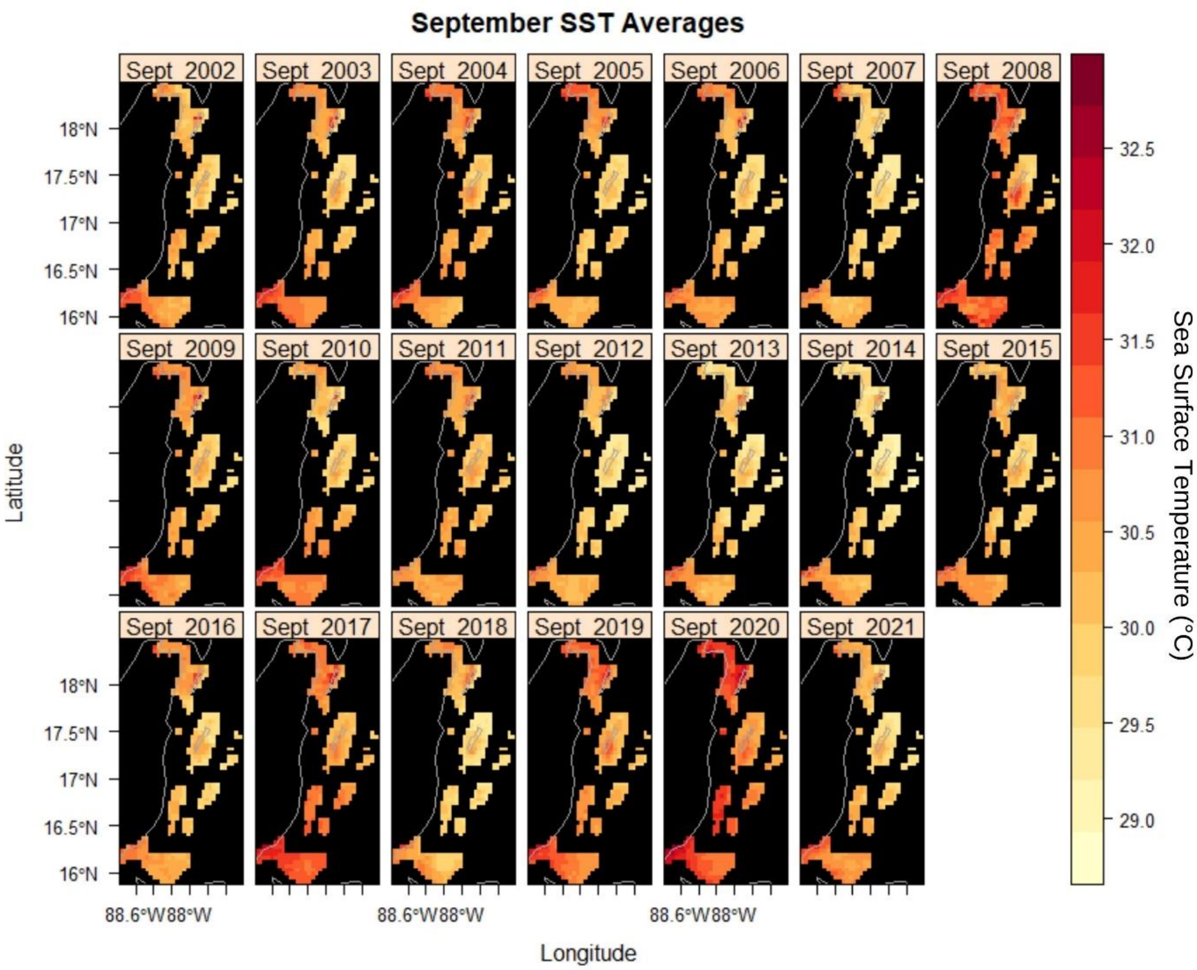

Figure 2-4. Maps show mean sea surface temperature for the month of September (hottest month) in Marine Protected Areas of Belize from 2002 to 2022.

4. Discussion

There are international efforts being made toward the protection and conservation of coral reefs, including the "Life Below Water" goal outlined in UN SDG 14. As a result, scientists have created indices and use remote sensing to monitor environmental stressors impacting coral health. The accessible GEE toolkit presented in this work was applied to identify locations at risk for coral decline in Belize as a proof of concept for its use more broadly. Several locations in the region are shown to have multiple stressors for corals, as has been observed previously at other locations. In 2008, a coral susceptibility model was created using environmental stressors including SST, chlorophyll-a, solar radiation, and other parameters for corals in the western Indian Ocean[68]. In this study, the north-western regions of the study area had high vulnerability which may be due to high SST and photosynthetically active radiation, where high solar irradiance at the surface indicates potential for heating and photochemical damage. A remote sensing coral stress index was created for corals in Saudi Arabia using the Quickbird satellite, environmental stressors, and water depth[69]. The areas with higher coral stress index values were areas that were near large towns and cities with fishing pressure accounting for the majority of variation. Most recently, a Google Earth Engine based tool used a combination of stressors and reducers to find strong correlations between their stress exposure score and El Niño bleaching events for corals in the Red Sea, Chagos Archipelago, and Gilbert Islands[19]. While this tool extensively uses SST in their score along with other factors like wind, they do not include water clarity as the toolkit presented here.

Using our toolkit, we saw that nearshore MPAs such as Swallow Caye, Corozal Bay, Port Honduras, and South Water Caye had the highest z-scores based on Kd(490) alone. This is supported by previous studies that show physical connectivity as evidence through chlorophyll-a between land and the BBRRS[70], sewage plumes off Caye Caulker, Belize[41], and excess nutrients near Belize City[46]. Deviating from the typical use of thermal data for indices, Canto et al. created a light-based index for the Great Barrier Reef based on MODIS Kd data. Using a color-coded scoring system, similar to the methodology in our workflow, the study found strong correlations between "wet" years and discharge data with water clarity for inshore locations[71]. If runoff and discharge indeed play a major role in water clarity patterns nearshore, then we may expect these patterns to change in the future as the southern region of Belize is projected to experience less precipitation and runoff by 2090[42].

Arora et al. (2019) employed remotely sensed data in the calculation of coral stress indices including DHW for five major Indian coral reef regions from 1982 to 2018[72]. De et al. (2021)

successfully integrated remotely sensed SST data into a coral health monitoring program in the Eastern Arabian Sea. Large scale bleaching events resulting from the marine heatwave associated with the 2014–2016 El Niño-Southern Oscillation were indicated by bleaching indices relying on remotely sensed data and corroborated with underwater coral health surveys[16]. DHWs for this study site were 4.80, 5.09, and 6.92 for the years 2014, 2015, and 2016, respectively. These values are comparable with max DHW values for vulnerable Belizean MPAs such as Corozal Bay (3.17 in 2014 and 5.25 in 2015 and 2016) and Port Honduras (6.08 in 2014, 6.65 in 2015, and 8.34 in 2016). Baumann et al., 2019 found DHW ranged between 3.80 and 6.55 in Belize in 2015. The highest instances of Mortality and Bleaching Risk instances calculated with this workflow were greatest in 2002, 2003, 2006, 2011, 2012, and the years following 2017, which align well with years reported for having mass bleaching events in the Caribbean[15]. This shows that using Aqua MODIS-derived SST to calculate DHW is also comparable to NOAA Coral Reef Watch DHW. Future studies and uses of this workflow should verify these types of findings with coral bleaching data or El Niño-Southern Oscillation years.

The upward trend in September SST is in line with what is being observed globally due to climate change. SST has increased on average by 0.14°F each decade for the past 120 years[73]. Additional studies have shown especially high temperature increases in September, such as a paper comparing coral reef bleaching and SST over a 30 year time period in La Parguera, Puerto Rico[74]. This study demonstrated recurring severe coral bleaching in coincidence with sharp temperature rises in September, with an overall increasing trend throughout the assessed time period. SST has increased by at least 1.1°C since the pre-industrial area, and an estimated 60% of marine ecosystems have been degraded[75]. A SST increase of 1.5°C could threaten 70%–90% of coral reefs, while a 2°C increase is predicted to destroy nearly 100% of all coral reefs permanently[75].

In 1998, the government of Belize passed the Coastal Zone Management Act to mitigate issues surrounding rapid development, overfishing, and rapid population growth. The Belize Coastal Zone Management Authority and Institute (CZMAI) is the leading authority in the nation's management of coastal resources and is responsible for the development of the National Integrated Coastal Zone Management Plan (ICZMP). The goal of the ICZMP involves a set of recommended actions to ensure sustainable use of coastal resources with conservation and social and economic needs in mind[76]. The most recent plan released in 2016 developed projected scenarios for 2025 based on three approaches: conservation, informed management, and development. Since 2016, additional development activities such as dredging have occurred which may have effects on water clarity along with general climate change effects. CZMAI is currently looking to revise the 2016 ICZMP by looking at impacts of development on their coastline with specific interest on effects following the plan itself. This document is paving the way for the recently launched Marine Spatial Planning (MSP) process, renamed the Belize Sustainable Ocean Plan, which is a partnership between the Government of Belize and The Nature Conservancy. The MSP is part of a set of agreements that will enable the country's debt conversion for marine conservation and will be legally enforceable. Under this plan, biodiversity protection zones will be increased from 15.9% to 30% of Belize's open ocean[77].

Through this work, we identified Port Honduras, Swallow Caye, Sapodilla Cayes Marine Reserve, and Corozal Bay as recommended MPAs for closer monitoring. In particular, Corozal Bay showed a high level of turbidity and heat stress consistently. Swallow Caye had turbidity stress most of the time, while Port Honduras and South Water Caye showed strong seasonal trends. This GEE workflow has the potential to be used in conjunction with in situ data to continue to monitor climatic and anthropogenic changes in water quality. The flexibility and dynamic nature of the toolkit will enable governmental entities to monitor new areas, especially with the expansion of protection zones under the new MSP.

For future research, it would be beneficial to add other potential variables as indicators of coral vulnerability that could be remotely detected such as chlorophyll-a measurements and toxic heavy metals concentrations. Chlorophyll-a is a key indicator of phytoplankton biomass, which can be used to assess the eutrophic status of water bodies, or the level of nutrients enriched within the water. Some papers have had success integrating chlorophyll-a as a variable among SST and turbidity to assess coral health[78,79]. Coastal areas such as the MPAs of Belize assessed in this study are especially important for chlorophyll-a monitoring because of their vulnerable ecosystems. Toxic heavy metals are also a major threat to coral health and their existence in marine ecosystems indicates a major concern for marine life. Even at low concentrations, heavy metals released into the oceans via anthropogenic activity such as mercury, lead, and arsenic can kill corals[80]. Existent studies sample heavy metal concentrations in marine water with respect to coral health[81,82]. Therefore, with further research, it should be possible to use remote sensing techniques such as those described in these studies to also map chlorophyll-a and heavy metal concentrations as additional indicators of coral health.

Prior to the creation of this workflow, coral indices and remote sensing products used to monitor water quality are mainly on thermal variables and geared toward well-studied reef systems such as the Great Barrier Reef. The workflow outlined here draws attention to certain Belizean MPAs in terms of conservation of coral health using freely-available data on SST and water clarity in Google Earth Engine and downstream analysis in RStudio. The accessibility of the data used and ability to replicate the analysis with ready to use tools and workflows is necessary to have robust management of coastal resources and understanding of climate impacts. Users are able to adapt thresholds to their own needs, add other stressors, and change the weights of the variable in the index. This toolkit is critical in areas that lack long-term measures of water quality parameters like Belize. Aside from the integration of additional coral stress indicators, future improvements of this toolkit could include comparisons of data with *in situ* samples for further validation. Because current marine sampling data is limited in Belize, it is necessary to collect more in situ data to assess water quality indicators, especially in the significant MPAs in this paper such as Port Honduras, Swallow Caye, Sapodilla Cayes Marine Reserve, and Corozal Bay.

5. Conclusion

The monitoring of water quality is extremely important for assessing the health of coral reefs and protecting coastal and marine resources. Remote sensing is a powerful tool for monitoring thermal stress and water clarity, two very important environmental stressors for coral. The work presented here used both Aqua MODIS-derived SST and Kd(490) with imagery from 2002 to 2022 to identify seasonal and long-term patterns in 24 of Belize's MPAs. Coral stress was analyzed using two approaches, one based on previously identified thresholds for SST and Kd(490) for suitable conditions for corals, and one based on the distribution of these parameters among all sites in the study. With the use of this workflow, certain MPAs are revealed to suffer from either high SST, turbidity, or both, which was the case with Port Honduras. The hottest month in Belize is September, and an analysis of mean SST for that month over the time period of the study revealed statistically significant upward trends at all sites ($p < 0.01$). The easy accessibility and reproducibility of results for MPAs and corals in general can help other data scarce nations manage their coastal resources while striving to meet the UN SDGs. Future work should aim to involve other known environmental stressors such as chlorophyll-a as well as in situ data.

6. References

1. Kenchington, R. Science and the management of coral reefs. *Mar. Pollut. Bull.* **136**, 508–515 (2018).

2. Obura, D. O. *et al.* Coral reef monitoring, reef assessment technologies, and ecosystem-based management. *Front. Mar. Sci.* **6**, 580 (2019).

3. Mason, R. A. B., Skirving, W. J. & Dove, S. G. Integrating physiology with remote sensing to advance the prediction of coral bleaching events. *Remote Sens. Environ.* **246**, 111794 (2020).

4. Lazuardi, W., Wicaksono, P. & Marfai, M. A. Remote sensing for coral reef and seagrass cover mapping to support coastal management of small islands. *IOP Conf. Ser. Earth Environ. Sci.* **686**, 012031 (2021).

5. Hoegh-Guldberg, O., Poloczanska, E. S., Skirving, W. & Dove, S. Coral reef ecosystems under climate change and ocean acidification. *Front. Mar. Sci.* **4**, 158 (2017).

6. United Nations. THE 17 GOALS - Sustainable Development. *Sustainable Development* https://sdgs.un.org/goals (2016).

7. Hedley, J. D. *et al.* Coral reef applications of Sentinel-2: Coverage, characteristics, bathymetry and benthic mapping with comparison to Landsat 8. *Remote Sens. Environ.* **216**, 598–614 (2018).

8. United Nations. Goal 14. (2022).

9. United Nations Environment Programme. *Understanding the State of the Ocean: A Global Manual on Measuring SDG 14.1.1, SDG 14.2.1 and SDG 14.5.1.* (2021).

10. Obura, D. O. Getting to 2030 - Scaling effort to ambition through a narrative model of the SDGs. *Mar. Policy* **117**, 103973 (2020).

11. Eakin, C. M. *et al.* Caribbean Corals in Crisis: Record Thermal Stress, Bleaching, and Mortality in 2005. *PLoS One* **5**, e13969 (2010).

12. Helmuth, B. *et al.* High resolution spatiotemporal patterns of seawater temperatures across the Belize Mesoamerican Barrier Reef. *Sci. Data* **7**, 1–6 (2020).

13. de Oliveira Soares, M. *et al.* Thermal stress and tropical reefs: mass coral bleaching in a stable temperature environment? *Mar. Biodivers.* **49**, 2921–2929 (2019).

14. Putra, R. D. *et al.* Detection of reef scale thermal stress with Aqua and Terra MODIS satellite for coral bleaching phenomena. *AIP Conf. Proc.* **2094**, 020024 (2019).

15. Baumann, J. H. *et al.* Nearshore coral growth declining on the Mesoamerican Barrier Reef System. *Glob. Chang. Biol.* **25**, 3932–3945 (2019).

16. De, K. *et al.* Application of remotely sensed sea surface temperature for assessment of recurrent coral bleaching (2014-2019) impact on a marginal coral ecosystem. *Geocarto Int.* 1–22 (2021) doi:10.1080/10106049.2021.1886345.

17. Johnson, J. V., Dick, J. T. A. & Pincheira-Donoso, D. Marine protected areas do not buffer corals from bleaching under global warming. *BMC Ecol. Evol.* **22**, (2022).

18. Wouthuyzen, S., Abrar, M. & Lorwens, J. A comparison between the 2010 and 2016 El-Ninō induced coral bleaching in the Indonesian waters. *IOP Conf. Ser. Earth Environ. Sci.* **118**, 1–15 (2018).

19. Williamson, M. J. *et al.* Monitoring shallow coral reef exposure to environmental stressors using satellite earth observation: the reef environmental stress exposure toolbox (RESET). *Remote Sens. Ecol. Conserv.* (2022) doi:10.1002/RSE2.286.

20. Déath, G. & Fabricius, K. Water quality as a regional driver of coral biodiversity and macroalgae on the Great Barrier Reef. *Ecol. Appl.* **20**, 840–850 (2010).

21. Doron, M., Babin, M., Mangin, A. & Hembise, O. Estimation of light penetration, and horizontal and vertical visibility in oceanic and coastal waters from surface reflectance. *J. Geophys. Res. Ocean.* **112**, 6003 (2007).

22. Zoffoli, L. M., Kampel, M. & Frouin, R. Temporal characterization of the diffuse attenuation coefficient in Abrolhos Coral Reef Bank, Brazil. *An. XVI Simp. Bras. Sensoriamento Remoto - SBSR, Foz do Iguaçu, PR, Bras. 13 a 18 abril 2013, INPE* 6917–6922 (2013).

23. Sommer, B., Beger, M., Harrison, P. L., Babcock, R. C. & Pandolfi, J. M. Differential response to abiotic stress controls species distributions at biogeographic transition zones. *Ecography (Cop.).* **41**, 478–490 (2018).

24. Sully, S. & van Woesik, R. Turbid reefs moderate coral bleaching under climate-related temperature stress. *Glob. Chang. Biol.* **26**, 1367–1373 (2020).

25. Freitas, L. M., Oliveira, M. de D. M., Leão, Z. M. A. N. & Kikuchi, R. K. P. Effects of turbidity and depth on the bioconstruction of the Abrolhos reefs. *Coral Reefs* **38**, 241–253 (2019).

26. Vega Sequeda, J. C., Zea, S. & Bernal, G. Efectos De Eventos Oceánicos Extremos En Formaciones Coralinas De Islas Del Rosario, Caribe Colombiano. *CICIMAR Oceánides* **32**, 25 (2017).

27. Muñiz-castillo, A. I. & Mcfield, M. Additive influence of extreme events and local stressors on coral diversity in the Mesoamerican Reef during the last decade. 1–25 (2022).

28. George, G. *et al.* Citizen Scientists Contribute to Real-Time Monitoring of Lake Water Quality Using 3D Printed Mini Secchi Disks. *Front. Water* **3**, 40 (2021).

29. Solangi, G. S., Siyal, A. A., Babar, M. M. & Siyal, P. Groundwater Quality Mapping using Geographic Information System: A Case Study of District Thatta, Sindh. *Mehran Univ. Res. J. Eng. Technol.* **36**, 1059–1072 (2017).

30. Sahoo, K. *et al.* Big Data Analysis Framework for Water Quality Indicators with Assimilation of IoT and ML. *Electron. 2022, Vol. 11, Page 1927* **11**, 1927 (2022).

31. D'Angelo, C. & Wiedenmann, J. Impacts of nutrient enrichment on coral reefs: new perspectives and implications for coastal management and reef survival. *Curr. Opin. Environ.*

Sustain. **7**, 82–93 (2014).

32. Mollica, N. R. *et al.* Ocean acidification affects coral growth by reducing skeletal density. *Proc. Natl. Acad. Sci. U. S. A.* **115**, 1754–1759 (2018).

33. Trnovsky, D., Stoltenberg, L., Cyronak, T. & Eyre, B. D. Antagonistic effects of ocean acidification and rising sea surface temperature on the dissolution of coral reef carbonate sediments. *Front. Mar. Sci.* **3**, 211 (2016).

34. UNESCO. *World Heritage Committee; 20th; Convention concerning the Protection of the World Cultural and Natural Heritage; report; 1997*. (1996).

35. Claudino-Sales, V. Belize Barrier Reef System, Belize. in *Coastal Research Library* vol. 28 451–456 (Springer, 2019).

36. Perkins, J. S. & Carr, A. The Belize Barrier Reef: Status and prospects for conservation management. *Biol. Conserv.* **31**, 291–301 (1985).

37. Cho, L. Marine protected areas: a tool for integrated coastal management in Belize. *Ocean Coast. Manag.* **48**, 932–947 (2005).

38. Morales-Vela, B., Olivera-Gómez, D., Reynolds, J. E. & Rathbun, G. B. Distribution and habitat use by manatees (Trichechus manatus manatus) in Belize and Chetumal Bay, Mexico. *Biol. Conserv.* **95**, 67–75 (2000).

39. Almada-Villela, P., McField, M., Kramer, P. A., Richards, P. & Arias-Gonzalez, E. Status of Coral Reefs of Mesoamerica – Mexico, Belize, Guatemala, Honduras, Nicaragua and El Salvador. *Status Coral Reefs World 2002* 303–324 (2002).

40. Verutes, G. M. *et al.* Integrated planning that safeguards ecosystems and balances multiple objectives in coastal Belize. *Int. J. Biodivers. Sci. Ecosyst. Serv. Manag.* **13**, 1–17 (2017).

41. Emrich, K., Martinez-Colon, M. & Alegria, H. Is untreated sewage impacting coral reefs of Caye Caulker, Belize? *J. Foraminifer. Res.* **47**, 20–33 (2017).

42. Martín-Arias, V. *et al.* Modeled Impacts of LULC and Climate Change Predictions on the Hydrologic Regime in Belize. *Front. Environ. Sci.* **10**, 1–16 (2022).

43. Blanke, J. M., Steinberg, M. K. & Donlevy, J. P. A baseline analysis of marine debris on southern islands of Belize. *Mar. Pollut. Bull.* **172**, 112916 (2021).

44. Maidens, J. & Burke, L. Belize Coastal Threat Atlas. *World Resour. Inst.* 20 (2005).

45. Callejas, I. A. *et al.* Effect of COVID-19 Anthropause on Water Clarity in the Belize Coastal Lagoon. *Front. Mar. Sci.* **8**, 490 (2021).

46. Lapointe, B. E., Tewfik, A. & Phillips, M. Macroalgae reveal nitrogen enrichment and elevated N:P ratios on the Belize Barrier Reef. *Mar. Pollut. Bull.* **171**, 112686 (2021).

47. Gibson, J., McField, M. & Wells, S. Coral reef management in Belize: An approach through integrated coastal zone management. *Ocean Coast. Manag.* **39**, 229–244 (1998).

48. Diedrich, A. The impacts of tourism on coral reef conservation awareness and support in

coastal communities in Belize. *Coral Reefs* **26**, 985–996 (2007).

49. Cheng, J., Zetina, Z., Cheng, J. & Zetina, Z. A Study to Investigate the Impact of the COVID-19 Pandemic on Tourist Arrivals in Belize. *Open J. Soc. Sci.* **9**, 326–334 (2021).

50. Edgar, G. J., Russ, G. R. & Babcock, R. C. *Chapter 19 Marine protected areas*. *Marine Ecology* (2007).

51. Cox, C., Valdivia, A., McField, M., Castillo, K. & Bruno, J. F. Establishment of marine protected areas alone does not restore coral reef communities in Belize. *Mar. Ecol. Prog. Ser.* **563**, 65–79 (2017).

52. Werdell, P. J. & Bailey, S. W. An improved in-situ bio-optical data set for ocean color algorithm development and satellite data product validation. *Remote Sens. Environ.* **98**, 122–140 (2005).

53. Aronson, R. B., Precht, W. F., Toscano, M. A. & Koltes, K. H. The 1998 bleaching event and its aftermath on a coral reef in Belize. *Mar. Biol. 2002 1413* **141**, 435–447 (2002).

54. NOAA. NOAA Coral Reef Watch Methodology Page. *NOAA Coral Reef Watch: Methodology* https://coralreefwatch.noaa.gov/product/5km/methodology.php#dhw (2020).

55. Chollett, I., Mumby, P. J., Müller-Karger, F. E. & Hu, C. Physical environments of the Caribbean Sea. *Limnol. Oceanogr.* **57**, 1233–1244 (2012).

56. Lasagna, R. *et al.* A new synthetic index to evaluate reef coral condition. *Ecol. Indic.* **40**, 1–9 (2014).

57. Pisapia, C., El Kateb, A., Hallock, P. & Spezzaferri, S. Assessing coral reef health in the North Ari Atoll (Maldives) using the FoRAM Index. *Mar. Micropaleontol.* **133**, 50–57 (2017).

58. Kumagai, J. A. *et al.* Habitat Protection Indexes - new monitoring measures for the conservation of coastal and marine habitats. *Sci. Data 2022 91* **9**, 1–11 (2022).

59. Fabricius, K. E. & De'ath, G. IDENTIFYING ECOLOGICAL CHANGE AND ITS CAUSES: A CASE STUDY ON CORAL REEFS. *Ecol. Appl.* **14**, 1448–1465 (2004).

60. Guest, J. R. *et al.* A framework for identifying and characterising coral reef "oases" against a backdrop of degradation. *J. Appl. Ecol.* **55**, 2865–2875 (2018).

61. Yin, Y. *et al.* DTEx: A dynamic urban thermal exposure index based on human mobility patterns. *Environ. Int.* **155**, 106573 (2021).

62. R Core Team. R: A language and environment for statistical computing. *R Foundation for Statistical Computing* https://www.r-project.org/ (2020).

63. Kuznetsova, A., Brockhoff, P. B. & Christensen, R. H. B. lmerTest Package: Tests in Linear Mixed Effects Models. *J. Stat. Softw.* **82**, 1–26 (2017).

64. Kokic, P., Crimp, S. & Howden, M. Forecasting climate variables using a mixed-effect state-space model. *Environmetrics* **22**, 409–419 (2011).

65. Fincham, J. I., Rijnsdorp, A. D. & Engelhard, G. H. Shifts in the timing of spawning in sole linked to warming sea temperatures. *J. Sea Res.* **75**, 69–76 (2013).

66. Johnston, D. W., Bowers, M. T., Friedlaender, A. S. & Lavigne, D. M. The Effects of Climate Change on Harp Seals (Pagophilus groenlandicus). *PLoS One* **7**, e29158 (2012).

67. Brienen, R. J. W. *et al.* Long-term decline of the Amazon carbon sink. *Nat. 2015 5197543* **519**, 344–348 (2015).

68. Maina, J., Venus, V., McClanahan, T. R. & Ateweberhan, M. Modelling susceptibility of coral reefs to environmental stress using remote sensing data and GIS models. *Ecol. Modell.* **212**, 180–199 (2008).

69. Rowlands, G. *et al.* Satellite imaging coral reef resilience at regional scale. A case-study from Saudi Arabia. *Mar. Pollut. Bull.* **64**, 1222–1237 (2012).

70. Soto, I. *et al.* Physical connectivity in the Mesoamerican Barrier Reef System inferred from 9 years of ocean color observations. *Coral Reefs* **28**, 415–425 (2009).

71. Canto, M. M. *et al.* A benthic light index of water quality in the Great Barrier Reef, Australia. *Mar. Pollut. Bull.* **169**, 112539 (2021).

72. Arora, M., Gujrati, A., Chaudhury, N. R., Chauhan, P. & Patel, R. C. Assessment of coral reef thermal stress over India based on remotely sensed sea surface temperature. *https://doi.org/10.1080/10106049.2019.1624983* **36**, 740–757 (2019).

73. EPA. Climate Change Indicators: Sea Surface Temperature | US EPA. *United States Environmental Protection Agency* https://www.epa.gov/climate-indicators/climate-change-indicators-sea-surface-temperature (2021).

74. Winter, A., Appeldoorn, R. S., Bruckner, A., Williams, E. H. & Goenaga, C. Sea surface temperatures and coral reef bleaching off La Parguera, Puerto Rico (northeastern Caribbean Sea). *Coral Reefs 1998 174* **17**, 377–382 (1998).

75. United Nations. *How is climate change impacting the world's ocean*. https://www.un.org/en/climatechange/science/climate-issues/ocean-impacts.

76. Coastal Zone Management Authority and Institute (CZMAI). Belize Integrated Coastal Zone Management Plan: The Vision for our Coast (ICZMP). *Minsitry Agric. For. Fish. Environ. Sustain. Dev.* 265 (2016).

77. Government of Belize Press Office. PRESS RELEASE: Official Launch of Belize's Marine Spatial Planning Process. (2022).

78. Otero, E. & Carbery, K. K. Chlorophyll a and turbidity patterns over coral reefs systems of La Parguera Natural Reserve,Puerto Rico. *Rev. Biol. Trop.* **53**, 25–32 (2005).

79. Ennis, R. S., Brandt, M. E., Wilson Grimes, K. R. & Smith, T. B. Coral reef health response to chronic and acute changes in water quality in St. Thomas, United States Virgin Islands. *Mar. Pollut. Bull.* **111**, 418–427 (2016).

80. Goodchild van Hilten, L. How copying coral could help remove toxins from the ocean. *Elsevier Connect* https://www.elsevier.com/connect/archive/how-copying-coral-could-help-remove-toxins-from-the-ocean (2015).

81. Sabdono, A. Heavy Metal Levels and Their Potential Toxic Effect on Coral Galaxea

fascicularis from Java Sea, Indonesia. *Res. J. Environ. Sci.* **3**, 96–102 (2009).

82. Berry, K. L. E. *et al.* Sources and spatial distribution of heavy metals in scleractinian coral tissues and sediments from the Bocas del Toro Archipelago, Panama. *Environ. Monit. Assess.* **185**, 9089 (2013).

7. Supplementary Materials

Supplementary Table 1: SDG 14 indicators relevant to this study, as documented by the United Nations. (Dep. of Eco. & Soc. Affairs)

Goal	Indicator
14.1 By 2025, prevent and significantly reduce marine pollution of all kinds, in particular from land-based activities, including marine debris and nutrient pollution.	14.1.1 (a) Index of coastal eutrophication
14.2 By 2020, sustainably manage and protect marine and coastal ecosystems to avoid significant adverse impacts, including by strengthening their resilience, and take action for their restoration in order to achieve healthy and productive oceans	14.2.1 Number of countries using ecosystem-based approaches to managing marine areas
14.3 Number of countries using ecosystem-based approaches to managing marine areas	14.3.1 Average marine acidity (pH) measured at agreed suite of representative sampling stations
14.5 By 2020, conserve at least 10 percent of coastal and marine areas, consistent with national and international law and based on the best available scientific information	14.5.1 Coverage of protected areas in relation to marine areas

Supplementary Table 2. Results of the criteria literature review search via Web of Science, last updated on July 26, 2022. Search criteria were applied to all fields for maximum range of papers.

Search Criteria	**# of results for all fields**
• remote sensing OR satellite OR Earth Observation OR EO OR Google Earth Engine OR GEE • water quality OR coastal OR recreational water OR marine OR coral OR corals • monitoring OR sampling OR measurement OR measuring	41,718
+	
• sustainable development goals OR sustainable development goal OR SDGs OR SDG	139
+	
• turbidity OR Kd490 OR SST OR sea surface temperature	6

Supplementary Table 3. Median z-scores and indices for SST, Kd(490), and a combination of both SST and Kd(490) in the coral index.

MPA	Median Z-Score (Kd(490))	Median Z-Score (SST)	SST Index	Kd(490) Index	Coral Index
Port Honduras	0.139	0.437	6	4	10
Swallow Caye	0.658	-0.158	3	6	9
Sapodilla Cayes Marine Reserve	-0.090	0.293	5	3	8
Corozal Bay	4.076	-0.491	1	6	7
Gladden Spit	-0.167	0.071	4	3	7
Gladden Spit and Silk Cayes	-0.074	0.098	4	3	7
Hol Chan	-0.132	0.046	4	3	7
Laughing Bird Caye	-0.064	0.143	4	3	7
South Water Caye	0.178	-0.015	3	4	7
Blue Hole	-0.097	-0.158	3	3	6
Glover's Reef	-0.234	0.060	4	2	6
Bacalar Chico	-0.259	-0.111	3	2	5
Caye Bokel Turneffe Atoll	-0.257	-0.044	3	2	5
Caye Caulker	-0.241	-0.026	3	2	5
Dog Flea Caye Turneffe Atoll	-0.268	-0.079	3	2	5
Emily or Caye Glory	-0.234	-0.037	3	2	5
Halfmoon Caye	-0.270	-0.115	3	2	5
Maugre Caye Turneffe Atoll	-0.256	-0.125	3	2	5
Northern Glover's Reef	-0.237	-0.067	3	2	5
Rocky Point Ambergris Caye	-0.269	-0.101	3	2	5
Sandbore	-0.270	-0.164	3	2	5
South Point	-0.262	-0.072	3	2	5
Turneffe Atoll	-0.257	-0.100	3	2	5
Northern Two Cayes	-0.267	-0.208	2	2	4

Supplementary Table 4: Results of the fixed linear effect model on September SST data assessed via the lme4 package in R. df refers to the degrees of freedom based on Satterthwaite's approximation, and Pr(>|t|) refers to the p value for the t test. The resulting p-value shows that time is highly significant in determining sea surface temperature.

Random Effects (MPAs)	**Variance**	**Std. Dev**			
Intercept	0.119	0.3449			
Residual	0.5552	0.7451			
Fixed Effect (Year)	**Estimate**	**St. Error**	**df**	**t value**	**Pr(>|t|)**
Intercept	3.00E+01	7.25E-02	2.50E+01	413.474	< 2e-16
Slope	1.07E-02	1.52E-03	6.91E+03	7.051	1.95E-12
Correlation of Fixed Effect:					
Year	-0.2				

Supplementary Table 5: Same as **Table S5** but for the full SST dataset.

Random Effects (MPAs)	**Variance**	**Std. Dev**			
Intercept	**0.06302**	**0.251**			
Residual	**1.89565**	**1.377**			
Fixed Effect (Year)	**Estimate**	**St. Error**	**df**	**t value**	**Pr(>|t|)**
Intercept	**2.81E+01**	**5.21E-02**	**2.42E+01**	**539.17**	**< 2e-16**
Slope	**1.31E-02**	**8.21E-04**	**8.89E+04**	**15.92**	**< 2e-16**
Correlation of Fixed Effect:					
Year	**-0.156**				

Supplementary Table 6. Total stress days divided by total observed days by MPA as a percentage. Only MPAs with one or more stress days are included in the table. Northern Glover's Reef had one stress day and therefore the ratio of stress days to total days was insignificant and rounded to 0.00 for all months.

Total Stress Days/Total Observed Days by Region (2002-2022)

MPA	All Days	April	May	June	July	Aug	Sep	Oct	Nov
Blue Hole	1.35	0.00	15.79	20.00	14.29	5.26	0.00	0.00	0.00
Corozal	17.83	0.00	5.88	15.38	95.00	96.97	92.73	41.90	3.89
Gladden Spit	0.43	0.00	2.22	6.85	0.00	0.00	0.00	0.00	0.00
Gladden Spit and Silk Cayes	1.08	6.59	5.13	5.48	0.00	0.00	0.00	0.00	0.00
Glover's Reef	0.26	0.00	0.00	5.45	0.00	0.00	0.00	0.00	0.00
Halfmoon Caye	0.08	0.00	1.22	0.00	0.00	0.00	0.00	0.00	0.00
Hol Chan	2.22	2.27	16.67	9.52	0.00	0.00	0.00	0.00	0.00
Laughing Bird Caye	0.62	4.55	2.67	5.41	0.00	0.00	0.00	0.00	0.00
Northern Glover's Reef	0.00	0.00	0.00	0.00	0.00	0.00	0.00	0.00	0.00
Port Honduras	12.93	0.00	0.00	0.00	43.42	43.86	40.41	29.19	8.67
Sapodilla Cayes Marine Reserve	2.40	5.49	8.05	10.64	1.41	2.75	6.29	2.76	0.64
South Water Caye	12.05	0.00	0.00	0.00	38.89	38.46	45.90	22.86	1.10
Swallow Caye	19.66	0.00	0.00	0.00	36.36	82.61	90.00	47.37	7.78

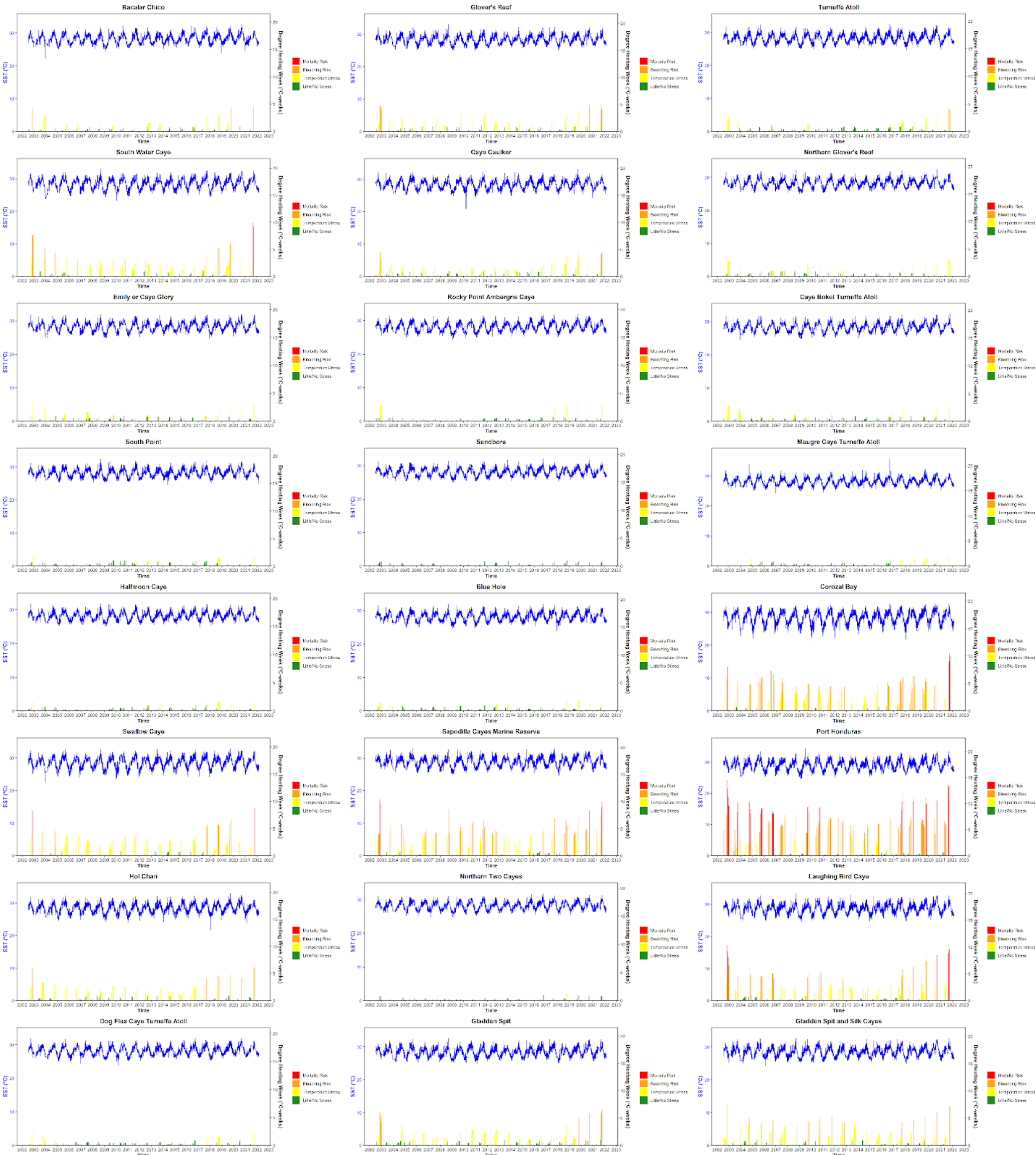

Supplementary Figure 1: SST and DHW plotted from 2002-2022 for all MPAs. The blue lines represent SST values, while the bars represent DHW. Red bars indicate mortality risk, orange bars indicate bleaching risk, yellow bars represent temperature stress, and green bars represent little or no stress.

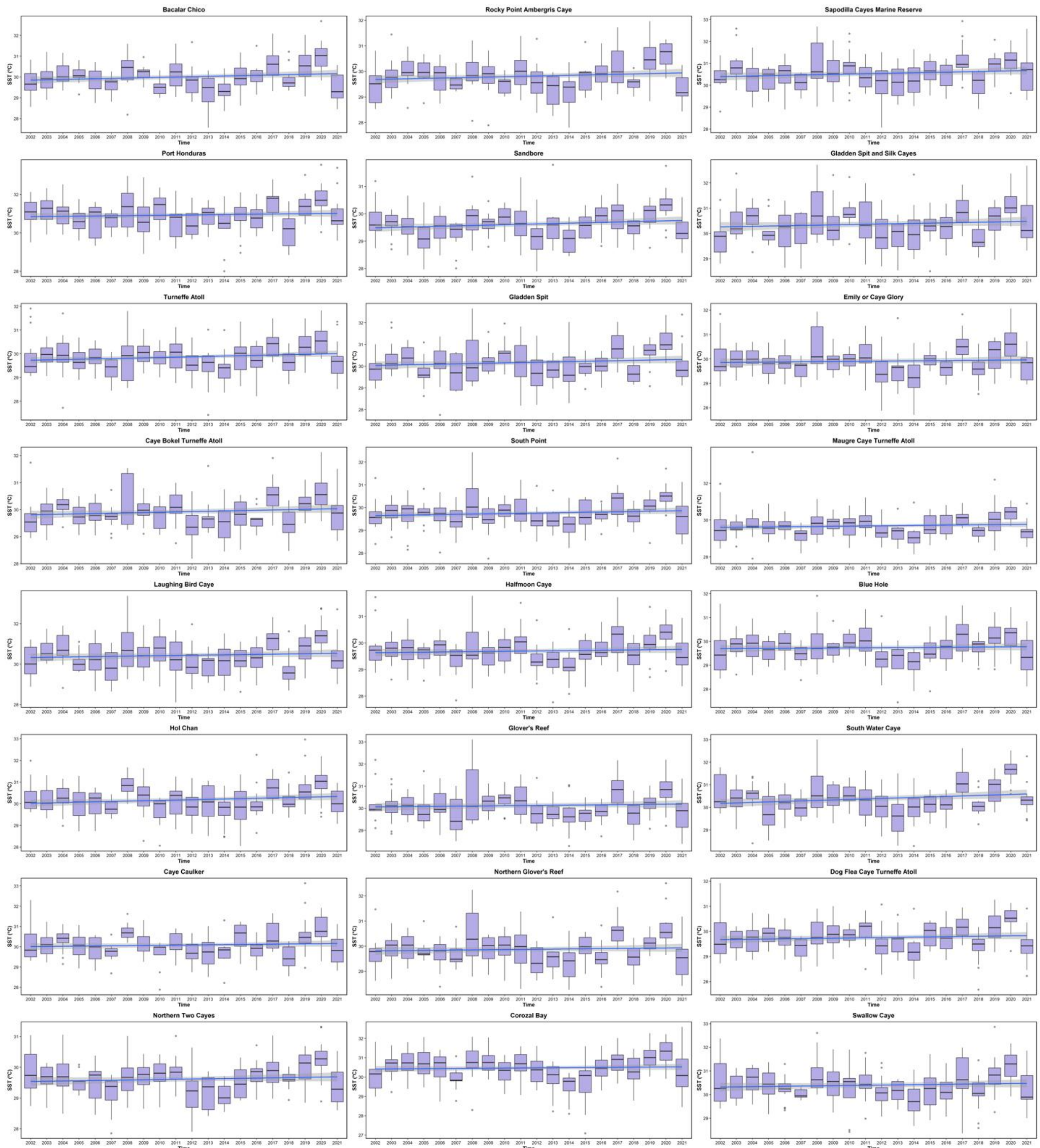

Supplementary Figure 2: September SST values for all MPAs from 2002-2022. Blue lines are the linear regression lines using the "lm" method in RStudio.

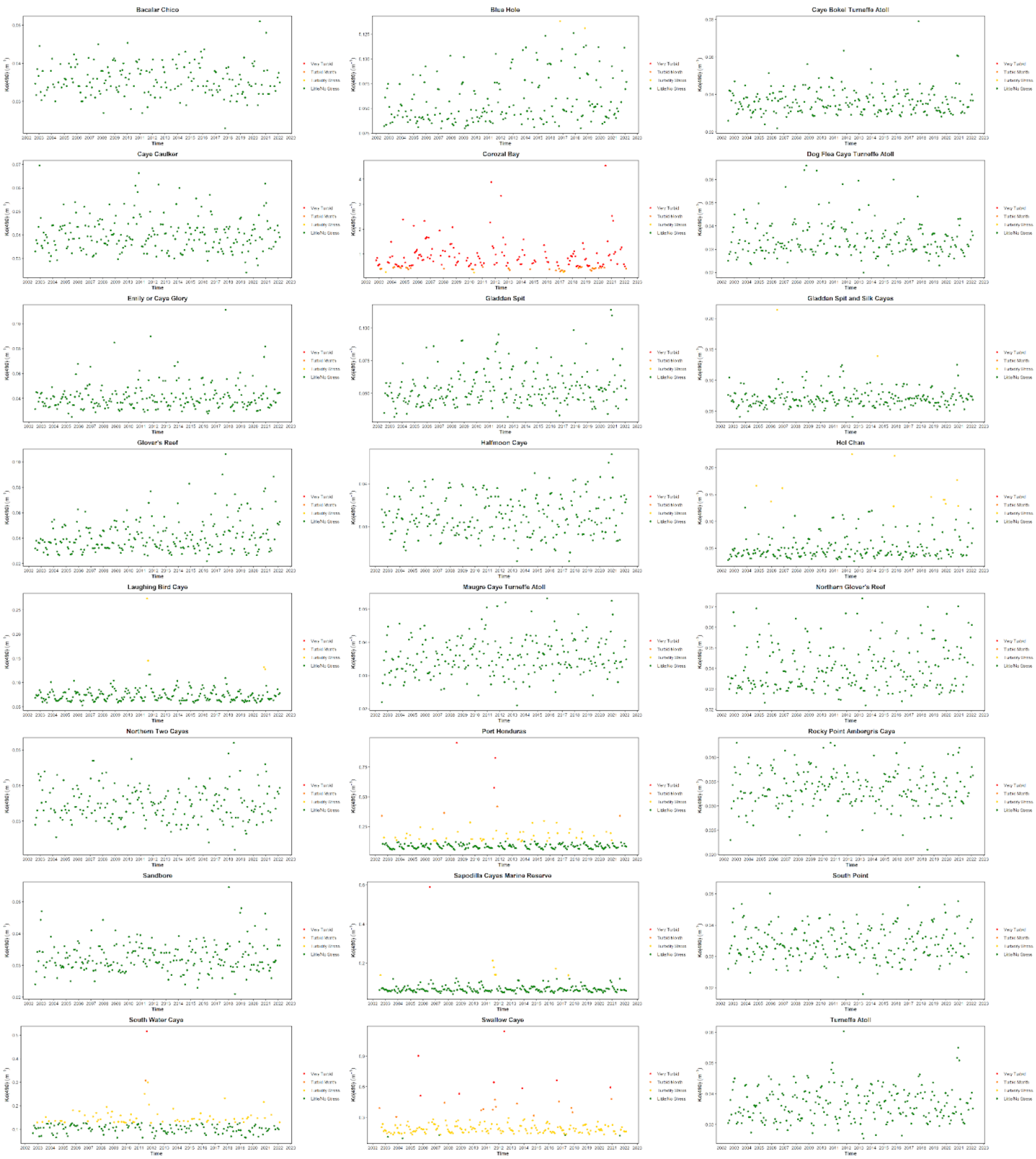

Supplementary Figure 3: Kd(490) values for all MPAs from 2002-2022. Red points indicate very turbid waters, orange points indicate a turbid month, yellow points indicate turbidity stress, and green points indicate little or no stress.

Chapter 3: The Influence of Land Use and Water Reclamation Plants on Fecal Indicator Bacteria and Antibiotic Resistance in the Los Angeles River Watershed

1. Introduction

Antibiotic resistance is deemed one of the world's greatest public health challenges. Over 2.8 million infections in the United States are caused by antibiotic resistance annually, and over 35,000 people die annually from these infections[1]. Although use of antibiotics is known to cause resistance in clinical isolates in as little as a year[2], antibiotics are still widely used in humans and animals. Presence of antibiotics as well as other stressors in the environment such as detergents, heavy metals, and consistent temperature, pH, and nutrient loadings give rise to the emergence, persistence, and dissemination of antibiotic resistance genes (ARGs) in bacteria[3,4]. ARGs can be transferred among bacteria through vertical gene transfer (VGT) and horizontal gene transfer (HGT)[5]. Mobile genetic elements (MGEs) such as integrons, plasmids, and transposons facilitate the transfer of ARGs among opportunistic microorganisms[6,7]. Due to the health threats to the public, research studies are quantifying and characterizing ARGs and antibiotic resistant bacteria (ARB) in various environmental compartments. Though these environmental compartments are recognized as hotspots for the proliferation and dissemination of antibiotic resistance, routine monitoring and standard methods for monitoring antibiotic resistance in them currently doesn't exist. Of these environmental compartments, studies on ARGs and ARB in surface waters, especially in populous coastal areas are increasing[8,9].

Anthropogenic pollution is largely responsible for the dissemination of antibiotic resistance in water ways. These sources include discharges from wastewater treatment plants (WWTPs)[10–16] livestock operations, agriculture, and land applications of manure[17–23], and hospitals[5,24–27]. Larger and denser cities were found to increase the impacts of antibiotic resistance in surface waters[28], with urban runoff contributing significant amounts of chemical pollutants, bacteria, sediments, and nutrients in water[29]. Direct discharge sources from WWTPs were found to contribute to ARG loadings in urban rivers in Beijing, China[28]. Sewage was found to greatly influence ARG reservoirs in coastal waters in the capital of Uruguay[30]. Though many studies have been conducted on quantifying antibiotic resistance in surface waters, not many have been conducted in large cities in the coast of the western United States[9] or tested existing frameworks and standardized methods for doing so[31–33].

There are various techniques employed to quantify and characterize antibiotic resistance. The most prevalent technologies for monitoring environmental antibiotic resistance in water include microbial source tracking, qPCR, whole genome sequencing, metagenomics, and culture-based methods[12,34,35] each with their own pros and cons. Culture-based methods allow for isolation of viable target organisms[36], but is time and labor intensive and many organisms are unculturable[34,37]. Amplification methods like qPCR are more sensitive than metagenomics, but require higher efforts to cover a wide variety of genes and taxonomic markers[12]. Metagenomics is thought to be superior in identifying ARGs in complex environmental and clinical metagenomes using an array of databases, but is a costly method[4,38]. Some experts argue for antibiotic susceptibility tests for phenotypic data and suggest combining that with molecular analysis from whole genome sequencing[37,39]. However, there is still no standard method to quantify AR or standard ARG unit[40], and dose and response models for ARB are still being explored[41].

This study aimed to test an existing framework for antibiotic resistance and cross-validate between culture, qPCR, and metagenomic techniques in varying land types and applying it to one of the most populous cities in the United States—Los Angeles, California. The Los Angeles River (LAR) watershed was evaluated for ARGs, fecal indicator bacteria, and Extended-spectrum beta-lactamase (ESBL) producing *E. coli* in varying land use types. Quantified ARGs and MGEs include *sul*1 (resistance to sulfonamides), *tet*W (resistance to tetracyclines), *intI*1 (proxy for anthropogenic pollution), *erm*F (resistance to macrolides), and *bla*SHV (resistance to beta-lactams) as well as 16S rRNA genes. DNA samples were sent for shotgun sequencing in order to compare them against relevant antibiotic resistance databases, calculate ARG abundance, and resistome risk. Water samples were taken in the river at points above and below three different water reclamation plants (WRPs), swimming and kayak sites, and from beaches near the coastal pour point using a snapshot study approach.

2. Materials and methods

2.1 Study Area

The LAR watershed is approximately 824 mi^2 and is home to approximately 4.5 million people. The LAR is 51 miles long and is bounded by the San Gabriel, Santa Susana, and Santa Monica Mountains in the west and north, the San Gabriel River Watershed in the east, and the Pacific Ocean in the south. The river outpours at the San Pedro/Los Angeles and Long Beach Harbor complex which has a semi-enclosed breakwater of 7.5 miles. The river's estuary is about three miles from where it meets Queensway Bay. The LAR watershed is diverse in land use distribution with 324 mi^2 being open space and forest and the rest being highly developed residential, industrial, and commercial areas. Land use distributions are as follows: 35% residential, 5% commercial, 8% industrial, and 51% open land[42]. Most of the river in the developed area is lined with concrete, but some areas in the Glendale Narrows and Sepulveda Flood Control Basin are unlined to provide riparian habitat.

Currently, most water volume in the LAR stem from three water reclamation plants with some inputs from runoff and groundwater upwelling. Approximately 27.1 million gallons per day (MGD) originate from the DC Tillman WRP, 7.8 MGD from the LA Glendale WRP, 4.5 MGD from the Burbank WRP, 3.6 MGD from groundwater upwelling, and a range between 0.032 and 7.8 MGD from runoff[43]. All WRPs use tertiary treatment technologies to treat municipal and industrial waste before discharging effluent into the river. Burbank and LA Glendale WRPs discharge directly into the river while Tillman WRP discharges partially to nearby garden and lake systems before reaching the river.

The LAR has multiple recreational sites for kayaking, fishing, and swimming. There are two recreation zones along the main stem of the river—the Elysian Valley and Sepulveda Basin LA River Recreation Zones[44]. Reportedly, thousands of people swim in unpermitted and designated areas in the LAR[45]. Most recreational swimming sites are in the upper LAR watershed in Hansen Dam and the Angeles National Forest.

2.2 Sample collection and filtration

Sample collection took place at sixteen sites with varying land uses as mapped in **Figure 3-1**. Five locations were above and below the three WRPs (Tillman Above, Tillman Below, Burbank Below, Glendale Above, Glendale Below), with exception of above the Burbank WRP due to no flow. Three kayaking sites (Sepulveda Dam, Rattlesnake Park, Steelhead Park) and four swim sites (Eaton Canyon Falls, Switzer Canyon Falls, Big Tujunga Creek, and Tujunga Wash) were sampled. Three beaches (Alamitos Beach, Long Beach City Beach, and Rosie's Dog Beach) and one estuary/tidal site (LA River in Long Beach) were included where the LAR discharges to the ocean. Each location was classified as "Developed", "Undeveloped," and "Beach" based on a land use map of Los Angeles County. Land use designations, coordinates, and sampling dates are located in **Table 3-1**. Site locations were selected based on water quality sample locations by the Council for Watershed Health[45] and Heal the Bay for their river and beach report cards[46,47]. Samples were collected during a one-week time range between October and November 2021.

Water sample collection occurred during the early morning hours to ensure minimal UV solar radiation. Four liters of water was collected in sterile polypropylene bottles first which were rinsed three times with ambient water before collection. Samples were transported on ice (4 °C) to the laboratory, and processed within six hours of collection. Water temperature, pH, conductivity, dissolved oxygen, and turbidity were measured for each location using a multiparameter sonde (Hydrolab HL4, OTT Hydromet, Loveland, CO).

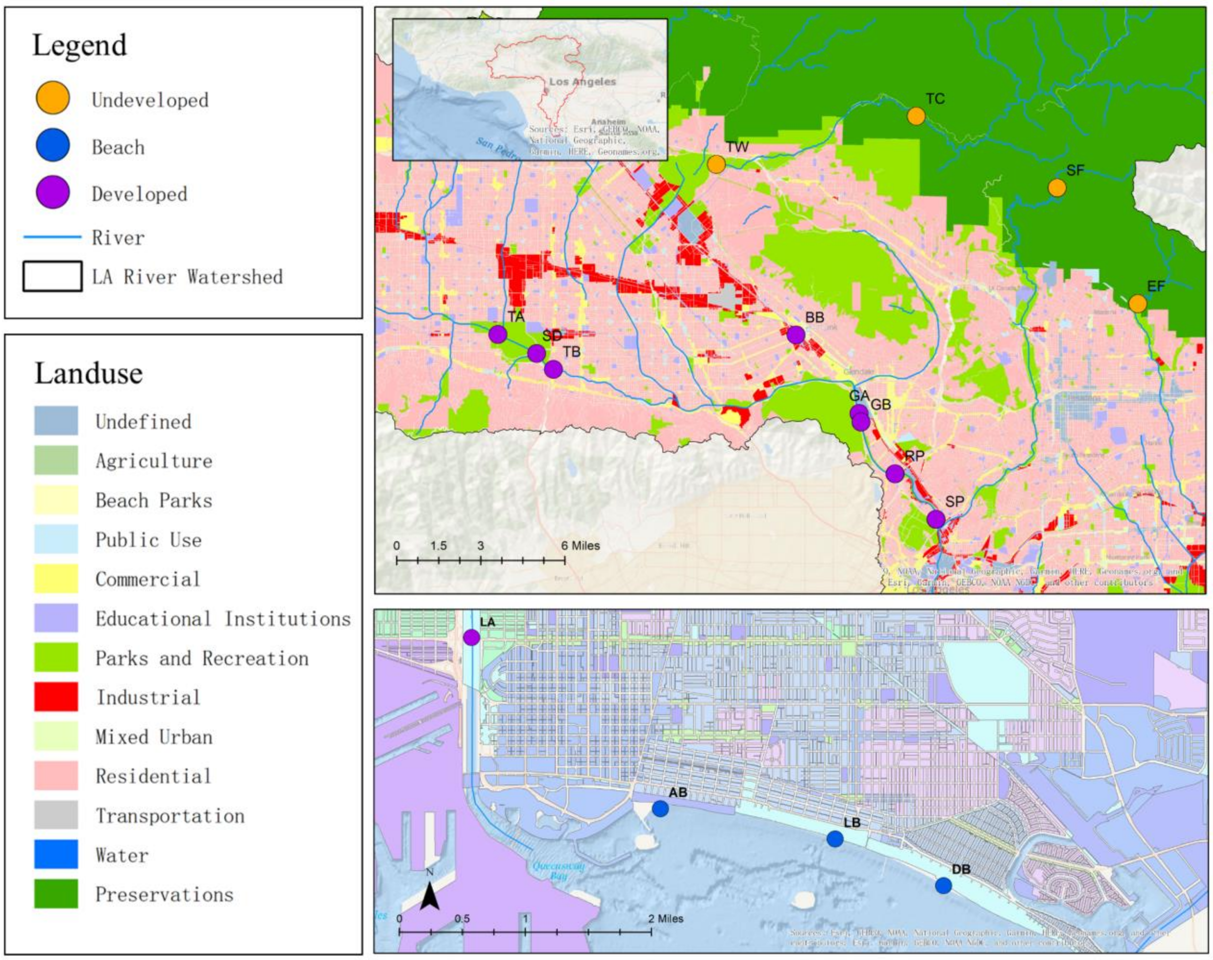

Figure 3-1. Land Use Types and Sampling Sites in the LAR Watershed.

Upon arrival at the laboratory, water samples were filtered in at least triplicate samples on 0.2 µm polycarbonate filters (MilliporeSigma, Burlington, MA). Volumes of water necessary to clog the filter ranged from 100-600 mL per sample and were recorded per replicate. Filters were stored in 2 mL screw cap tubes with flame sterilized tweezers and fixed with 50% ethanol. Samples were stored at -20 °C prior to DNA extraction. A phosphate buffer solution blank was filtered and stored during each sampling event.

2.3 DNA extraction, qPCR, and ddPCR

Ethanol-fixed filters were cut into approximately 1 cm^2 pieces with flame-sterilized scissors and placed into lysing matrix tubes from the FastDNA SPIN Kit for Soil (MP Biomedicals, Irvine, CA). The remaining ethanol solution was subjected to centrifugation at 5000 x g for 10 minutes before being resuspended with the sodium phosphate buffer contained in the DNA kit and added to the lysing matrix tube. All samples were extracted according to manufacturer instructions taking the longest suggested times for incubation, mixing, and settling. An extraction blank was extracted per each extraction batch. Total DNA concentrations and 260/280 absorbance ratios were determined through spectrophotometry via a NanoDrop 2000c (Thermo Scientific, Waltham, MA).

All samples were analyzed for ARG abundance of *sul*1, *tet*W, bla_{SHV}, and *erm*F. The *intI*1 gene was quantified as a proxy for anthropogenic pollution and the 16S rRNA gene was quantified as a surrogate for total bacteria. Gene target sequences and cycling conditions are in the **Supplementary Material**. qPCR amplification was performed using the StepOnePlus system (Applied Biosystems, Foster City, CA) in 25 µL reaction volumes containing 12.5 µL PowerUp SYBR Green Master Mix (Applied Biosystems, Foster City, CA), 1.25 µL of each forward and reverse primer, 2 µL of template DNA, and molecular grade water for the remaining volume for all genes except 16S rRNA. The 16S rRNA gene was performed in a 20 µL reaction volume with 10 µL of PowerUp SYBR Green Master Mix, 1 µL of each forward and reverse primer, 3 µL of template DNA, and molecular grade water for the remaining volume. All assays were performed in 96-well plates. At least a five-point standard curve was run with each plate utilizing double-stranded gBlock gene fragments resuspended according to manufacturer instructions (IDT, Coralville, IA) and quantified on the NanoDrop 2000c (Thermo Scientific, Waltham, MA). Ten-fold dilutions were carried out for the 16S rRNA gene to uncover the presence of PCR inhibitors. The minimum accepted qPCR efficiency was 83% and the lowest R^2 value was 0.997. The limit of detection was set based on the lowest standard per assay.

Molecular quantification of human associated fecal maker targets was conducted using a Bio-Rad QX200 Droplet Digital PCR System (Bio-Rad Laboratories, Hercules, CA). The assay primers targeting crAssphage and HF183/BacR287 molecular indicator region were adapted and performed (Supplementary Material). 20-µL reactions were made using 4x Supermix of Probes (Bio-Rad Laboratories, Hercules, CA). Targets were analyzed in duplex. Droplets were generated with a Bio-Rad QX200 Auto Droplet Generator, and amplification was performed using a C1000 Touch Thermal Cycler (Bio-Rad Laboratories, Hercules, CA) according to manufacturer's recommendations: 94°C for 10 minutes, followed by 40 cycles of 94°C for 30 seconds, then 60°C for 1 minute. At least two no template control (NTC) assays were performed for each assay by replacing the DNA with molecular grade water. Droplets were read on a QX200 Droplet Reader (Bio-Rad Laboratories, Hercules, CA). QA/QC was performed for all samples. Samples with less than 10,000 accepted droplets were excluded from data analysis. Copy number concentrations were calculated by taking the data generated and normalizing to 100 mL of sampled water to compare all markers on the same scale.

Table 3-1. Coordinates and Dates Sampled for Sampling Locations.

Sample Site	Abbreviation	Date sampled	Latitude	Longitude
Tillman Above	TA	10/30/2021	34.179716	-118.50097
Tillman Below	TB	10/30/2021	34.161736	-118.466389
Burbank Below	BB	10/30/2021	34.180021	-118.315391
Glendale Above	GA	10/30/2021	34.139541	-118.275949
Glendale Below	GB	10/30/2021	34.13503	-118.274646
Sepulveda Dam	SD	10/30/2021	34.169951	-118.476915
Rattlesnake Park	RP	10/30/2021	34.108343	-118.253356
Steelhead Park	SP	10/30/2021	34.084798	-118.227951
Eaton Canyon Falls	EF	10/28/2021	34.196567	-118.102397
Switzer Canyon Falls	SF	10/28/2021	34.256484	-118.152752
Big Tujunga Creek	TC	10/28/2021	34.29346	-118.240723
Tujunga Wash	TW	10/28/2021	34.268204	-118.365301
Alamitos Beach	AB	11/1/2021	33.763226	-118.179424
Long Beach City Beach	LB	11/1/2021	33.759783	-118.155302
Rosie's Dog Beach	DB	11/1/2021	33.754426	-118.140329
LA River in Long Beach	LA	11/1/2021	33.782896	-118.2055

2.4 FIB, heavy metal analysis, and ESBL E. coli enumeration

FIB enumeration includes quantifying levels of total coliforms, *Escherichia coli* (Colilert-18, IDEXX), and *Enterococci* (Enterolert, IDEXX) bacteria using standard methods and kits (IDEXX Laboratories, Westbrook, ME). Final concentrations were reported in MPN/100 mL. Marine samples and samples along the main stem of the river were diluted ten-fold and up to 1,000-fold respectively according to manufacturer recommendations.

For quantifying ESBL *E. coli*, 100 µL of 1 mg/mL cefotaxime was added to each prepared 100 mL IDEXX bottle with Colilert-18 media. Samples were diluted at most 100-fold.

Heavy metals were quantified from the water samples using ICP-OES for Cu, Ni, Cr, Mn, Fe, V, and Al expressed in mg/L.

2.5 Sequencing and Bioinformatics

Approximately 100 ng of DNA for all 16 samples were sequenced via 2x150 bp paired-end shotgun metagenomic sequencing on an Illumina NovaSeq 6000 by Mr. DNA (Shallowater, TX). Each library ranges from 10 - 30 million paired-end sequences. All sequence data were deposited into the public NCBI Short Read Archive (SRA) database. The raw sequences were uploaded into Galaxy (https://usegalaxy.org) for processing and assembly. Trimmomatic (Galaxy Version 0.38.0) was used to remove low quality reads from our pair-end data[48]. The Trimmomatic operation SLIDINGWINDOW was set to 4 bases and a quality score of 20, the MINLEN operation was set to a length of 50 bases, and AVGQUAL operation was set to a score of 20. The paired data was assembled using *de novo* metagenomic assembly by MEGHIT (Galaxy Version 1.2.9) using the default settings of 2 for minimum multiplicity and 200 bp for the minimum length of output contigs[49]. FastQC (Galaxy Version 0.73) and Fasta Statistics (Galaxy Version 2.0) were used for quality control.

ARGs were characterized using the ARGs-OAP pipeline (v2.3) which uses the Structured Antibiotic Resistance Genes database to quantify ARG subtypes by cell number and 16S rRNA[50]. Environmental resistome risk scores were calculated using the MetaCompare pipeline which assigns a risk score based on the co-occurrence of ARGs, MGEs, and pathogens on assembled contigs[51]. Read-based taxonomic classification was performed via the Kraken2 (v2.0.8) software on the National Microbiome Data Collaborative (NMDC) EDGE bioinformatics platform (https://nmdc-edge.org/).

2.6 Statistical Analysis

Data were analyzed and visualized in RStudio (v4.0.2). ARG data categorized by land use and tested for statistical significance through the Wilcoxon test at the 0.05 alpha level. Correlation plots were created with the "corrplot" (v0.90) package. The principal component analysis plot was created using the "prcomp" function and "ggbiplot" (v0.55) package. The "ggplot2" (v3.3.6) package was used to create all bar plots. The 3D plot of the resistome risk factors was created using the "plot3D" (v1.4) package. Heatplots and chord plots were created using the "pheatmap" (v1.0.1) and "circlize" (v0.4.1) package, respectively.

3. Results and discussion

3.1 Absolute gene abundances of ARGs and intI1

In this study, four ARGs (*sul*1, *erm*F, *bla*SHV, and *tet*W), 16S rRNA, and *intI*1 were quantified using qPCR in all water samples. The absolute abundances of all genes per land use are displayed in **Figure 3-2**. The undeveloped areas consistently had the lowest gene values, while sites in developed areas had the highest, and beaches had moderate levels for all genes, except *tet*W where beaches had similar values to developed sites. On average, developed sites exhibited median gene values from 1-3 orders of magnitude greater than undeveloped sites and 1-2 orders of magnitude greater than beach sites, except for *tetW*. LA River in Long Beach (LA), the lowest developed area, consistently had the highest average absolute gene value. Big Tujunga Creek (TC) had the lowest average relative abundance for *sul*1, *intI*1, and *tet*W, and Switzer Canyon Falls (SF) had the lowest for *bla*SHV and *erm*F. Absolute gene abundances were statistically significant between developed and undeveloped land uses for all genes ($p < 0.05$). Developed gene abundances for *sul*1, *intI*1, and *erm*F were significantly different compared to beaches ($p < 0.05$). Beach and undeveloped gene abundances were not statistically significant.

Similar results where downstream concentrations of genes increased for all genes except *tet*W were also found in a study that measured ARGs in a wastewater effluent receiving river in the Netherlands[14]. Comparing the same gene targets (*sul*1, *intI*1, and *tet*W), the values in the Netherlands were only similar to our developed locations and our *tet*W values were lower. Our *sul*1 gene values in developed areas were the most comparable to that in the Funan[52] and Zenne Rivers, which are both impacted by wastewater. We had significantly less *tet*W levels which may be due to tetracycline being most commonly detected in the Zenne River[13]. Our absolute *sul*1 and *intI*1 values were also similar to the river Murg in Switzerland which receives WWTP effluent with increased values during bypass events[11].

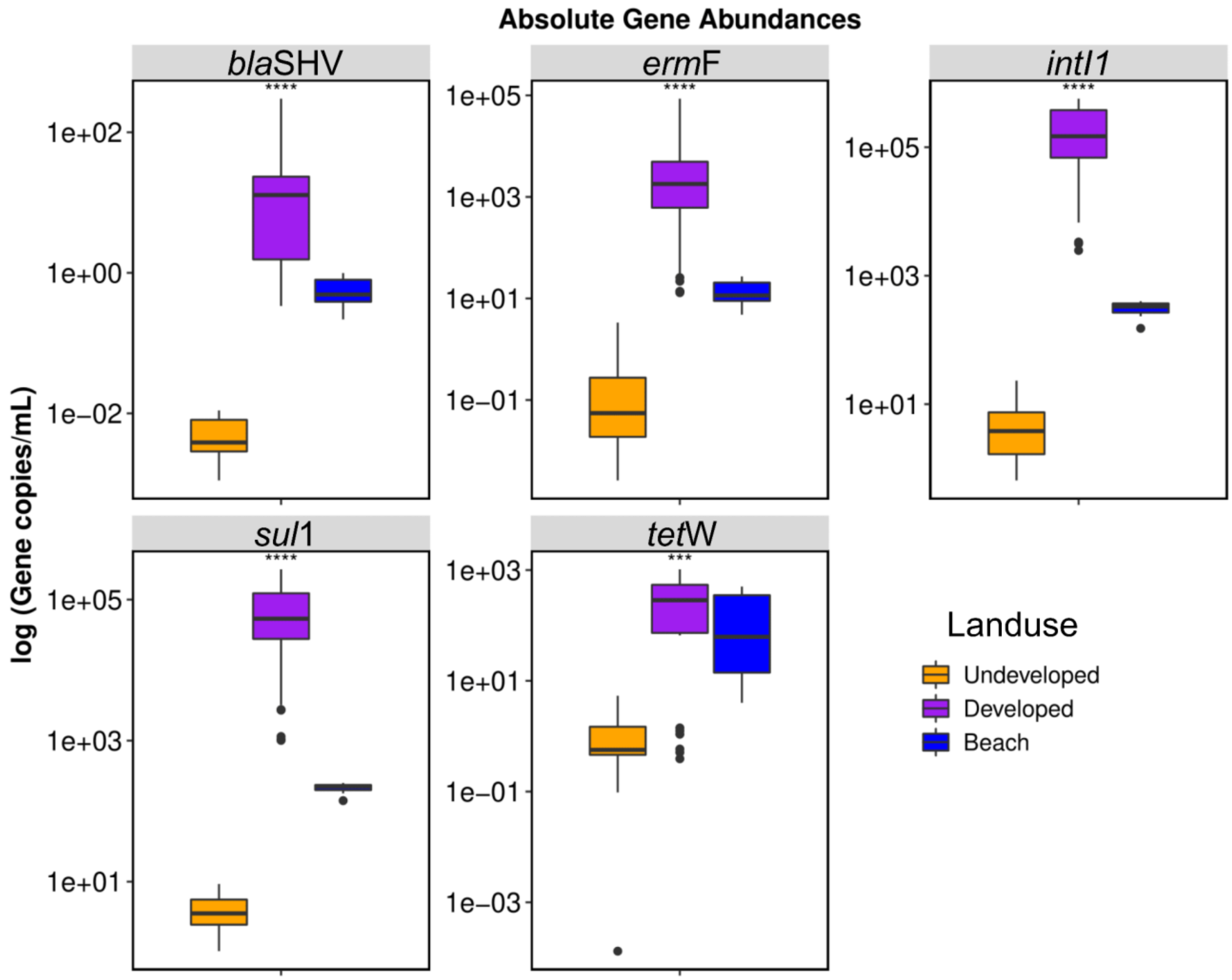

Figure 3-2. Absolute gene abundances per land use.

3.2 AMR trends in the watershed captured by qPCR versus metagenomic data

Comparing normalized gene abundances between qPCR data (**Figure 3-3A**) and metagenomic data (**Figure 3-3B**) reveal similar trends through the LAR watershed. The four undeveloped sites begin with low AMR abundances with Eaton Canyon Falls (EF) displaying higher values. Both methods capture increases in AMR in developed regions beginning at Tillman Above (TA) with qPCR capturing significant increases in *sul*1 and *intI*1 at Tillman Below (TB). High AMR values increase until they are diluted by the Pacific Ocean as evidenced by the lower values at the three beaches. In the qPCR data, higher AMR values are retained compared to the undeveloped sites whereas in the metagenomic data the AMR values are lower than the undeveloped sites.

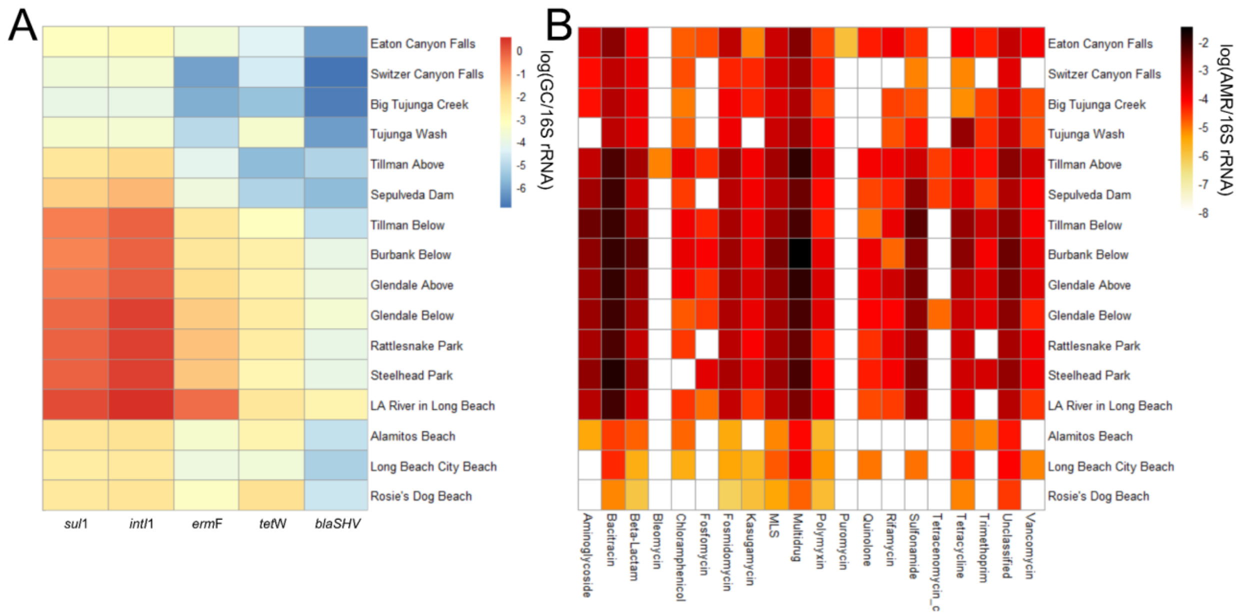

Figure 3-3. Heat plots of relative gene abundances through the watershed from (A) qPCR and (B) metagenomic data.

3.3 Diversity of AMR through metagenomic data

The use of sequencing data enables the search of a greater diversity of ARGs from different classes. 20 out of the 24 antibiotic classes that the ARGsOAP pipeline searches for were found in the water samples. Based on the relative abundance ARG data from the pipeline, there is a greater diversity of antibiotic classes represented in the developed sites (**Figure 3-4A**). Burbank Below (BB) had the highest relative abundance mainly stemming from multidrug resistance ARG types. **Figure 3-4B**, depicts the top 10 ARG classes among all samples. Multidrug resistant ARG types were the most abundant followed by bacitracin, unclassified, MLS, sulfonamide, aminoglycoside, beta-lactam, fosfomycin, tetracycline, and vancomycin. Multidrug resistant ARGs were also the largest proportion of ARGs in an urban stream in Nebraska, USA[53]. Lee et al. 2022, also found high abundance of MLS, aminoglycosides, beta-lactam, sulfonamide, and tetracycline resistance classes in metagenomic data in WWTP effluent and bypass in a Swiss river[11]. Multidrug, MLS, and beta-lactam ARG types were also most abundantly found in a WWTP in Virgina, USA[54]. Developed land uses have the highest portion of ARGs, followed by undeveloped and beaches.

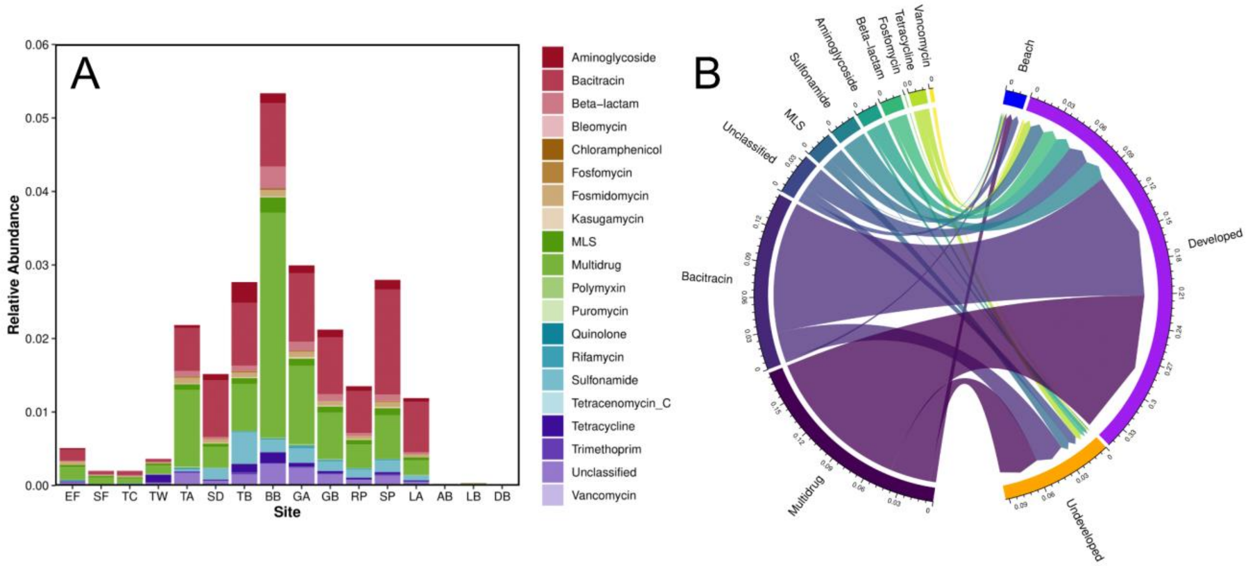

Figure 3-4. Diversity and relative abundance of ARG classes (A) and top 10 ARG classes per land use.

3.4 Bacterial diversity

After comparing the top three taxonomies for each site, there were nineteen unique species and *Limnohabitans* sp. 63ED37-2 appeared in half of the sites. This organism is commonly found in freshwater habitats[55], and was found in LA, SP, RP, GB, TB, GA, SD, and TA. *Limnohabitans* sp. 63ED37-2 was the most predominant species in six of their taxonomies. The eight sites that lacked *Limnohabitans* sp. 63ED27-2 in their top ten taxonomies were the three beach sites (AB, LB, DB), the four undeveloped sites (TW, TC, SF, EF), and one developed site, Burbank Below (BB). BB was the closest site downstream from the undeveloped sites, which could explain why its taxonomy differs from the other eight developed sites, in that it lacks an organism that typically features in the taxonomies of freshwater sites. 12 out of the 16 samples had *Homo sapiens* as a top contributor which was commonly found in large US rivers[56].

3.5 Resistome risk

Resistome risk scores were calculated for all samples from assembled contigs containing ARGs with the potential for mobility and presence in pathogens (**Figure 3-5A**). The MetaCompare results were then plotted in a 3-dimensional hazard space based on the hits from the Comprehensive Antibiotic Resistance Database (CARD), ACLAME, and PATRIC databases (**Figure 3-5B**). Resistome risk scores are greater in developed areas with the highest being at the Burbank Below (BB) location (RR = 27.94). Beach and undeveloped land use sites had similar resistome risk scores ($18.80 < RR < 22.80$), where Switzer Canyon Falls (SF) had the lowest score. Co-occurrence of ARGs, MGEs, and pathogens increase from undeveloped to the developed sites and decrease at the beaches though not to the extent on the undeveloped sites. Notably, the sites below water reclamation plants (TB) have higher instances of co-occurrence than the sites above the respective plants (TA). Here the highest score was a river sample impacted by treatment plant water which was also seen in a study in Puerto Rico[32]. The resistome risk scores in the developed areas were similar to those of secondary effluent of a US-based treatment plant[54]. Compared to European samples, our beach and undeveloped resistome risk scores were similar to WWTP effluent ($18.42 < RR < 22.77$) and the developed sites were similar to that of dairy lagoons ($22.71 < RR < 29.02$) but lower than hospital sewage ($RR > 34.47$)[51].

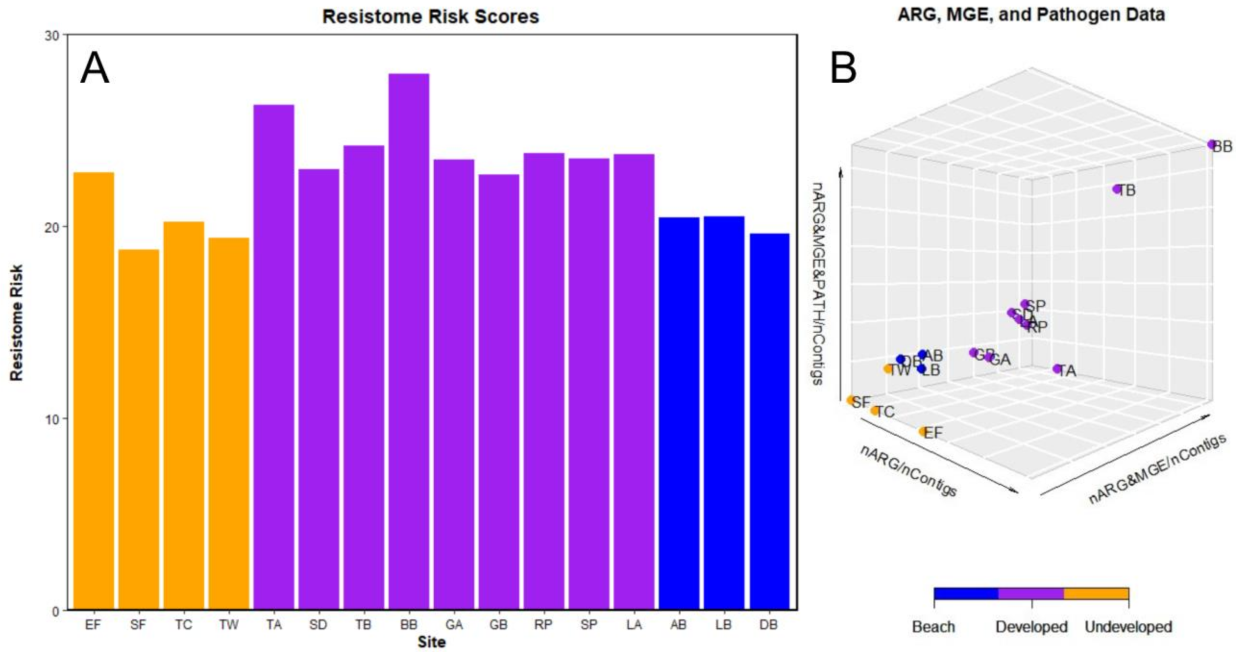

Figure 3-5. (A) Resistome risk scores and (B) co-occurence of ARGs, MGEs, and pathogens in a 3D hazard space.

3.6 Correlation of ARGs and water quality parameters

Figure 3-6A depicts the correlation coefficients between normalized ARGs, 16S rRNA, *int*I1, FIB, heavy metals, and other physicochemical properties. There were statistically significant positive correlations among turbidity and ESBL *E.coli* ($p < 0.01$), Fe ($p < 0.05$), total coliforms ($p<0.05$). There were also positive correlations between 16S rRNA, total coliforms, ESBL *E.coli*, and *E. coli*. All ARGs and *intI*1 correlated positively with each other and with pH. There are statistically significant negative correlations between dissolved oxygen and ESBL *E. coli* ($p < 0.05$), *E. coli* ($p < 0.001$), total coliforms ($p < 0.001$), and 16S rRNA ($p < 0.01$). There were strong negative correlations between 16S rRNA and Ni ($p < 0.05$) and Mn ($p <0.05$) concentrations. Ni concentrations also correlated negatively with ESBL *E. coli* ($p < 0.05$) and the ESBL *E. coli* resistance ratio ($p<0.01$).

The principal component analysis (PCA) displayed sample separation based on land use classification where the principal components together accounted for 63% of the total variation

(**Figure 3-6B**). The first PCA axis correlates best with *Enterococcus* and the *sul*1 and *intI*1 genes. The second PCA axis generally separated the developed sites from beach and undeveloped samples. Within the developed sites, the most upstream (TA) and downstream developed sites (LA) were outliers. All genes and FIB were driving factors in developed sites and dissolved oxygen and conductivity were big drivers for beach sites.

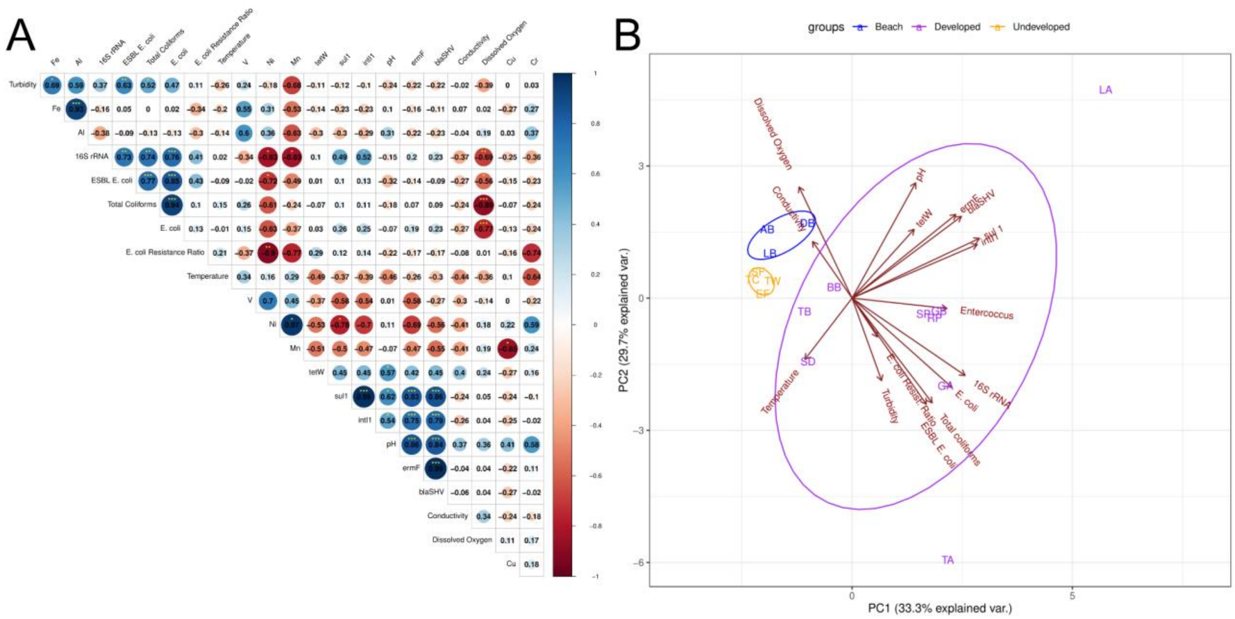

Figure 3-6. (A) Correlation plot of ARGs, heavy metals, FIB, and physicochemical properties. One star ('*'), Two stars ('**'), Three stars ('***') denote p-values less than 0.05, 0.01, and 0.001, respectively. (B) PCA plot of ARGs, FIB, and physicochemical properties by land use.

3.7 FIB and ESBL E. coli

Figures 3-7A-D depict the results from FIB, ESBL *E. coli* for the sampling campaign. In the undeveloped areas in the Angeles National Forest, there were low levels of FIB and ESBL *E. coli*. In the developed areas of the river where the kayaking sites and WRPs are located, levels of FIB and ESBL *E. coli* increase and remain high until the tidal/estuarine area. Most areas exceed their respective recreational limits. Levels of FIB and ESBL *E. coli* decrease at the beaches near the LAR pour point. WRPs mostly have a dilution effect on FIB and ESBL *E. coli* due to high treatment standards for the effluent before it is discharged to the river.

Our *E. coli* levels were comparable to Funan River in Chengdu, China where higher levels were found downstream from residential areas, a hospital, and a WWTP[52]. A study on antibiotic resistant *E. coli* in a wastewater-impacted Belgian river also reported higher levels of bacteria downstream compared to upstream sampling sites[13]. However, the bacterial levels and resistance were amplified by inputs from the wastewater treatment plants. These contrasting results may be due to their treatment plants encompassing processes equivalent to secondary treatment in the US, whereas the WRPs discharging in the LAR have tertiary treatment technologies.

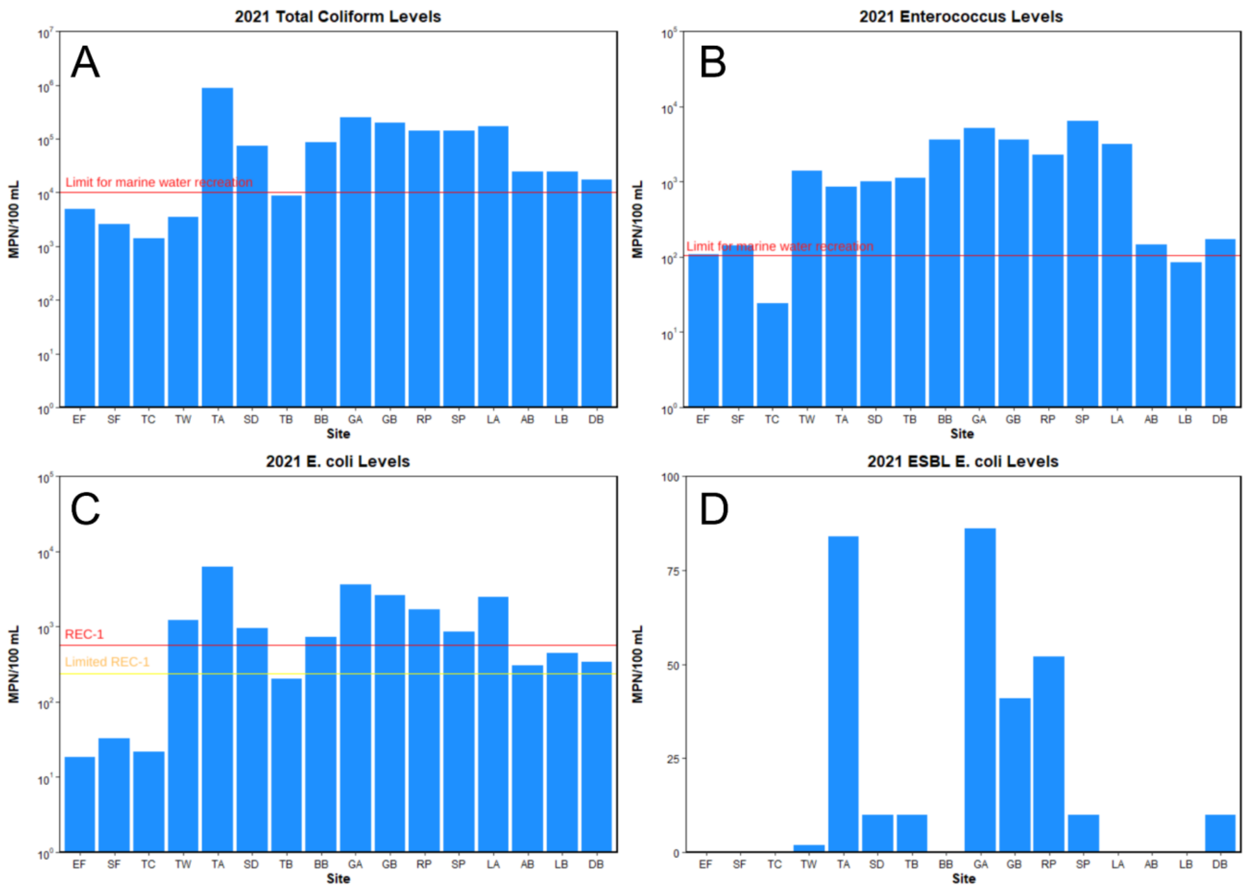

Figure 3-7. (A) Total coliforms, (B) *Enterococcus*, (C) *E. coli*, and (D) ESBL *E. coli* levels for all sampling locations. EPA recreational limits for total coliforms, *Enterococcus*, and *E. coli* are denoted by horizontal lines.

3.8 HF183 and crAssphage

A total of sixteen field samples were analyzed for HF183 and crAssphage targets using the ddPCR method (**Figure 3-8**). The average concentrations of crAssphage were 0.32, 3.62, and 1.62

$\log_{10}$ copies/100 ml for undeveloped, developed, and beach sites, respectively, while HF183 concentrations were 0, 3.062, and 0.92 $\log_{10}$ copies/100 ml for undeveloped, developed, and beach sites, respectively. Overall, the levels of HF183 and crAssphage were highest in developed areas, followed by beach sites. The Burbank Below (BB) site exhibited the highest concentration of HF183, which corresponds to the resistome risk scores obtained. The concentrations measured in our study were comparable to or greater than concentrations measured in other studies. For instance, in an impacted urban watershed in Pittsburgh, PA, USA, crAssphage concentrations ranged from 3.0 to 5.2 $\log_{10}$ copies/100 ml, which is similar to the average concentrations of crAssphage observed in our developed area sites[57]. Ahmed et al. reported HF183 ranging from 2.18 to 4.83 $\log_{10}$ copies/100 ml and crAssphage ranging from 2.17 to 3.80 $\log_{10}$ copies/100 ml for crAssphage, respectively, in the stormwater collected from urban sites and peri-urban sites in Australia[58]. The co-occurrence of the two human fecal markers is more obvious at the developed sites. Moreover, the crAssphage and HF183 concentrations in our study sites were strongly correlated ($r=0.9$, $p<0.05$), suggesting that both markers may originate from similar sources and undergo similar environmental fates within the time scale required for water to pass through the Los Angeles River watershed. These findings contribute to our understanding of human fecal markers and microbial source marker dynamics in the study areas.

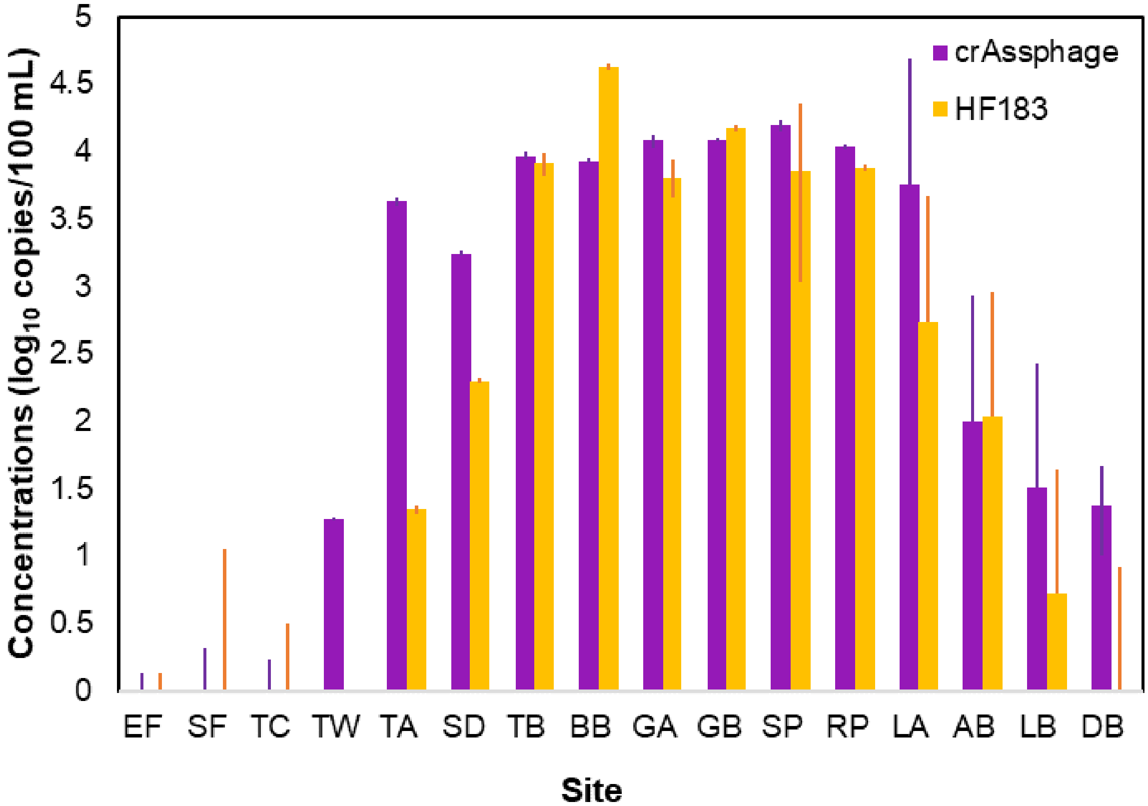

Figure 3-8. ddPCR results for HF183 and crAssphage expressed in log copies per 100 mL of water filtered.

4. Conclusions

This study compared ARG and FIB trends in the Los Angeles River watershed based on land use and influence of water reclamation plants. Metagenomic and amplification-based analysis of ARGs revealed increased loadings of ARGs in the river in the developed areas compared to undeveloped sites and beaches. Viability-based methods for FIB display similar trends where there are larger FIB concentrations in developed sites compared to beaches and undeveloped places exceeding recreational limits. Though WRPs in general diluted FIB due to high water quality standards in effluent water, ARG loadings were higher and downstream of WRPs and there were greater instances of ARGs being co-located on MGEs and pathogens. Our work shows that both qPCR and metagenomics are comparable in elucidating ARG trends based on land use and anthropogenic pollution which can be supplemented by viability-based methods. This work serves to compare various methods in monitoring ARGs and FIB in one of the most populated cities in the United States in the hopes of standardizing methods for monitoring these contaminants in aquatic environments.

5. References

1. CDC. The biggest antibiotic-resistant threats in the U.S. *Centers for Disease Control and Prevention* (2019).
2. Ventola, C. L. The Antibiotic Resistance Crisis. *Pharm. Ther.* **40**, 277–283 (2015).
3. Bombaywala, S., Mandpe, A., Paliya, S. & Kumar, S. Antibiotic resistance in the environment: a critical insight on its occurrence, fate, and eco-toxicity. *Environ. Sci. Pollut. Res.* 1–28 (2021) doi:10.1007/s11356-021-13143-x.
4. Vikesland, P. J. *et al.* Toward a Comprehensive Strategy to Mitigate Dissemination of Environmental Sources of Antibiotic Resistance. 13061–13069 (2017) doi:10.1021/acs.est.7b03623.
5. Narciso-Da-Rocha, C., Varela, A. R., Schwartz, T., Nunes, O. C. & Manaia, C. M. blaTEM and vanA as indicator genes of antibiotic resistance contamination in a hospital–urban wastewater treatment plant system. *J. Glob. Antimicrob. Resist.* **2**, 309–315 (2014).
6. Ma, L., Li, A.-D., Yin, X.-L. & Zhang, T. The Prevalence of Integrons as the Carrier of Antibiotic Resistance Genes in Natural and Man-Made Environments. *Environ. Sci. Technol.* **51**, 5721–5728 (2017).
7. Partridge, S. R., Kwong, S. M., Firth, N. & Jensen, S. O. Mobile genetic elements associated with antimicrobial resistance. *Clin. Microbiol. Rev.* **31**, (2018).
8. A. A. Hatha, M., Sukumaran, D. P., Silvester, R. & John, N. Polluted Coastal and Estuarine Environments: A Potential Reservoir for AMR Determinants in Various Pathogenic Bacteria. in *Antimicrobial Resistance* 101–134 (Springer Singapore, 2020). doi:10.1007/978-981-15-3658-8_5.
9. Zheng, D. *et al.* A systematic review of antibiotics and antibiotic resistance genes in estuarine and coastal environments. *Sci. Total Environ.* **777**, (2021).
10. Eramo, A., Morales Medina, W. R. & Fahrenfeld, N. L. Viability-based quantification of antibiotic resistance genes and human fecal markers in wastewater effluent and receiving waters. *Sci. Total Environ.* **656**, 495–502 (2019).
11. Lee, J., Beck, K. & Bürgmann, H. Wastewater bypass is a major temporary point-source of antibiotic resistance genes and multi-resistance risk factors in a Swiss river. *Water Res.* **208**, 117827 (2022).
12. Miłobedzka, A. *et al.* Monitoring antibiotic resistance genes in wastewater environments: The challenges of filling a gap in the One-Health cycle. *J. Hazard. Mater.* **424**, 127407 (2022).
13. Proia, L. *et al.* Antibiotic resistance along an urban river impacted by treated wastewaters.

Sci. Total Environ. **628**–**629**, 453–466 (2018).

14. Sabri, N. A. *et al.* Prevalence of antibiotics and antibiotic resistance genes in a wastewater effluent-receiving river in the Netherlands. *J. Environ. Chem. Eng.* **8**, 102245 (2020).

15. Tang, Y., Liang, Z., Li, G., Zhao, H. & An, T. Metagenomic profiles and health risks of pathogens and antibiotic resistance genes in various industrial wastewaters and the associated receiving surface water. *Chemosphere* **283**, 131224 (2021).

16. Wang, R., Ji, M., Zhai, H., Guo, Y. & Liu, Y. Occurrence of antibiotics and antibiotic resistance genes in WWTP effluent-receiving water bodies and reclaimed wastewater treatment plants. *Sci. Total Environ.* **796**, 148919 (2021).

17. Barrios, R. E. *et al.* Fate and transport of antibiotics and antibiotic resistance genes in runoff and soil as affected by the timing of swine manure slurry application. *Sci. Total Environ.* **712**, 136505 (2020).

18. Chee-Sanford, J. *et al.* Fate and Transport of Antibiotic Residues and Antibiotic Resistance Genes following Land Application of Manure Waste. *J. Environ. Qual.* **38**, 1086–1108 (2009).

19. Cira, M. *et al.* Commercially available garden products as important sources of antibiotic resistance genes—a survey. *Environ. Sci. Pollut. Res.* 1–8 (2021) doi:10.1007/s11356-021-13333-7.

20. He, Y. *et al.* Antibiotic resistance genes from livestock waste: occurrence, dissemination, and treatment. *npj Clean Water* **3**, 4 (2020).

21. Hung, W. C. *et al.* Tracking antibiotic resistance through the environment near a biosolid spreading ground: Resistome changes, distribution, and metal(loid) co-selection. *Sci. Total Environ.* **823**, 153570 (2022).

22. Jacobs, K., Wind, L., Krometis, L.-A., Hession, W. C. & Pruden, A. Fecal Indicator Bacteria and Antibiotic Resistance Genes in Storm Runoff from Dairy Manure and Compost-Amended Vegetable Plots. *J. Environ. Qual.* **48**, 1038–1046 (2019).

23. West, B. M., Liggit, P., Clemans, D. L. & Francoeur, S. N. Antibiotic resistance, gene transfer, and water quality patterns observed in waterways near cafo farms and wastewater treatment facilities. *Water. Air. Soil Pollut.* **217**, 473–489 (2011).

24. Hassoun-Kheir, N. *et al.* Comparison of antibiotic-resistant bacteria and antibiotic resistance genes abundance in hospital and community wastewater: A systematic review. *Sci. Total Environ.* **743**, 140804 (2020).

25. Hocquet, D., Muller, A. & Bertrand, X. What happens in hospitals does not stay in hospitals: antibiotic-resistant bacteria in hospital wastewater systems. *J. Hosp. Infect.* **93**, 395–402 (2016).

26. Paulus, G. K. *et al.* The impact of on-site hospital wastewater treatment on the downstream communal wastewater system in terms of antibiotics and antibiotic resistance genes. *Int. J. Hyg. Environ. Health* **222**, 635–644 (2019).

27. Petrovich, M. L. *et al.* Microbial and Viral Communities and Their Antibiotic Resistance Genes Throughout a Hospital Wastewater Treatment System. *Front. Microbiol.* **11**, 153

(2020).

28. Xu, Y. *et al.* Occurrence and distribution of antibiotics, antibiotic resistance genes in the urban rivers in Beijing, China. *Environ. Pollut.* **213**, 833–840 (2016).

29. Almakki, A., Jumas-Bilak, E., Marchandin, H. & Licznar-Fajardo, P. Antibiotic resistance in urban runoff. *Sci. Total Environ.* **667**, 64–76 (2019).

30. Fresia, P. *et al.* Urban metagenomics uncover antibiotic resistance reservoirs in coastal beach and sewage waters. *Microbiome 2019 71* **7**, 1–9 (2019).

31. Borchardt, M. A. *et al.* The Environmental Microbiology Minimum Information (EMMI) Guidelines: QPCR and dPCR Quality and Reporting for Environmental Microbiology. *Environ. Sci. Technol.* **55**, 10210–10223 (2021).

32. Davis, B. C. *et al.* Demonstrating an Integrated Antibiotic Resistance Gene Surveillance Approach in Puerto Rican Watersheds Post-Hurricane Maria. *Environ. Sci. Technol.* **54**, 15108–15119 (2020).

33. Keenum, I. *et al.* A framework for standardized qPCR-targets and protocols for quantifying antibiotic resistance in surface water, recycled water and wastewater. (2022) doi:10.1080/10643389.2021.2024739.

34. Ishii, S. Quantification of antibiotic resistance genes for environmental monitoring: Current methods and future directions. *Curr. Opin. Environ. Sci. Heal.* **16**, 47–53 (2020).

35. Sanderson, H., Fricker, C., Brown, R. S., Majury, A. & Liss, S. N. Antibiotic resistance genes as an emerging environmental contaminant. *Environ. Rev.* **24**, 205–218 (2016).

36. McLain, J. E., Cytryn, E., Durso, L. M. & Young, S. Culture-based methods for detection of antibiotic resistance in agroecosystems: Advantages, challenges, and gaps in knowledge. *J. Environ. Qual.* **45**, 432–440 (2016).

37. Sukhum, K. V., Diorio-Toth, L. & Dantas, G. Genomic and Metagenomic Approaches for Predictive Surveillance of Emerging Pathogens and Antibiotic Resistance. *Clin. Pharmacol. Ther.* **106**, 512–524 (2019).

38. Guitor, A. K. *et al.* Capturing the resistome: A targeted capture method to reveal antibiotic resistance determinants in metagenomes. *Antimicrob. Agents Chemother.* **64**, (2020).

39. Diallo, O. O. *et al.* Antibiotic resistance surveillance systems: A review. *J. Glob. Antimicrob. Resist.* **23**, 430–438 (2020).

40. Nguyen, A. Q. *et al.* Monitoring antibiotic resistance genes in wastewater treatment: Current strategies and future challenges. *Sci. Total Environ.* **783**, 146964 (2021).

41. Chandrasekaran, S. & Jiang, S. C. A dose response model for quantifying the infection risk of antibiotic-resistant bacteria. *Sci. Reports 2019 91* **9**, 1–11 (2019).

42. Ackerman, D., Schiff, K. C., Trim, H. & Mullin, M. Characterization of water quality in the Los Angeles River. *Bull. South. Calif. Acad. Sci.* **102**, 86–91 (2003).

43. LA City Sanitation. *One Water LA 2040 Plan. Volume 4: LA River Flow Study*. https://www.lacitysan.org/san/faces/wcnav_externalId/s-lsh-es-owla-r-owlap-v4larfs?_adf.ctrl-state=102i39qu11_5&_afrLoop=15347373152922746#! (2018).

44. Mountains Recreation & Conservation Authority. LA River Recreation. http://lariverrecreation.org/.

45. Council for Watershed Health. Los Angeles River Watershed Monitoring Program (LARWMP) 2020 Annual Report. (2020).

46. Heal the Bay. River Report Card. (2020).

47. Heal the Bay. 2019-2020 Beach Report Card. (2020).

48. Bolger, A. M., Lohse, M. & Usadel, B. Trimmomatic: a flexible trimmer for Illumina sequence data. *Bioinformatics* **30**, 2114–2120 (2014).

49. Li, D., Liu, C.-M., Luo, R., Sadakane, K. & Lam, T.-W. MEGAHIT: an ultra-fast single-node solution for large and complex metagenomics assembly via succinct de Bruijn graph. doi:10.1093/bioinformatics/btv033.

50. Yin, X. *et al.* ARGs-OAP v2.0 with an expanded SARG database and Hidden Markov Models for enhancement characterization and quantification of antibiotic resistance genes in environmental metagenomes. *Bioinformatics* **34**, 2263–2270 (2018).

51. Oh, M. *et al.* MetaCompare: a computational pipeline for prioritizing environmental resistome risk. *FEMS Microbiol. Ecol.* **94**, 79 (2018).

52. Yang, Y. *et al.* Prevalence of antibiotic resistance genes in bacteriophage DNA fraction from Funan River water in Sichuan, China. *Sci. Total Environ.* **626**, 835–841 (2018).

53. Baral, D. *et al.* Tracking the Sources of Antibiotic Resistance Genes in an Urban Stream during Wet Weather using Shotgun Metagenomic Analyses. *Environ. Sci. Technol.* **52**, 9033–9044 (2018).

54. Majeed, H. J. *et al.* Evaluation of Metagenomic-Enabled Antibiotic Resistance Surveillance at a Conventional Wastewater Treatment Plant. *Front. Microbiol.* **12**, 1–19 (2021).

55. Lee, J. *et al.* Unraveling the riverine antibiotic resistome: The downstream fate of anthropogenic inputs. *Water Res.* **197**, 117050 (2021).

56. Linz, D. M. *et al.* Metagenomic mapping of cyanobacteria and potential cyanotoxin producing taxa in large rivers of the United States. *Nat. Sci. Reports* **13**, 1–13 (2023).

57. Stachler, E., Crank, K. & Bibby, K. Co-Occurrence of crAssphage with Antibiotic Resistance Genes in an Impacted Urban Watershed. *Environ. Sci. Technol. Lett.* **6**, 216–221 (2019).

58. Ahmed, W., Payyappat, S., Cassidy, M. & Besley, C. A duplex PCR assay for the simultaneous quantification of Bacteroides HF183 and crAssphage CPQ_056 marker genes in untreated sewage and stormwater. *Environ. Int.* **126**, 252–259 (2019).

6. Supplementary Materials

Supplementary table 1. qPCR assay information.

Target		**Oligo**	**Size (bp)**	**Annealing Temperature (°C)**	**N of cycles**	**LOD**	**Efficiency (%)**	**R^2**	**Reference**
Gene	**Name**	**Sequence (5'-3')**							
intI1	intI1-FW	CCTCCCGCACGATGATC	280	58	40	3.59	89.26%	0.9992	Goldstein et al. 2001
	intl1-RV	TCCACGCATCGTCAGGC							
sul1	sul1-FW	CGCACCGGAAACATCGCTGCAC	163	65	45	5.11	89.32%	0.9995	Pei et al. 2006
	sul1-RV	TGAAGTTCCGCCGCAAGGCTCG							
tetW	tetW-FW	GAGAGCCTGCTATATGCCAGC	168	60	45	5.23	88.78%	0.9983	Zhou et al. 2014
	tetW-RV	GGGCGTATCCACAATGTTAAC							
ermF	ermF-FW	TCGTTTTACGGGTCAGCACTT	268	50	45	0.6	95.34%	0.9993	Knapp et al. 2010
	ermF-RV	CAACCAAAGCTGTGTCGTTT							
blaSHV	blaSHV-FW	TGATTTATCTGCGGGATACG	215	55	40	3.64	96.19%	0.9995	Knapp et al. 2010
	blaSHV-RV	TTAGCGTTGCCAGTGCTCG							
16S rRNA	16S-FW	CGGTGAATACGTTCYCGG	124	56	40	16.9	88.08%	0.999	Suzuki et al., 2000
	16S-RV	GGWTACCTTGTTACGACTT							

Chapter 4: Antibiotic Resistance Genes and Nutrients in the Lower Belize River and Belize Barrier Reef

1. Introduction

Antibiotic resistance has been widely regarded as a global health crisis since the mid 1900s[1,2]. In 2019, about 1.27 million deaths were attributed to antibiotic resistance globally[3]. Antibiotic resistance arises due through misuse and overuse of antibiotics among humans and animals. Though antibiotic resistance genes (ARGs) have evolved and exist in natural and remote environments, anthropogenic stressors such as heavy metals and pharmaceuticals can promote the conferring of ARGs by bacteria. Aside from clinical settings, environment compartments, such as air, soil, and water, play an important role in the proliferation and dissemination of antibiotic resistance[4]. Sources of anthropogenic activities that impact the human resistome include livestock operations[5–7], land application of manure to crop fields[8–10], composting and biosolid production[11–14], non-point discharges[15–18], and effluent from wastewater treatment plants that have industrial, hospital, and residential influents[19–23]. Thus, the need to monitor and understand the intersection between environment and humans in terms of antibiotic resistance is warranted[24–28].

Antibiotic resistance disproportionately affects low- and middle- income countries (LMICs)[29–31]. In fact, multidrug resistant organisms are the main cause of healthcare-associated infections (HAI) in Latin America[29] which may be attributed to high population density, poor living conditions, ineffective healthcare systems, and poor quality of antibiotics. Additionally, poor infrastructure leads to sanitation and water issues resulting in inaccessibility to potable water, illegal discharges, untreated wastewater, and poor solid waste disposal[29,32]. Though behavioral interventions have been proven to have positive impact on use of antibiotics in LMICs[33], antibiotic resistance in these countries is still prevalent[29,34–36]. A review of studies conducted in Latin America found that plasmid-mediated quinolone resistance genes are prevalent in humans, animals, food, and the environment[37]. Antibiotic resistant *Helicobacter pylori* had also been identified in Latin America and the Caribbean[38,39]. However, disparities among studies conducted within LMICs also exist. For example, most studies in Latin America are in Brazil and Mexico[40] with not many investigations being conducted in Central America. There are very few studies that elucidate the impacts of antibiotic resistance in coral reefs, with all studies being concentrated in China[41,42]. The urgent need to monitor antibiotic resistance in other LMICs and various environmental matrices such as coral reefs, groundwater, soil, and coastal areas still remains[40].

Belize, a country in Central America, has previously identified antibiotic-resistant bacteria (ARB) as an issue in its healthcare system. Though antibiotics are prohibited for sale without a prescription through the Belize Antibiotic Act, a study showed that around 47.2 % of surveyed community pharmacies were willing to sell antibiotics without a prescription[43] most likely due to seeking of economic gain, weak regulatory enforcement, and consumer demands. Another survey of Belizean college students reported that around 29% of students self-medicate with antibiotics, which may potentially lead to adverse drug reactions, bacterial resistance, and drug interactions[44]. Children from San Pedro were found to have tetracycline- and sulfonamide-resistant *Enterobacteriaceae*[45] and 56.97% of *Neisseria Gonorrhoeae* isolates collected were penicillinase-producing[46]. Belize has a large tourism economy accounting for over 40% of gross domestic product (GDP)[47] and many international visitors chose to recreate along Belize's coastline, cayes, and atolls. There are several potential inputs of pollution into Belizean waterways such as agricultural runoff, waste, nutrients, and sewage[48–51]. Particularly, high tourism and poor sewage system is thought to be the reason for ARB in nurse sharks near the Hol Chan Marine Reserve[52]. There are also anecdotes of community members experiencing itching, rashes, and other health effects from recreating in rivers[53]. As the nation continues to develop, the need to elucidate sources of ARGs and ARB in waterways is crucial to ensure the safety of Belizeans and tourists alike.

Current gaps in the AR surveillance in LMICs involve sampling the environmental resistome to understand resistance determinants and potentially contributing niches[34]. There are multiple ways to monitor antibiotic resistance in waterways such as use of qPCR, sequencing and metagenomics, and culture-based methods[25,54,55]. However, there is a need to cross-validate between different AR monitoring methods and move towards standardization protocols[20,25]. The World Health Organization (WHO) has a set of standard protocols under the Global Tricycle Surveillance for ESBL- producing *E. coli* aimed at monitoring ARGs in different environments. For environmental samples, a study conducted in a major city would consist of sampling from surface waters downstream and upstream from the city, near wet market or poultry market areas, and wastewater treatment plant inputs[56]. Additionally, Davis et al. describes an integrated approach to AR monitoring using qPCR and metagenomics analysis[20]. Incorporating the Davis approach and WHO standard protocols, the purpose of this study was to assess ARGs and ARB using qPCR and metagenomics in the lower Belize River watershed, reef system near Belize City, and Glover's Reef Atoll. Five ARGs (*sul*1, *sul*2, *erm*F, *tet*A, and *bla*SHV) were quantified through qPCR, along with *intI*1 and 16S rRNA at 18 locations in Belize where a subset of six samples were sent for shotgun sequencing. Nutrients (nitrate, phosphate, total nitrogen, and ammonia), total organic carbon (TOC), and turbidity were also measured at all sites. To our knowledge, this study is the first of its kind in comprehensively surveying antibiotic resistance in Belize and Central America.

2. Methods and Materials

2.1 Study Area

Belize is a small Central American country bordered by Mexico, Guatemala, and the Caribbean Sea. Belize is in the heart of the Mesoamerican Barrier Reef System which is the world's second largest barrier reef. The Belize Barrier Reef Reserve System (BBRRS) is a UNESCO world heritage site which encompasses a variety of the country's biodiverse ecosystems including seagrass, coral reefs, and mangroves[57]. The reef system contributes about 30% of the nation's GDP through coastal protection, fisheries, and tourism[58,59]. The BBRRS has seven protected sites which include the Glover's Reef Marine Reserve established in 1993[60]. Glover's Reef Atoll (260 km^2) is 45 km offshore from Belizean coastline and contains around 850 coral reef patches in its interior lagoon[61]. Glover's Reef has designated zones for spawning, general use, and conservation. Glover's Reef is home to a variety of fish species[62,63] and the Glover's Reef Research Station owned by the Wildlife Conservation Society located in the reef's conservation zone.

The Belize River is the largest river in Belize running across the center of the country and flowing from the Peten District of Guatemala to the Belize coastal lagoon. The river outpours near Belize City, the most populous city in Belize (around 60,000 residents) and is approximately 290 km in length. It's a source for drinking water, tourism, fisheries, and mangrove cayes. Excessive nutrient loading, sediments, and pesticides have depleted the water quality of the river in part from deforestation and unsustainable agricultural practices. The pour point of the Belize River is located around 20 km away from the BBRRS. Studies have found trace metals, color dissolved organic matter, and nitrogen loading enrichment in the reef system from land-based pollution[49,51,64].

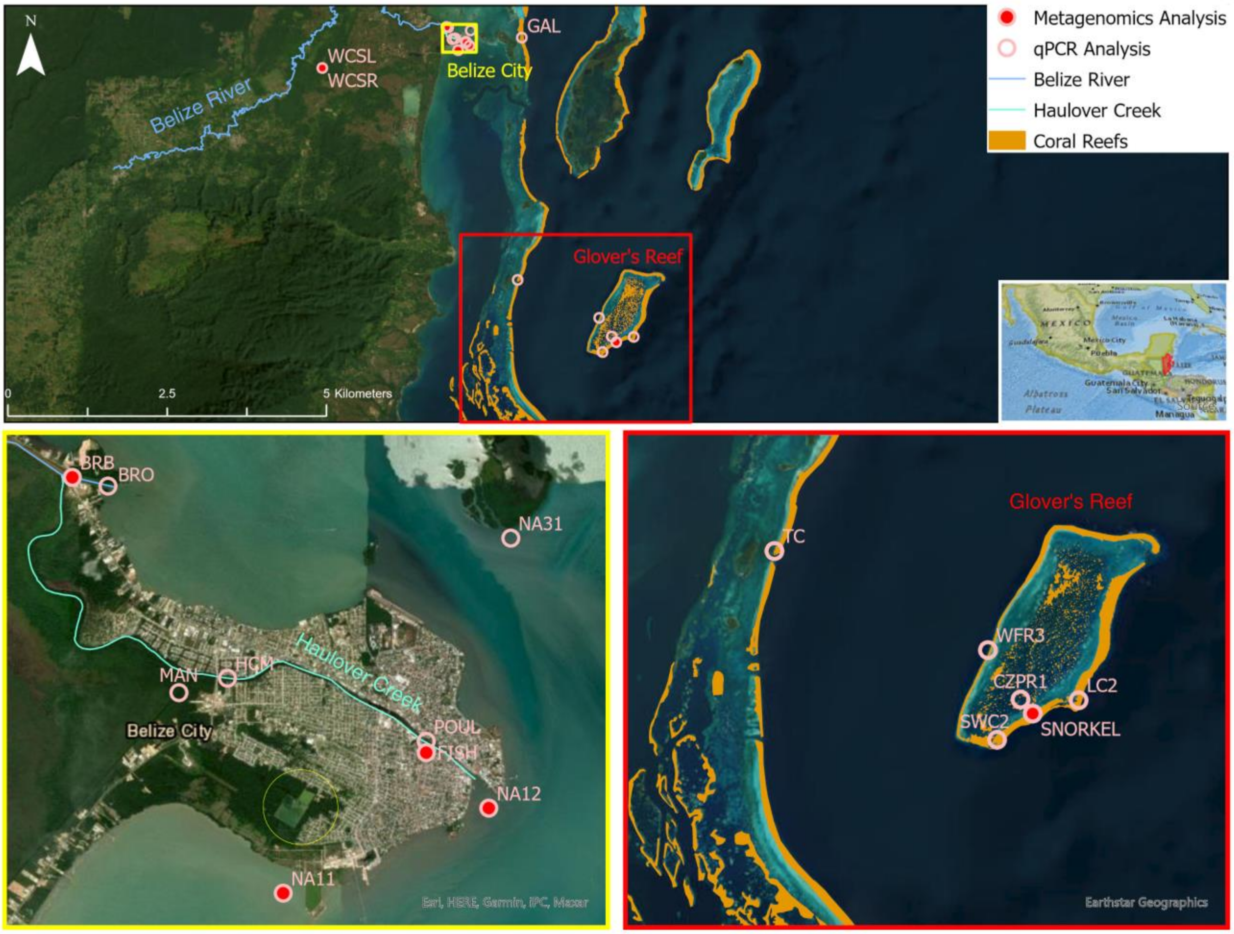

Figure 4-1. Sampling locations in the lower Belize River watershed and Belize coastal lagoon. The top panel shows all of the sampling locations (pink circles) between inland forested areas and coral reefs. The subset of samples sent for shotgun sequencing are filled in red. The bottom yellow panel depicts where the Belize River outpours to the coastal lagoon in the top left corner and Haulover Creek flows through Belize City. In this panel, the yellow circle in the bottom center is the wastewater treatment lagoon system. The bottom red panel shows the Glover's Reef and Tobacco Caye (TC) sampling locations.

2.2 Sample Collection and filtration

Water samples were collected at 18 sites in Belize: eight within the lower portion of the Belize River watershed, three near the surrounding coast of Belize City, two in coral areas in the BBRRS, and five locations at Glover's Reef Atoll (**Figure 4-1** and **Table 4-1**). Water samples were taken using sterile polypropylene bottles within a four-day time period between August and

September 2022. Bottles were rinsed three times with ambient water before collection, transported on ice to the laboratory, and processed within twelve hours of collection.

At the laboratory, water samples were filtered on 0.2 µm polycarbonate filters (MilliporeSigma, Burlington, MA). Volume of water necessary to clog the filter ranged from 100 - 750 mL and was recorded for each replicate. Filters were stored in 2 mL screw cap tubes with flame sterilized tweezers and fixed with 50% ethanol. Samples were stored at -20 °C prior to arrival in the US. Filters were flown to the US on ice and stored at -20 °C immediately upon arrival until DNA extraction.

Table 4-1. Name and Coordinates of Sampling Sites.

Name	Date	Description	Latitude	Longitude
BRB	8/29/2022	Belize River bridge	17.535921	-88.241917
BRO	8/29/2022	Belize River outpour	17.534666	-88.236874
MAN	8/29/2022	Mangrove canal	17.50556	-88.22691
HCM	8/29/2022	Upper Haulover Creek	17.50763	-88.22006
POUL	8/29/2022	Downstream from poulty operations	17.49872	-88.19202
FISH	8/29/2022	Near fish market	17.49715	-88.19202
NA12	8/29/2022	Haulover Creek outpour	17.48931	-88.18317
NA11	8/29/2022	Near wastewater treatment lagoons	17.477333	-88.2121667
NA31	8/30/2022	Offshore Belize City	17.52735	-88.1800833
GAL	8/30/2022	Gallow's Point Reef	17.50889	-88.05099
TC	8/31/2022	Tobacco Caye	16.89898	-88.06194
WFR3	8/31/2022	Glover's Reef: West/Forereef	16.80375	-87.85625
CZPR1	8/31/2022	Glover's Reef: Conservation zone/Patch reefs	16.75611	-87.82483
LC2	8/31/2022	Glover's Reef: Long Caye	16.75541	-87.76903
SNORKEL	8/31/2022	Glover's Reef: Glover's Reef Research Station	16.74251	-87.8131
SWC2	8/31/2022	Glover's Reef: Southwest Caye	16.71761	-87.8476
WCSL	9/1/2022	Inland Belize River: Lagoon	17.432719	-88.5546919
WCSR	9/1/2022	Inland Belize River: River	17.432562	-88.5545589

2.3 DNA Extraction and qPCR

To prepare for the DNA extraction, filters were cut into approximately 1 cm^2 pieces with flame-sterilized scissors and placed into lysing matrix tubes from the FastDNA SPIN Kit for Soil (MP Biomedicals, Irvine, CA). The remaining ethanol solution was subjected to centrifugation at 5000 x g for 10 minutes before being resuspended with the sodium phosphate buffer contained in the DNA kit and added to the lysing matrix tube. All samples were extracted according to manufacturer instructions taking the longest suggested times for incubation, mixing, and settling. An extraction blank was extracted per extraction batch. Total DNA concentrations and 260/280 absorbance ratios were determined through spectrophotometry via a NanoDrop 2000c (Thermo Scientific, Waltham, MA).

Five ARGs, *sul*1, *sul*2, *erm*F, *tet*A, and *bla*SHV, were targeted for analysis through qPCR along with *intI*1 (a proxy for anthropogenic pollution) and the 16S rRNA gene (a surrogate for total bacteria). Gene target sequences are in **Table 4-2**. qPCR amplification was performed using the StepOnePlus system (Applied Biosystems, Foster City, CA) in 25 µL reaction volumes containing 12.5 µL PowerUp SYBR Green Master Mix (Applied Biosystems, Foster City, CA), 1.25 µL of each forward and reverse primer, 2 µL of template DNA, and molecular grade water for the remaining volume for all genes except 16S rRNA. The 16S rRNA gene was performed in a 20 µL reaction volume with 10 µL of PowerUp SYBR Green Master Mix, 1 µL of each forward and reverse primer, 3 µL of template DNA, and molecular grade water for the remaining volume. All assays were performed in 96-well plates. At least a five-point standard curve was run with each plate utilizing double-stranded gBlock gene fragments resuspended according to manufacturer instructions (IDT, Coralville, IA) and quantified on the NanoDrop 2000c (Thermo Scientific, Waltham, MA). Ten-fold dilutions were carried out for the 16S rRNA gene to detect the presence of PCR inhibitors. The lowest qPCR efficiency was 90.6% and the lowest R^2 value was 0.998. The limit of detection was set based on the lowest standard per assay.

Table 4-2. qPCR assay information.

Target		Oligo	Size (bp)	Annealing Temperature (°C)	N of cycles	LOD	Efficiency (%)	R^2	Reference
Gene	Name	Sequence (5'-3')							
sul1	sul1-FW	CGCACCGGAAACATCGCTGCAC	258	65	45	2.87	91.8535	0.9995	Pei et al., 2006
	sul1-RV	TGAAGTTCCGCCGCAAGGCTCG							
intI1	intI1-FW	GGCTTCGTGATGCCTGCTT	424	55	45	1.5	95.4015	0.999	Luo et al., 2010
	intI1-RV	CATTCCTGGCCGTGGTTCT							
ermF	ermF-FW	TCGTTTTACGGGTCAGCACTT	246	50	45	2.59	97.7745	0.9995	Knapp et al., 2010
	ermF-RV	CAACCAAAGCTGTGTCGTTT							
blaSHV	blaSHV-FW	TGATTTATCTGCGGGATACG	215	55	40	3.99	89.6275	0.9995	Knapp et al., 2010
	blaSHV-RV	TTAGCGTTGCCAGTGCTCG							
tetA	tetA-FW	GCTACATCCTGCTTGCCTTC	250	55	45	4.11	95.559	1	Ng et al., 2001
	tetA-RV	CATAGATCGCCGTGAAGAGG							
sul2	sul2-FW	CTCCGATGGAGGCCGGTAT	190	60	45	2.08	92.6135	1	Luo et al., 2010
	sul2-RV	GGGAATGCCATCTGCCTTGA							
16S rRNA	16S-FW	CGGTGAATACGTTCYCGG	124	56	40	16.9	91.7358	0.9994	Suzuki et al., 2000
	16S-RV	GGWTACCTTGTTACGACTT							

2.4 Sequencing

Approximately 100 ng of DNA for a subset of six locations were sequenced via paired-end shotgun metagenomic sequencing (2x150 bp) on an Illumina NovaSeq 6000 by Mr. DNA (Shallowater, TX). Each library ranges from 10 - 30 million paired-end sequences. All sequence data were deposited into the public NCBI Short Read Archive (SRA) database. The raw sequences were uploaded into Galaxy (https://usegalaxy.org) for processing and assembly. Trimmomatic (Galaxy Version 0.38.0) was used to remove low quality reads from our pair-end data[65]. The following Trimmomatic operations were used: SLIDINGWINDOW: 4, 20, MINLEN: 50, and AVGQUAL: 20. The paired data was assembled using de novo metagenomic assembly by MEGHIT (Galaxy Version 1.2.9) using the default settings of 2 for minimum multiplicity and 200 bp for the minimum length of output contigs[66]. FastQC (Galaxy Version 0.73) and Fasta Statistics (Galaxy Version 2.0) were used for quality control.

ARGs were characterized using the ARGs-OAP pipeline (v2.3) which uses the Structured Antibiotic Resistance Genes database to quantify ARG subtypes by cell number and 16S rRNA[67]. Environmental resistome risk scores were calculated using the MetaCompare pipeline which assigns a risk score based on the co-occurrence of ARGs, MGEs, and pathogens on assembled contigs in a 3D hazard space[68]. Read-based taxonomic classification was performed via the

Kraken2 (v2.0.8) software on the National Microbiome Data Collaborative (NMDC) EDGE bioinformatics platform (https://nmdc-edge.org/).

2.5 Nutrients and turbidity

Total organic carbon (TOC), nitrate, phosphate, total nitrogen, and ammonia concentrations were measured in mg/L for all samples using a Hach DR 2800 spectrophotometer and DRB 200 reactor block (Hach Company, Loveland, CO) according to manufacturer's instructions.

Turbidity was measured on an Orion AQUAfast AQ3010 turbidity meter (Thermo Scientific, Waltham, MA) in NTU.

2.6 Fecal indicator bacteria and antibiotic resistant E. coli enumeration

Fecal indicator bacteria and antibiotic resistant *E. coli* were measured in areas samples taken in Belize City and surrounding coast (n=8). FIB enumeration includes quantifying levels of total coliforms, *Escherichia coli* (Colilert-18, IDEXX), and Enterococci (Enterolert, IDEXX) bacteria using standard methods and kits (IDEXX Laboratories, Westbrook, ME). Final concentrations were reported in MPN/100 mL. Marine samples and samples along the main stem of the river were diluted 10-fold and up to 1,000-fold respectively according to manufacturer recommendations.

For quantifying ESBL *E. coli*, 100 µL of 1 mg/mL cefotaxime was added to each prepared 100 mL IDEXX bottle with Colilert-18 media. Samples were diluted at most 10-fold.

2.7 Statistical analysis

Data were analyzed and visualized in RStudio (v4.0.2). Correlation plots were created with the "corrplot" (v0.90) package. The principal component analysis plot was created using the "prcomp" function and "ggbiplot" (v0.55) package. The "ggplot2" (v3.3.6) package was used to create all bar plots. The 3D plot of the resistome risk factors was created using the “plot3D” (v1.4) package. Heatplots and chord plots were created using the “pheatmap” (v1.0.1) and “circlize” (v0.4.1) package, respectively.

3. Results and discussion

3.1 Concentrations of ARGs and intI1

In this study, five ARGs (*sul*1, *sul*2, *erm*F, *tet*A, and *bla*SHV) were quantified along with *intI*1 via qPCR. **Figure 4-2** depicts the absolute abundances of ARGs and *intI*1 across 18 water samples. The genes sul1, intI1, and sul2 clustered together while ermF and tetA had similar trends. The sites displayed four general clusters with genes being the highest at through Haulover Creek in Belize City (FISH and POUL), the creek’s pourpoint at the coast (NA12), and near the treatment lagoons discharge point (NA11). The next highest groups encompass the other inland samples from Belize River (BRO, BRB, WCSR) and areas in Haulover Creek just before Belize City (MAN and HCM). The third group clustered together areas that are further from the coast of Belize (TC and NA31) and the other inland location in Belize River (WCSL). The sites with the lowest gene concentrations include all locations at Glover’s Reef Atoll (WFR3, CZPR1, LC2, SNORKEL, SWC2) and the coral reef area closest to Belize City, Gallow’s Point Reef (GAL).

Compared to a study in China that surveyed ARGs in corals, our ARG values (2.62×10^{-3} copies/L to 5.42×10^{3} copies/L) are significantly lower than theirs (7.34×10^{4} copies/L to 1.33×10^{7} copies/L). The *sul*1 values in Belize are in the range of three magnitudes lower than those in their study while the *sul*2 in our study are higher[41]. This may be due to the larger populations on one of the islands studied which receive thousands of tourists per day. Another study in Chinese corals also had very high gene copies in their reefs (3.96×10^{7} to 1.65×10^{9} copies/L). In their case, *sul*2 was the most prevalent among their samples[42].

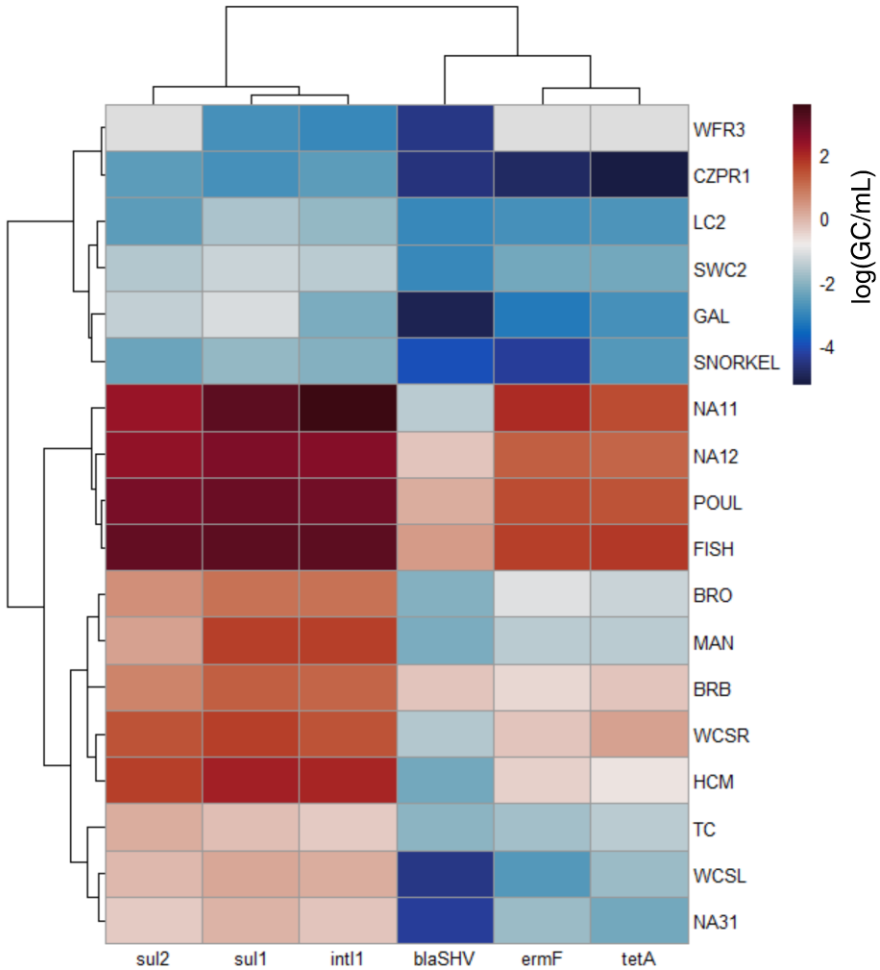

Figure 4-2. Absolute gene abundances for water samples with clustering among genes and locations.

3.2 AMR trends via metagenomic data

Out of the 24 antibiotic classes searched for by the ARGsOAP pipeline, 17 were represented among the samples. The inland locations (WCSR, BRB, FISH) had the highest relative abundances and distribution of AMR classes compared to the coastal waters (NA12 and NA11) and coral reef location (SNORKEL) (**Figure 4-3A**). The fish market location had the highest gene levels while the coral reef location had the lowest. **Figure 4-3B** shows the distribution of the top 10 AMR classes among the six samples sent for sequencing. The top 10 antibiotic classes are bacitracin, multidrug, unclassified, MLS, tetracycline, beta-lactam, sulfonamide, vancomycin, aminoglycoside, and rifamycin. This data also shows the fish market having the highest partition of AMR gene occurrences. 161 out of the 1244 gene were found across the six samples with *bac*A, *mdt*B, and CpxR being the three most prevalent.

A similar study that utilized shotgun sequencing in the coastal waters near the capital of Uruguay also found differing AMR classes between surface waters influenced by sewage and beaches not near sewage pipes[69]. A study in China monitoring the influence of wastewater on antibiotic resistance in surface waters also found bacitracin to be most prevalent among samples. This study attributes this to the inability of the treatment system to eradicate bacitracin resistance genes and its common use for topical therapy and growth promotion in animals[70]. A study in Puerto Rico found higher relative ARG abundances in urbanized surface waters compared to rural and less impacted areas. The most dominant AMR class represented in their samples were multidrug and beta-lactam ARGs revealed through metagenomic data[20].

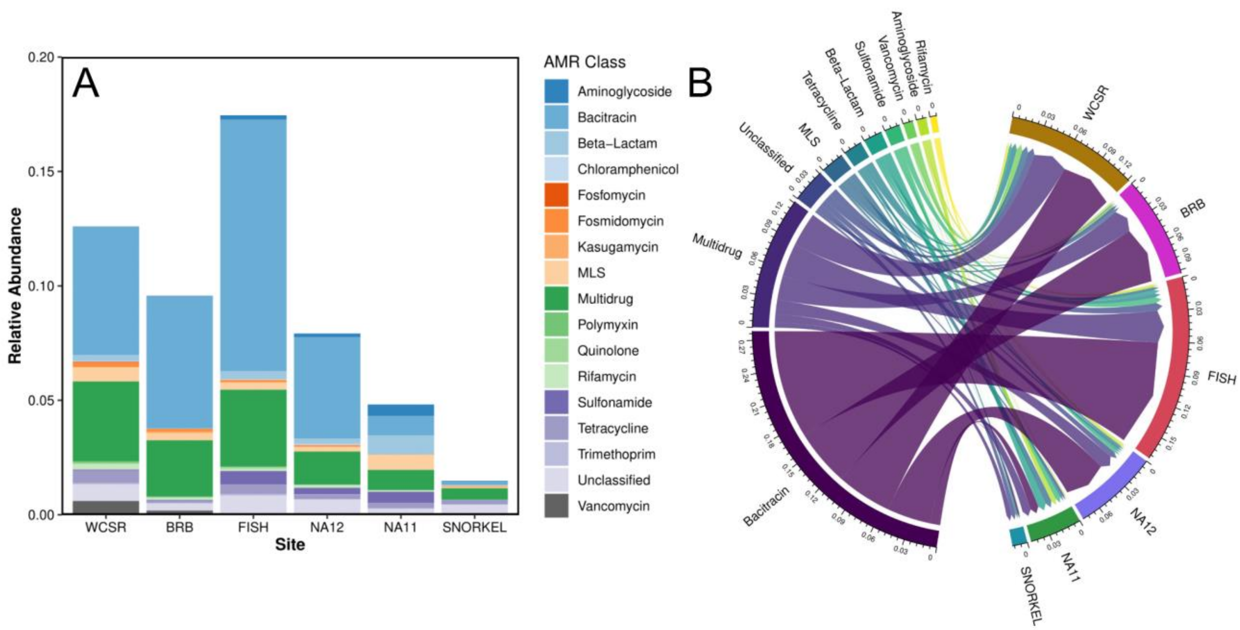

Figure 4-3. (A) Stacked bar plot and (B) chord plot of relative gene abundances of AMR classes among metagenomic samples.

3.3 Microbial diversity

After comparing the top five taxonomies for each site, there were fifteen unique species, with *Polynucleobacter necessarius* (n=4) and *Limnohabitans* sp. 103DPR2 (n=3) being the only two organisms that appeared in over half of the sites. *Polynucleobacter necessarius* and *Limnohabitans* sp. 103DPR2 are ubiquitous in freshwater habitats[71,72], and both are found in sites such as FISH, BRB, and WCSR. The presence of *Polynucleobacter necessariu*s is a key indicator of freshwater habitats[73], thus it is absent from the SNORKEL and NA11 sites.

3.4 Resistome risk

Resistome risk (RR) scores were calculated using the MetaCompare pipeline (**Figure 4-4A**). The inland most site (WCSR) had the highest resistome risk score of 27.6 with the lowest, RR of 21.7, being the coral reef site at Glover's Reef Atoll (SNORKEL). Inland sites in both the Belize River (FISH) and Haulover Creek (BRB) were slightly higher than the corresponding pourpoint samples, NA12 and NA11. The 3-dimensional hazard space was plotted to visualize the co-location of ARGs, MGEs, and pathogens as seen in **Figure 4-4B**. Here the fish market sample had the highest co-location per contig of ARGs, MGEs, and pathogens while the inland Belize River site (WCSR) had the lowest.

Compared to RR scores calculated for a diversity of European water samples, the Belizean samples had scores resembling that on dairy lagoons and wastewater treatment plant effluent[68]. WCSR, FISH, and NA12 sites had the highest RR scores among the samples (24.34 to 27.66) and were similar to the range of European dairy lagoons ($22.71 < RR < 29.02$). BRB, NA11, and SNORKEL had the lowest scores (21.69 -23.35) and most closely resembled the RR scores of European wastewater treatment plant effluent ($18.42 < RR < 22.77$). Our values are also comparable to those found in water samples in Puerto Rico where rural areas had lower values ($RR < 23$) compared to surface waters in urban areas that have impacts of wastewater ($RR > 25$)[20].

In general, RR scores range from 18 to 28 in surface waters where waters with sewage influences may have similar or even lower scores than those that do not. The RR scores are better suited to distinguish among surface waters and sewage and wastewater treatment plant influent.

In terms of co-location, FISH had the highest instances of contigs (n=7) with the presence of ARGs, MGEs, and pathogens which resulted in a high RR score. Though WCSR did not exhibit any contigs with co-location of ARGs with MGEs and pathogens, the higher ratio of ARGs per contig resulted in the highest RR score even compared to FISH which has the most co-location. This shows that the RR score is greatly influenced by the hits against the CARD database and number of contigs. Other MetaCompare users have also calculated similar RR scores despite having variations among co-located contigs, specifically for samples with decent water quality[74].

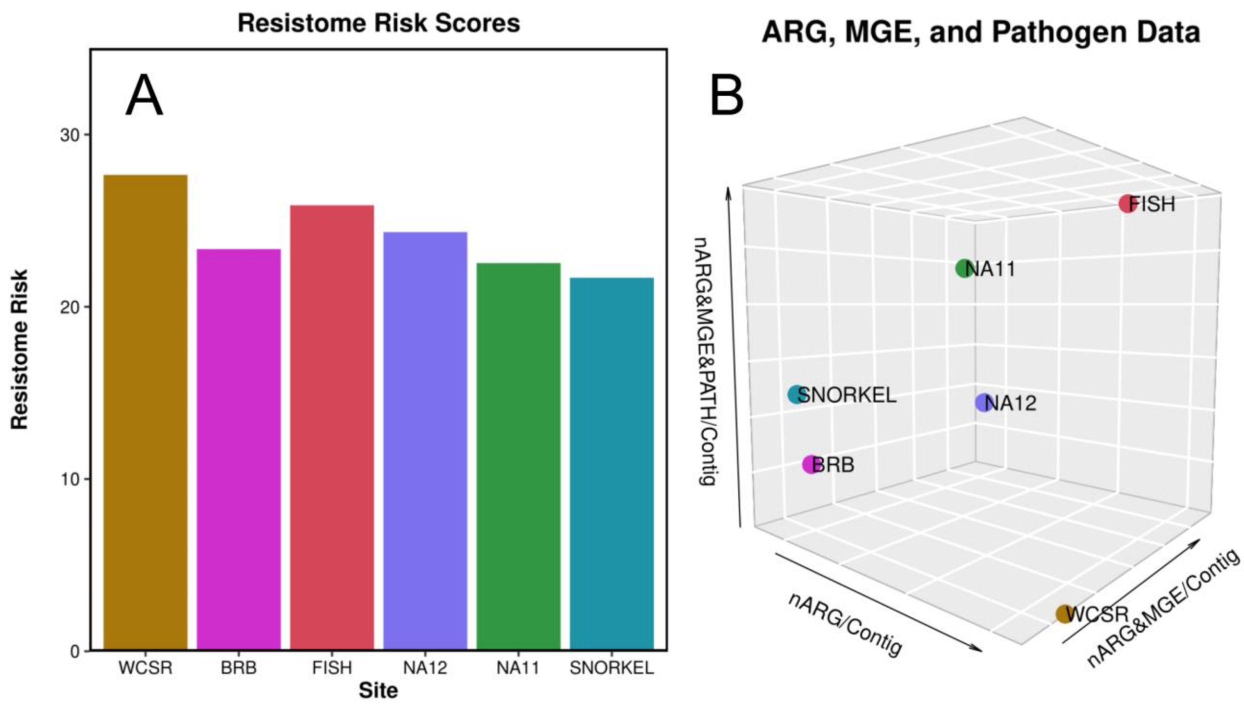

Figure 4-4. (A) Resistome risk scores and (B) 3D hazard space of co-located ARG, MGEs, and pathogens per contig.

3.5 Fecal indicator bacteria and ESBL E. coli

Figure 4-5A and **4-B** depict levels of total coliform and *E. coli* measured by the IDEXX Colilert-18 tests. The red and yellow lines signify the EPA standards for bacteria in recreational waters. From the eight sites measured, FIB levels were highest near the poultry (POUL) and fish market (FISH) along Haulover Creek. Total coliform and *E. coli* levels for FISH exceeded EPA standards, with POUL also being above recommendations for *E. coli*. With the addition of Cefotaxime to the Colilert-18 tests, ESBL-producing *E. coli* were detected mainly at FISH, although the resistance ratio was highest for POUL and NA12.

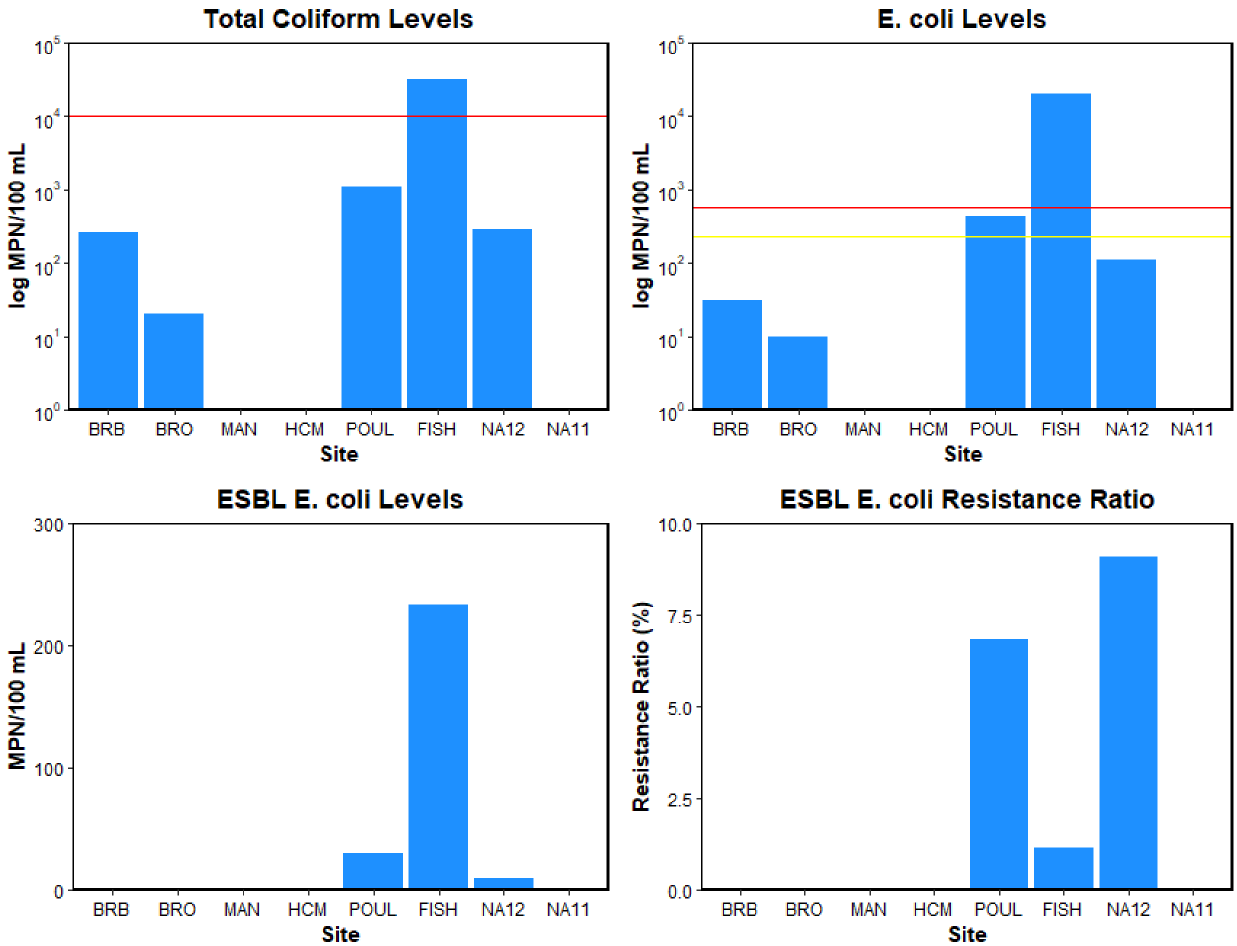

Figure 4-5. Results from IDEXX Colilert-18 tests measuring total coliform (A) and E. coli levels (B). Graphs (C) and (D) are results from Colilert-18 tests modified with Cefotaxime antibiotic.

3.6 Correlations among ARGs, nutrients, and FIB

Figure 4-6 shows the correlation coefficients for normalized ARGs, 16S rRNA, *intI*1, FIB, and nutrients. There were very strong positive correlations ($p < 0.001$) among all ARGs except *erm*F and *bla*SHV. The correlations between *sul*1, *sul*2, and *intI*1 are typically strong compared to macrolide and tetracycline resistance genes[75,76]. There were also strong positive correlations among FIB ($p < 0.001$) and FIB and ammonia ($p < 0.05$). Ammonia also had strong correlations with 16S rRNA ($p < 0.001$) and total nitrogen correlated with the *E. coli* resistance ratio ($p < 0.05$). The *bla*SHV gene also correlated with phosphate ($p < 0.05$) and ammonia ($p < 0.05$). A study in surface waters in Malaysia also found strong positive correlations among ARGs, ESBL *E. coli*, MGEs, and nutrients[77].

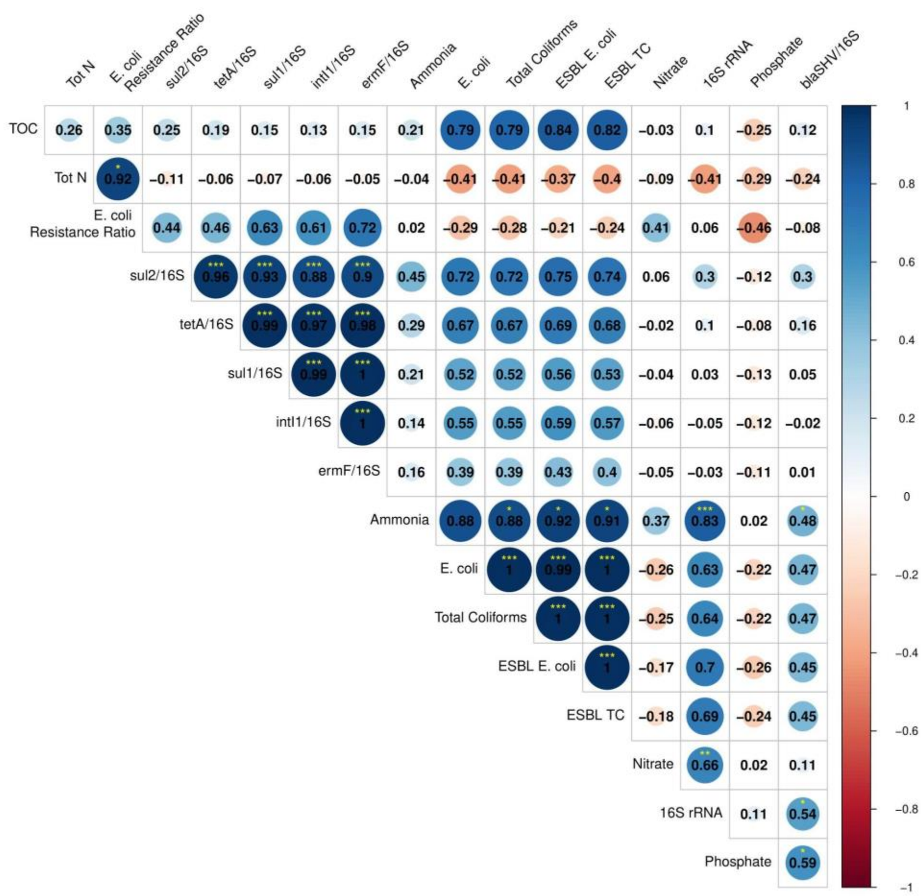

Figure 4-6. Correlation plot of ARGs, nutrients, and FIB. One star ('*'), Two stars ('**'), Three stars ('***') denote p-values less than 0.05, 0.01, and 0.001, respectively.

4. Conclusions

In this study, various methods to monitor antibiotic resistance were conducted in a variety of water types in Belize, including coral reefs. This study adhered to the World Health Organization's Tricyle environmental surveillance framework which calls for a collection of water samples in hotspot sources such as wet markets, wastewater discharge, and upstream and downstream of major cities. The areas closest to Belize City, the most populated city in Belize, had elevated ARGs, particularly the fish market in Haulover Creek and the area of the coast closest to the treatment lagoon. These two areas also had the greatest instances of co-location of ARGs, MGEs, and pathogens as revealed by metagenomic data and high FIB and ESBL *E. coli* by culture methods. Though coral reef areas had lower ARGs than the inland and coastal sites, they were not completely devoid of ARGs, indicating the influence of anthropogenic pollution. Here, viability, amplification, and sequencing methods for monitoring antibiotic resistance proved to be useful in identifying these dynamic pollutants in an understudied part of the world. Thus more studies should be conducted in Central America to reveal the threats of antibiotic resistance on human health and ecological impacts.

5. References

1. Levy, S. B. The Challenge of Antibiotic Resistance. **278**, 46–53 (1998).
2. Neu, H. C. The Crisis in Antibiotic Resistance. *Science (80-.).* **257**, 1064–1073 (1992).
3. Murray, C. J. *et al.* Global burden of bacterial antimicrobial resistance in 2019: a systematic analysis. *Lancet* **399**, 629–655 (2022).
4. Bombaywala, S., Mandpe, A., Paliya, S. & Kumar, S. Antibiotic resistance in the environment: a critical insight on its occurrence, fate, and eco-toxicity. *Environ. Sci. Pollut. Res.* 1–28 (2021) doi:10.1007/s11356-021-13143-x.
5. He, Y. *et al.* Antibiotic resistance genes from livestock waste: occurrence, dissemination, and treatment. *npj Clean Water* **3**, 4 (2020).
6. Luiken, R. E. C. *et al.* Farm dust resistomes and bacterial microbiomes in European poultry and pig farms. *Environ. Int.* **143**, 105971 (2020).

7. Yang, F., Han, B., Gu, Y. & Zhang, K. Swine liquid manure: a hotspot of mobile genetic elements and antibiotic resistance genes. *Sci. Rep.* **10**, 15037 (2020).

8. Chee-Sanford, J. *et al.* Fate and Transport of Antibiotic Residues and Antibiotic Resistance Genes following Land Application of Manure Waste. *J. Environ. Qual.* **38**, 1086–1108 (2009).

9. Cira, M. *et al.* Commercially available garden products as important sources of antibiotic resistance genes—a survey. *Environ. Sci. Pollut. Res.* 1–8 (2021) doi:10.1007/s11356-021-13333-7.

10. Zhao, X., Wang, J., Zhu, L., Ge, W. & Wang, J. Environmental analysis of typical antibiotic-resistant bacteria and ARGs in farmland soil chronically fertilized with chicken manure. *Sci. Total Environ.* **593–594**, 10–17 (2017).

11. Hung, W. C. *et al.* Tracking antibiotic resistance through the environment near a biosolid spreading ground: Resistome changes, distribution, and metal(loid) co-selection. *Sci. Total Environ.* **823**, 153570 (2022).

12. Jacobs, K., Wind, L., Krometis, L.-A., Hession, W. C. & Pruden, A. Fecal Indicator Bacteria and Antibiotic Resistance Genes in Storm Runoff from Dairy Manure and Compost-Amended Vegetable Plots. *J. Environ. Qual.* **48**, 1038–1046 (2019).

13. Munir, M. & Xagoraraki, I. Levels of Antibiotic Resistance Genes in Manure, Biosolids, and Fertilized Soil. *J. Environ. Qual.* **40**, 248–255 (2011).

14. Zhang, M. *et al.* Variation of antibiotic resistome during commercial livestock manure composting. *Environ. Int.* **136**, 105458 (2020).

15. Almakki, A., Jumas-Bilak, E., Marchandin, H. & Licznar-Fajardo, P. Antibiotic resistance in urban runoff. *Sci. Total Environ.* **667**, 64–76 (2019).

16. Baral, D. *et al.* Tracking the Sources of Antibiotic Resistance Genes in an Urban Stream during Wet Weather using Shotgun Metagenomic Analyses. *Environ. Sci. Technol.* **52**, 9033–9044 (2018).

17. Garner, E. *et al.* Stormwater loadings of antibiotic resistance genes in an urban stream. *Water Res.* **123**, 144–152 (2017).

18. Zhang, S. *et al.* Antibiotic concentration and antibiotic-resistant bacteria in two shallow urban lakes after stormwater event. *Environ. Sci. Pollut. Res.* **23**, 9984–9992 (2016).

19. Czekalski, N., Gascón Díez, E. & Bürgmann, H. Wastewater as a point source of antibiotic-resistance genes in the sediment of a freshwater lake. *ISME J. 2014 87* **8**, 1381–1390 (2014).

20. Davis, B. C. *et al.* Demonstrating an Integrated Antibiotic Resistance Gene Surveillance Approach in Puerto Rican Watersheds Post-Hurricane Maria. *Environ. Sci. Technol.* **54**, 15108–15119 (2020).

21. Eramo, A., Morales Medina, W. R. & Fahrenfeld, N. L. Viability-based quantification of antibiotic resistance genes and human fecal markers in wastewater effluent and receiving

waters. *Sci. Total Environ.* **656**, 495–502 (2019).

22. Proia, L. *et al.* Antibiotic resistance along an urban river impacted by treated wastewaters. *Sci. Total Environ.* **628**–**629**, 453–466 (2018).

23. Rodriguez-Mozaz, S. *et al.* Occurrence of antibiotics and antibiotic resistance genes in hospital and urban wastewaters and their impact on the receiving river. *Water Res.* **69**, 234–242 (2015).

24. Dalton, K. R., Rock, C., Carroll, K. C. & Davis, M. F. One Health in hospitals: how understanding the dynamics of people, animals, and the hospital built-environment can be used to better inform interventions for antimicrobial-resistant gram-positive infections. *Antimicrob. Resist. Infect. Control* **9**, 78 (2020).

25. Keenum, I. *et al.* A framework for standardized qPCR-targets and protocols for quantifying antibiotic resistance in surface water, recycled water and wastewater. (2022) doi:10.1080/10643389.2021.2024739.

26. Nielsen, M. C., Wang, N. & Jiang, S. C. Acquisition of antibiotic resistance genes on human skin after swimming in the ocean. *Environ. Res.* **197**, 110978 (2021).

27. Vikesland, P. J. *et al.* Toward a Comprehensive Strategy to Mitigate Dissemination of Environmental Sources of Antibiotic Resistance. 13061–13069 (2017) doi:10.1021/acs.est.7b03623.

28. Zhu, Y.-G. *et al.* Continental-scale pollution of estuaries with antibiotic resistance genes. *Nat. Microbiol.* **2**, 16270 (2017).

29. Domínguez, D. C., Chacón, L. M. & Wallace, D. Anthropogenic Activities and the Problem of Antibiotic Resistance in Latin America: A Water Issue. *Water 2021, Vol. 13, Page 2693* **13**, 2693 (2021).

30. Farrar, W. E. Antibiotic Resistance in Developing Countries. *Source J. Infect. Dis.* **152**, 1103–1106 (1985).

31. Vlieghe, E., Phoba, M. F., Tamfun, J. J. M. & Jacobs, J. Antibiotic resistance among bacterial pathogens in Central Africa: a review of the published literature between 1955 and 2008. *Int. J. Antimicrob. Agents* **34**, 295–303 (2009).

32. Husaini, D. C. *et al.* Field-based screening of selected oral antibiotics in Belize. *PLoS One* **15**, e0234814 (2020).

33. Cuevas, C., Batura, N., Wulandari, L. P. L., Khan, M. & Wiseman, V. Improving antibiotic use through behaviour change: a systematic review of interventions evaluated in low- and middle-income countries. *Health Policy Plan.* **36**, 754–773 (2021).

34. Iskandar, K. *et al.* Surveillance of antimicrobial resistance in low- and middle-income countries: a scattered picture. *Antimicrob. Resist. Infect. Control 2021 101* **10**, 1–19 (2021).

35. Nadimpalli, M. *et al.* Combating Global Antibiotic Resistance: Emerging One Health Concerns in Lower- and Middle-Income Countries. *Clin. Infect. Dis.* **66**, 963–969 (2018).

36. Sulis, G., Sayood, S. & Gandra, S. Antimicrobial resistance in low- and middle-income countries: current status and future directions. *Expert Rev. Anti. Infect. Ther.* **20**, 147–160 (2022).

37. Vieira, D. C., Lima, W. G. & de Paiva, M. C. Plasmid-mediated quinolone resistance (PMQR) among Enterobacteriales in Latin America: a systematic review. *Mol. Biol. Rep.* **47**, 1471–1483 (2020).

38. Martínez M, J. D., Henao R, S. C. & Lizarazo R, J. I. Antibiotic Resistance of Helicobacter pylori in Latin America and the Caribbean. *Rev Col Gastroenterol* **29**, 218–227 (2014).

39. Ortiz, V. *et al.* Helicobacter pylori antimicrobial resistance and antibiotic consumption in the low-resource Central America setting. *Helicobacter* **24**, e12595 (2019).

40. Reichert, G., Hilgert, S., Fuchs, S. & Azevedo, J. C. R. Emerging contaminants and antibiotic resistance in the different environmental matrices of Latin America. *Environ. Pollut.* **255**, 113140 (2019).

41. Liu, S., Su, H., Pan, Y. F. & Xu, X. R. Spatial and seasonal variations of antibiotics and antibiotic resistance genes and ecological risks in the coral reef regions adjacent to two typical islands in South China Sea. *Mar. Pollut. Bull.* **158**, 111424 (2020).

42. Zhongjie, W. *et al.* Occurrence and characteristics of antibiotic resistance genes in the coral reef ecosystems along the east coast of Hainan Island. *J. Trop. Biol.* **13**, (2022).

43. Husaini, D. C., Abubakar, Y., Harris-Thurton, L. & Mphuthi, D. D. Over-The-Counter Sales of Antibiotics at Community Pharmacies in Belize: A Cross-Sectional Simulated Client Visit study. *Integr. J. Med. Sci.* **8**, 1–5 (2021).

44. Husaini, D. C., Mphuthi, D. D. & Abubakar, Y. Self-Medication Practices Among College Students in Belize : a Nationwide Cross Sectional Study. *World J. Pharamceutical Res.* **8**, 238–254 (2019).

45. Shears, P., Hart, C. A. & Suliman, G. A preliminary investigation of antibiotic resistance in Enterobacteriaceae isolated from children with diarrhoea from four developing countries. *Ann. Trop. Med. Parasitol.* **82**, 185–188 (1988).

46. Dillon, J. A. R. *et al.* Challenges in the control of gonorrhea in South America and the Caribbean: Monitoring the development of resistance to antibiotics. *Sex. Transm. Dis.* **33**, 87–95 (2006).

47. Cheng, J., Zetina, Z., Cheng, J. & Zetina, Z. A Study to Investigate the Impact of the COVID-19 Pandemic on Tourist Arrivals in Belize. *Open J. Soc. Sci.* **9**, 326–334 (2021).

48. Emrich, K., Martinez-Colon, M. & Alegria, H. Is untreated sewage impacting coral reefs of Caye Caulker, Belize? *J. Foraminifer. Res.* **47**, 20–33 (2017).

49. Felgate, S. L. *et al.* Conversion of Forest to Agriculture Increases Colored Dissolved Organic Matter in a Subtropical Catchment and Adjacent Coastal Environment. *J. Geophys. Res. Biogeosciences* **126**, 1–19 (2021).

50. Wells, C. E. *et al.* Wastewater technopolitics on the southern coast of Belize. *Econ. Anthropol.* **6**, 277–290 (2019).

51. Lapointe, B. E., Tewfik, A. & Phillips, M. Macroalgae reveal nitrogen enrichment and elevated N:P ratios on the Belize Barrier Reef. *Mar. Pollut. Bull.* **171**, 112686 (2021).

52. Blackburn, J. K., Mitchell, M. A., Blackburn, M.-C. H., Curtis, A. & Thompson, B. A. EVIDENCE OF ANTIBIOTIC RESISTANCE IN FREE-SWIMMING , TOP-LEVEL MARINE PREDATORY FISHES. *J. Zoo Wildl. Med.* **41**, 7–16 (2010).

53. Drexler, K. The New River Report: Socio-Ecological System Impacts of Anthropogenic Pollution on New River Communities in Belize. *Glob. Secur. Intell. Stud.* **5**, (2020).

54. Miłobedzka, A. *et al.* Monitoring antibiotic resistance genes in wastewater environments: The challenges of filling a gap in the One-Health cycle. *J. Hazard. Mater.* **424**, 127407 (2022).

55. Nguyen, A. Q. *et al.* Monitoring antibiotic resistance genes in wastewater treatment: Current strategies and future challenges. *Sci. Total Environ.* **783**, 146964 (2021).

56. World Health Organization. *WHO integrated global surveillance on ESBL-producing E. coli using a "One Health" approach: implementation and opportunities*. (2021).

57. UNESCO. *World Heritage Committee; 20th; Convention concerning the Protection of the World Cultural and Natural Heritage; report; 1997*. (1996).

58. Cho, L. Marine protected areas: a tool for integrated coastal management in Belize. *Ocean Coast. Manag.* **48**, 932–947 (2005).

59. Claudino-Sales, V. Belize Barrier Reef System, Belize. in *Coastal Research Library* vol. 28 451–456 (Springer, 2019).

60. Cherrington, E. A. *et al.* Use of public Earth observation data for tracking progress in sustainable management of coastal forest ecosystems in Belize, Central America. *Remote Sens. Environ.* **245**, 111798 (2020).

61. Huntington, B. E., Karnauskas, M. & Lirman, D. Corals fail to recover at a Caribbean marine reserve despite ten years of reserve designation. *Coral Reefs* **30**, 1077–1085 (2011).

62. Babcock, E. A., Coleman, R., Karnauskas, M. & Gibson, J. Length-based indicators of fishery and ecosystem status: Glover's Reef Marine Reserve, Belize. *Fish. Res.* **147**, 434–445 (2013).

63. Flowers, K. *et al.* Varying reef shark abundance trends inside a marine reserve: evidence of a Caribbean reef shark decline. doi:10.3354/meps13954.

64. Prouty, N. G., Hughen, K. A. & Carilli, J. Geochemical signature of land-based activities in Caribbean coral surface samples. *Coral Reefs* **27**, 727–742 (2008).

65. Bolger, A. M., Lohse, M. & Usadel, B. Trimmomatic: a flexible trimmer for Illumina sequence data. *Bioinformatics* **30**, 2114–2120 (2014).

66. Li, D., Liu, C.-M., Luo, R., Sadakane, K. & Lam, T.-W. MEGAHIT: an ultra-fast single-node solution for large and complex metagenomics assembly via succinct de Bruijn graph. doi:10.1093/bioinformatics/btv033.

67. Yin, X. *et al.* ARGs-OAP v2.0 with an expanded SARG database and Hidden Markov Models for enhancement characterization and quantification of antibiotic resistance genes in environmental metagenomes. *Bioinformatics* **34**, 2263–2270 (2018).

68. Oh, M. *et al.* MetaCompare: a computational pipeline for prioritizing environmental resistome risk. *FEMS Microbiol. Ecol.* **94**, 79 (2018).

69. Fresia, P. *et al.* Urban metagenomics uncover antibiotic resistance reservoirs in coastal beach and sewage waters. *Microbiome 2019 71* **7**, 1–9 (2019).

70. Tang, Y., Liang, Z., Li, G., Zhao, H. & An, T. Metagenomic profiles and health risks of pathogens and antibiotic resistance genes in various industrial wastewaters and the associated receiving surface water. *Chemosphere* **283**, 131224 (2021).

71. Hahn, M. W., Lang, E., Brandt, U., Wu, Q. L. & Scheuerl, T. Emended description of the genus Polynucleobacter and the species P. necessarius and proposal of two subspecies, P. necessarius subspecies necessarius subsp. nov. and P. necessarius subsp. a symbioticus subsp. nov. *Int. J. Syst. Evol. Microbiol.* **59**, 2002 (2009).

72. Kasalický, V. *et al.* Aerobic anoxygenic photosynthesis is commonly present within the genus Limnohabitans. *Appl. Environ. Microbiol.* **84**, (2018).

73. Methe, B. A., Hiorns, W. D. & Zehr, J. P. Contrasts between marine and freshwater bacterial community composition: Analyses of communities in Lake George and six other Adirondack lakes. *Limnol. Oceanogr.* **43**, 368–374 (1998).

74. Majeed, H. J. *et al.* Evaluation of Metagenomic-Enabled Antibiotic Resistance Surveillance at a Conventional Wastewater Treatment Plant. *Front. Microbiol.* **12**, 1–19 (2021).

75. Sabri, N. A. *et al.* Prevalence of antibiotics and antibiotic resistance genes in a wastewater effluent-receiving river in the Netherlands. *J. Environ. Chem. Eng.* **8**, 102245 (2020).

76. Wang, R., Ji, M., Zhai, H., Guo, Y. & Liu, Y. Occurrence of antibiotics and antibiotic resistance genes in WWTP effluent-receiving water bodies and reclaimed wastewater treatment plants. *Sci. Total Environ.* **796**, 148919 (2021).

77. Ott, A. *et al.* Developing Surrogate Markers for Predicting Antibiotic Resistance "Hot Spots" in Rivers Where Limited Data Are Available. *Environ. Sci. Technol.* **55**, 7466–7478 (2021).

Chapter 5: Use of Google Earth Engine for teaching coding and monitoring of environmental change: a case study among STEM and non-STEM students

1. Introduction

Underrepresented minorities (URM) and women remain at disproportionately low numbers in science, technology, engineering, and math (STEM) and the research workforce despite efforts to increase diversity [1–4]. In 2016, women earned only 20% of Bachelor's degrees in engineering and URM students only received 22% of all engineering Bachelor's degrees in the United States [5]. Intervention efforts seeking to increase diversity in STEM include research experiences, mentoring, financial assistance, and graduate school preparation [6]. However, most first-generation and URM students do not have sufficient resources, time, and knowledge of opportunities to secure an intern position in a STEM laboratory [7]. This issue was heightened during the COVID-19 pandemic as students had limited research opportunities and weren't effectively able to explore and learn new skills to inform their future careers [8,9]. Interventions in the classroom setting have proven to increase self-efficacy, feelings of agency, and desire to pursue research among women and URM. Class modules incorporating research have been shown to improve female students' self-perception in inquiry skills and attitudes toward science [10]. Teaching undergraduate research skills in an engineering classroom found that 20% of participating students enjoyed research enough to pursue a Ph.D. degree [11].

Course-based undergraduate research experiences (CUREs) are considered to be the next generation of inquiry-based learning, which traditionally has engaged students in research that was not of wide interest to the scientific community. CUREs provide an opportunity for students to engage in research, such as through the collection and analysis of environmental samples, that could lead to important and relevant scientific discoveries [12]. The data from a CURE should either be of interest to the wider scientific community or contribute to a larger database. Notably, CUREs are viewed as an inclusive model for engaging students in research [13–15]. When research is included as part of college courses and all students take part in the research project, there is more equitable access to research opportunities, which bring significant and well-documented advantages for the learning process [7,16]. This practice is encouraged by the National Academies of Science, Engineering, and Mathematics as a way to increase inclusivity, encourage collaborative work, and expose more students to the research methodology of particular scientific disciplines [17]. Because outcomes are unknown, students can experience the excitement of true discovery. Further, when research embedded in courses contributes to a collective dataset, students feel part of a larger research community [18] and can promote conversations between scientists and students outside of class [19].

Coding, remote sensing, and data visualization are useful skills for undergraduate students to learn. Learning scientific and problem-solving skills should not be limited to only STEM majors, but also to non-STEM students to increase science literacy among all citizens [20,21]. Computational skills are necessary for fields beyond engineering and computer science, and a study has found utility in teaching these skills to non-STEM students [22]. Foundationally, programming encompasses the wider practice of conceptualizing and visualizing abstract data and translating it into other situations which develops one's critical thinking further [23]. Coding skills can further be used to popularize remote sensing skills which can be utilized to help students understand human-environment interaction [24,25].

It is important to increase students' self-efficacy and sense of agency to visualize environmental change and to gauge their interest in a career in STEM research, especially during the COVID-19 pandemic. Studies have yet to investigate the value of teaching remote sensing and computational skills to STEM and non-STEM students. The goal of this study was to integrate remote sensing modules in an engineering, upper-division class (STEM class) and freshman writing course with a focus on the environment (non-STEM class) and understand its influences on feelings of agency and self-efficacy in using the skills learned and interest in STEM research. The STEM students also partook in a CURE to apply their skills from the remote sensing modules on an original research topic.

2. Methods

2.1 Background on the courses

This study was implemented in two different courses at a large public research university in southern California during the winter term of 2022. During this term, the first two weeks of the courses were virtual due to rising COVID-19 cases in the university's county. The rest of the term was hybrid. The first course is an upper-division engineering course (STEM class) focused on the chemical fate and transport in aquatic environments. This 10-week course usually takes place once a year with around 50 students self-enrolling in the class. The course was taught by one professor with three 25% teaching assistants. These students are typically STEM majors in their junior or senior year at the university. The second course where the intervention was implemented is a freshman writing cluster course (non-STEM class) focused on food systems through the lens of the environment and sustainability. The class is offered yearlong with approximately 150 mainly non-STEM students self-enrolling to fulfill science and writing general education requirements. In this course, four instructors collaboratively taught different portions of the class with four teaching assistants and the intervention took place during two of the professors' instructional periods.

To gauge the demographics of the students in both classes, participants self-reported their information in a survey. The frequencies and percentages of student demographic information for the two classes including data for students who fully participated in the study are in **Table 5-1**. A first-generation student herein was defined as "a student whose parent(s)/guardian(s) have no education experience past high school" according to a definition from the US Department of Education [26]. Participating students were allowed to select one or multiple racial and ethnic identities and underrepresented minorities (URM) were classified based on three racial and ethnic groups—blacks, Hispanics, and American Indians or Alaska Natives according to the National Science Foundation [27]. In the STEM class (n=25), 44% female, 52% male, and 4% non-binary were reported. 24% of students were identified as first-generation students, and 16% were identified as URM. In the non-STEM class (n=95), 75%, 22%, 1%, and 1% of participants were identified as female, male, gender-nonconforming, and preferred not to answer, respectively. Among the same participants, approximately 24% identified as first-generation, and 33% URM were classified. At the institutional level, students are 58% female, 41% male, 31% first-generation students, and around 23% are classified as URM.

Table 5-1. Frequency and percent of student classification by gender, first-generation student, underrepresented minority, and COVID-19 pandemic research opportunity response per class.

Course	Category	Frequency	Percent (%)
Gender			
STEM	Female	11	44
	Male	13	52
	Non-binary	1	4
Non-STEM	Female	72	75.79
	Male	21	22.11
	Gender-nonconforming	1	1.05
	Prefer not to answer	1	1.05
First-generation Student			
STEM	No	19	76
	Yes	6	24
Non-STEM	No	72	75.79
	Yes	23	24.21
Underrepresented Minority Students (URM)			
STEM	Non-URM	21	84
	URM	4	16

Non-STEM	Non-URM	63	66.32
	URM	32	33.68
Research opportunity impacted by pandemic			
STEM	Maybe	3	12
	No	11	44
	Yes	11	44
Non-STEM	Maybe	41	43.16
	No	45	47.37
	Yes	9	9.47

2.2 The intervention

The intervention involved two modules consisting of both in-class instruction and assignments. Students learned the basics of Google Earth Engine (GEE) through the two modules over a three-week time span. GEE is a cloud-based geospatial analysis platform that allows users to visualize and analyze satellite-derived data. GEE may be used with JavaScript and Python, but in this intervention, we used the JavaScript Application Programming Interface (API). Throughout the class instruction, students were introduced to GEE with interactive tutorials with guidance from the instructor. Topics of the tutorials involve climate change effects on sea ice, sea surface temperature, and deforestation. Tutorials consist of pre-created and tested scripts adapted from existing Geospatial Ecology and Remote Sensing (GEARS) labs (www.gears-lab.com) that students were able to paste into their code editors in real-time. During in-class instruction, students learned how to change the area of analysis and the time frame within the coded script, learned about different satellite missions and their different properties, and how to create maps and charts for analysis.

2.3 Assignments

There were two short assignments following in-class instruction for students to explore the basic functionalities of GEE and begin to compare results from different locations and time frames. The objectives of the assignments were for students to learn to modify scripts to answer questions regarding environmental change and to identify potential causes (i.e., climate and/or anthropogenic causes). The students were required to create new maps in addition to their responses.

In Assignment 1, students visualized albedo, sea surface temperature, and sea ice cover around the world using 500 m Daily MODIS Albedo and 4 km NOAA AVHRR Pathfinder images. Students were asked to visualize a part of the world different from the example and explain why some areas have different values and characteristics for the respective parameters.

In Assignment 2, students used true color imagery to visualize the campus. In particular, they used a false-color composite to look at vegetation and calculated the normalized-difference vegetation index (NDVI) using Sentinel-2 MSI images. Students applied the same skills to examine deforestation in Rondonopolis, Brazil due to the edge effects of agricultural conversion.

The STEM students had an additional assignment before the CURE to prepare them for their respective projects. Since the CURE would involve using remote sensing to look at the effects of the COVID-19 anthropause on water quality during and after the pandemic, students read an article that conducted a similar analysis in Belize[28]. The STEM students completed a reading guide assignment based on this article to indicate an understanding of the appropriate background and methods for the CURE project.

2.4 The CURE

In the second half of the term, the STEM students were introduced to the CURE portion of the class. The project involved using a water quality remote sensing tool to investigate changes to water quality due to the COVID-19 anthropause. Students were assigned to randomized groups of three to five students and selected a region of interest for their project. The students used a modified version of the Optical Reef and Coastal Area Assessment (ORCAA) tool created by the Belize and Honduras Water Resources NASA DEVELOP team (https://github.com/NASA-

DEVELOP/ORCAA). In this tool, Sentinel-2 MSI and Aqua MODIS satellite imagery are used to visualize water quality changes in coastal areas around the world. Sentinel-2 imagery is used to visualize turbidity, color dissolved organic matter, chlorophyll-a, and normalized difference chlorophyll index. Sea surface temperature, chlorophyll-a, Kd(490) (a proxy for water clarity), and particulate organic carbon can be assessed with Aqua. The students had to identify two nearby locations in their study region for comparison: one where they suspect the anthropause will have affected water quality and a control site. A total of 15 STEM student groups analyzed the following areas: Thailand, Singapore, San Diego, California, USA, Port of Long Beach in California, Australia, Nigeria, Maldives, India, Houston, Texas, USA, Ho Chi Minh City, Vietnam, Hawaii, USA, and Alaska, USA. The students wrote a final report giving background on how COVID-19 shutdowns affected their area of interest in terms of travel and commerce and attempted to explain water quality findings during and after the COVID-19 shutdown using scientific literature and regional news articles. The report also included their maps and time series plots for each location and water quality parameters. The students augmented their conclusions through supplemental spreadsheets of their time series data and images of their maps.

2.5 Surveys

Confidential pre- and post-surveys were used to assess shifts in self-efficacy in coding, remote sensing, interest in science, and an environmental research career. The surveys were administered through Google Forms which collected responses anonymously. Previously, we've used similar assessment methods which revealed an increased interest in science among K-12 students through service learning research courses [29,30]. The surveys included a five-point Likert scale, free response, and multiple-choice questions. There were five core Likert statements in both surveys for students to rate their ability to modify code, understand remote sensing, interest in science, and have an environmental research career (**Table 5-2**). The first three questions of each survey asked for the students' favorite number, the name of their first best friend, and the name of their first pet to facilitate pairing the pre- and post-surveys. The pre-survey had additional questions on demographics, major, year, gender, and identification as a first-generation college student. The post-survey included additional multiple-choice and free-response questions on the effect of the pandemic on their ability to engage in a research experience. The surveys were approved by the university's Institutional Review Board.

Table 5-2. Likert statements included in both pre- and post-surveys.

Core Likert Statements
Q1. I am confident in my ability to leverage current coding skills to investigate environmental change.
Q2. I am confident in my ability to make small edits to code.
Q3. I understand remote sensing for studying the environment.
Q4. I have a strong interest in science.
Q5. I would consider a career in environmental research.

2.6 Statistical analysis

Survey results were processed and analyzed using Excel, RStudio, and Python. The survey data was screened for duplicate entries, typos, and inconsistent response entries in RStudio. The pre- and post-surveys were paired for students using Fuzzy Lookup in Excel using the first three questions. Python was then utilized for statistical processing and visualization of the paired data. Different student identities were grouped for analysis by gender, first-generation, and URM with the Pandas package. Likert statement results were visualized using the Plot_Likert and Pyplot extensions of Matplotlib in Python. The SciPy.Stats sub-package was used to calculate the means for the Likert responses based on each grouping and question and mean differences in the paired data. A paired t-test analysis was done in Python through SciPy.Stats library, at a 95% level of significance for each student grouping and Likert statement. The COVID-19 free responses were recorded into more meaningful categories where recurring themes were identified, such as lack of opportunity and financial burden.

3. Results

In the two courses, the non-STEM class had 160 students enrolled and 95 pairable surveys (59% response rate), and the STEM class had 60 students enrolled which resulted in 25 pairable surveys (41% response rate). In reporting summative gains for each goal, overall students in both courses demonstrated increased confidence values regarding their environmental literacy and ability to modify and apply code for research purposes (**Figure 5-1**). Additional Likert plots are in the **Supplementary Material**.

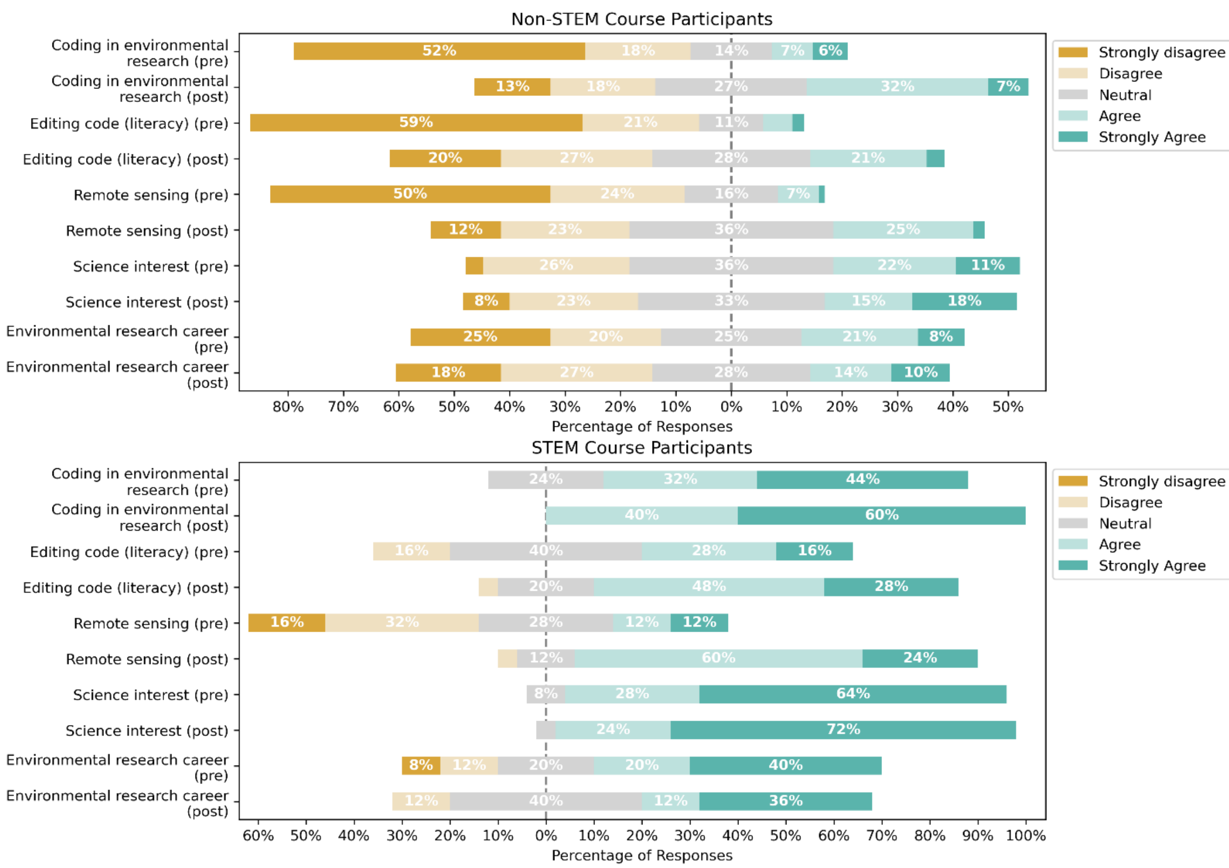

Figure 5-1. Likert plots of non-STEM and STEM student participants pre and post responses to the 5 Likert statements.

3.1 Non-STEM case study

In pre-course and post-course surveys, respondents in the non-STEM course in all concerned demographic groups increased their mean response score (on a scale of 1 to 5) regarding skill-based assessments (Q1: coding in environmental research relationship, Q2: coding edits (literacy), and Q3: remote sensing) indicating some gained knowledge and confidence (**Table 5-3**). Based on the paired t-test p-values all non-STEM students had statistically significant increases for Q1, Q2, and Q3. Most notably, non-STEM females displayed greater differences ($p \leq 0.001$) after the modules compared to the non-STEM males ($p \leq 0.01$). All first-generation and URM non-STEM students had statistically significant increases ($p \leq 0.001$) in their selections for Q1, Q2, and Q3.

Table 5-3. Mean differences for the five core Likert statements between pre- and post-surveys for paired student responses per student grouping. Three asterisks denote paired t-test p-values ≤ 0.001, 2 asterisks denote p-values ≤ 0.01, and one asterisk is p-values ≤ 0.05.

Category	Class	Q1	Q2	Q3	Q4	Q5
Female	STEM	0.364	0.636	1.455**	0.000	0.182
	Non-STEM	1.111***	0.986***	1.056***	0.000	0.125
Male	STEM	0.462***	0.462	1.154**	0.231	-0.154
	Non-STEM	0.857**	0.667*	0.714**	0.000	-0.286
First-Generation	STEM	0.333	0.500	1.666	0.166	-0.333
	Non-STEM	1.217***	1.217***	0.957***	-0.391	-0.13
Non-First-Generation	STEM	0.421*	0.579*	1.211***	0.105	0.105
	Non-STEM	1.000***	0.819***	0.972***	0.139	0.083
URM	STEM	0.750	1.000	1.250	0.750	0.000
	Non-STEM	0.969***	1.031***	0.969***	0.125	0.094
Not URM	STEM	0.333*	0.476	1.333***	0.000	0.000
	Non-STEM	1.095***	0.857***	0.968***	-0.048	0.000

The responses for interest-based assessment (Q4: science interest and Q5: environmental research career interest) exhibited marginal improvements. Based on **Figure 5-1**, non-STEM students display a wide range of selections on the Likert scale for Q4 and Q5. Concerning interest in science (Q4), a greater proportion of students had neutral responses (33-36%) compared to interest in a career in research (25-28%). There were no statistically significant increases in the mean responses for Q4 and Q5. The only identities to see marginal increases in mean response were females, non-first-generation students, and URM in the non-STEM class.

3.2 STEM CURE case study

Similar to the non-STEM students, STEM students displayed positive movement in confidence concerning coding (Q1 and Q2) and understanding of remote sensing (Q3) based on **Figure 5-1**. For Q1, there were no STEM students that selected “Disagree” or “Strongly Disagree” before the intervention. Following the modules and CURE, there were no “Neutral” responses for Q1 in the STEM class. For Q2, STEM students had increases in the proportion of students selecting “Agree” and “Strongly Agree” following the intervention. Q3 had the most drastic shift in movement among the Likert results for the STEM students where only 24% of students selected “Agree” and “Strongly Agree” for their understanding of remote sensing at the beginning of the course compared to 84% of students following the intervention. For the differences in mean responses, males, non-first-generation, and non-URM STEM students had statistically significant increases for Q1 and non-first-generation students for Q2. For Q3, females, males, non-first-generation, and non-URM students had statistically significant differences in their mean responses.

For the STEM students, there was less movement for Q4 and Q5 with most students already having a strong interest in science (92%) and interest in a career in environmental research (60%) at the start of the course. STEM males, first-generation, non-first-generation, and URM students had increases in their mean responses for Q4. For Q5, only females and non-first-generation STEM students had increased mean responses through the course.

3.3 CURE reports

Additionally, students in the STEM course utilized their new skills in accessing remotely-sensed data to compile their group research report on water bodies of their choosing. The students contributed water quality data and analysis for more than fifteen water regions spanning nine countries. Students tested their hypotheses on the anthropogenic effects on water quality by observing differences in indicators, including sea surface temperature, Kd(490), chlorophyll-a, particulate organic carbon, and turbidity. In the reports, some groups reported improvements in water quality while others found deteriorations.

Two exceptional student project reports uncovered improvements in areas with heavy marine traffic. The first group used the ORCAA tool for the Bangkok Port in Thailand and compared water quality during 2018 (01/01/2018-12/31/2018) to that in 2020 (01/01/2020-12/31/2020). The Bangkok Port is the largest in Thailand and is located in the nation's capital. The students' most notable finding was the improvement in turbidity in 2020 (**Figure 5-2C**) at the port compared to 2018 (**Figure 5-2A**) as shown in their created maps. Another group selected Hawaii for their region of interest and similarly noticed an improvement in turbidity in Kahului Bay in Hawaii, USA (**Figure 5-3**). The Kahului Harbor was contained in the area of interest and is the main port of Maui for receiving both commercial and tourist-based marine traffic. The students compared the water quality during part of 2018 (03/01/2018-11/30/2018) to 2020 (03/01/2020-11/30/2020) using Sentinel-2 imagery. Their time series plots in particular shows a decline in turbidity following the respective COVID-19 shutdown in Hawaii in March 2020 (**Figure 5-3D**).

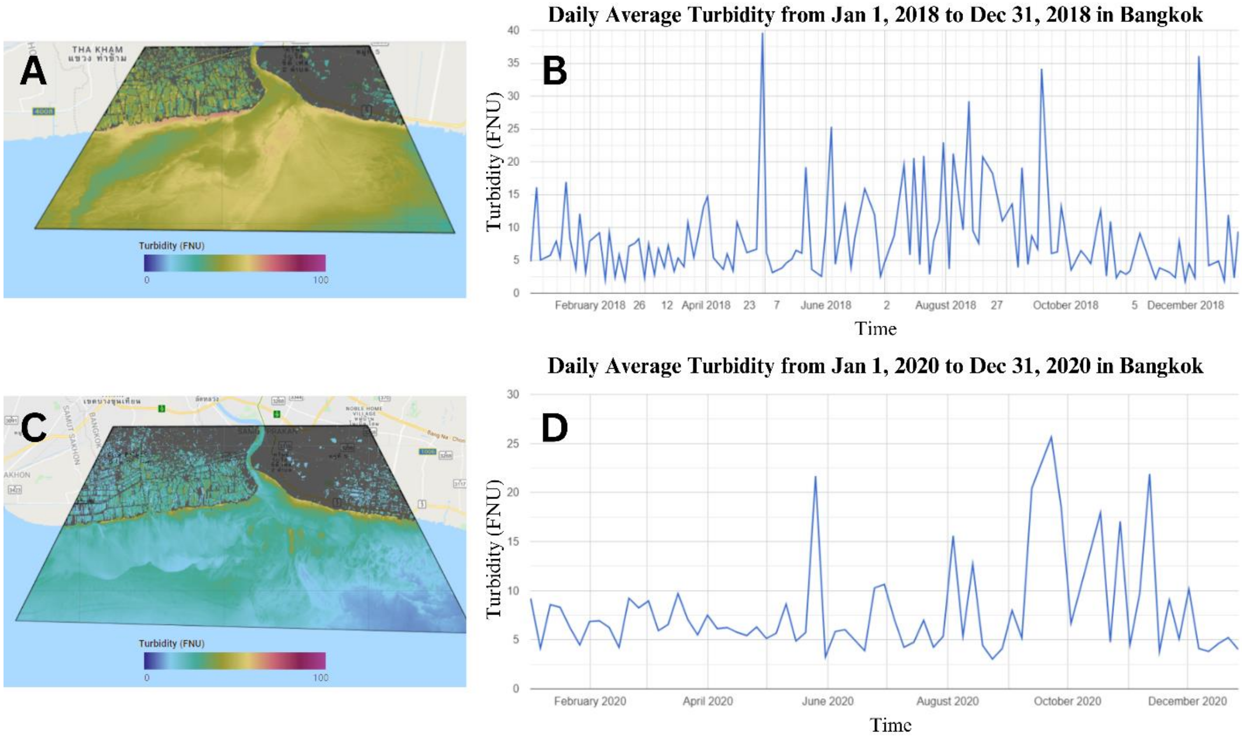

Figure 5-2. Turbidity Results from CURE on Bangkok Port in Thailand. (A) Map of average turbidity before COVID-19 anthropause. (B) Time series of daily average turbidity of Bangkok before COVID-19 anthropause. (C) Map of average turbidity during the COVID-19 anthropause. (D) Time series of daily average turbidity of Bangkok during the COVID-19 anthropause.

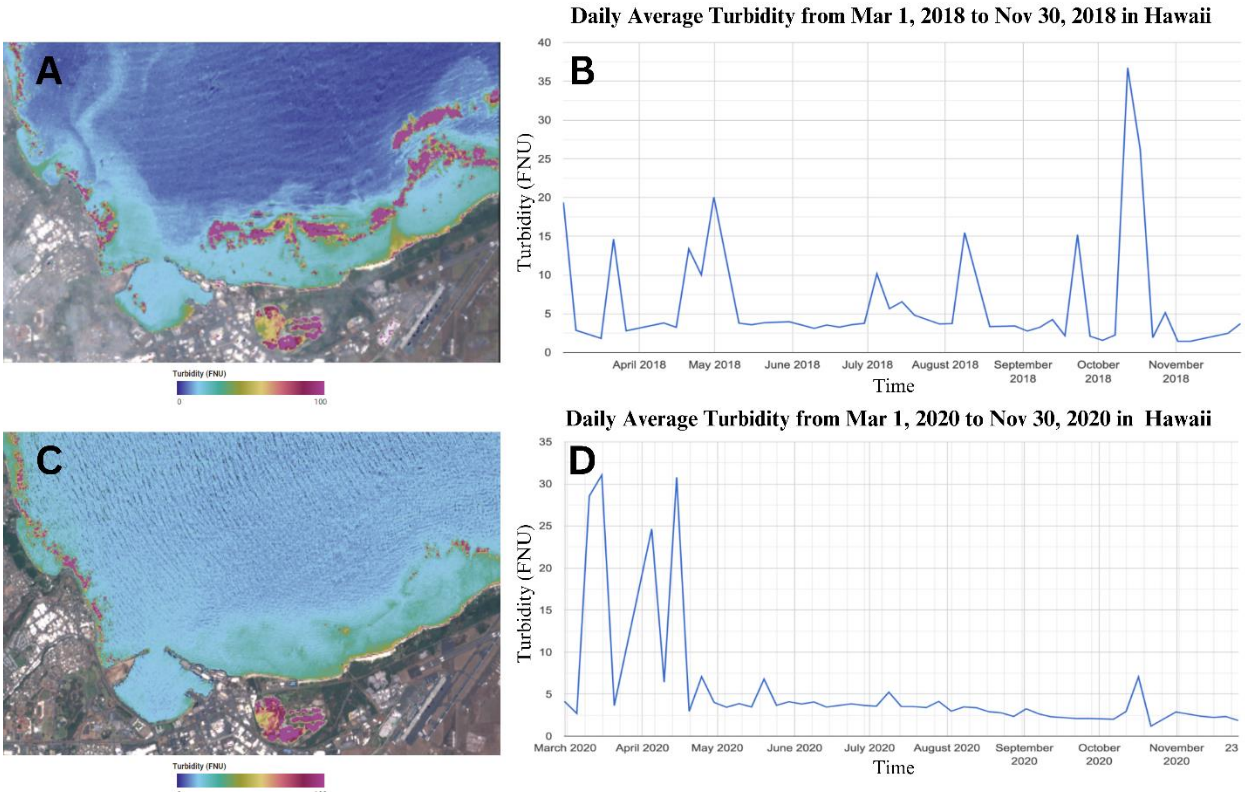

Figure 5-3. Turbidity Results from CURE on Kahului Bay in Hawaii, USA. (A) Map of average turbidity before COVID-19 anthropause. (B) Time series of daily average turbidity of Hawaii before COVID-19 anthropause. (C) Map of average turbidity during the COVID-19 anthropause. (D) Time series of daily average turbidity of Hawaii during the COVID-19 anthropause.

3.4 Research opportunities during the COVID-19 pandemic

Regarding research opportunities, 44% of STEM students and 9.5% of non-STEM students responded that they had experienced difficulties accessing research due to the pandemic. Among 22 free-response answers for both classes, 8 students in the STEM class and 5 students in the non-STEM class stated that there were limited research opportunities on campus and for obtaining internships. A couple of responses involved financial burden and lack of information on how to find research opportunities among first-year non-STEM students. A couple of STEM students mentioned partaking in research activities virtually or in-person despite the pandemic. Post CURE assessments, a couple of STEM students mentioned anecdotally that their applied skills in coding through Google Earth Engine helped them obtain internship positions through their ability to demonstrate competency and enthusiasm for their research projects during the interview stage.

4. Discussion

The study explored outcomes of remote sensing modules in environmental science and engineering courses containing participants from both STEM and non-STEM backgrounds. Implementation of these modules in both STEM- and non-STEM-based courses showed positive outcomes in scientific methodologies, coding skills, and attitudes toward scientific fields for all students. Equitable access to research skills benefits underrepresented demographics in equal if not greater proportions. For the duration of the study, positive growth was fostered directly in the STEM course through the modules and research applications that utilized CURE practices and pedagogy. Even without the scaffolding through the modules, the non-STEM class participants benefited and exhibited short-term growth from receiving lessons centered around CURE pedagogy. Student agency towards their learning and skills will become the building blocks for further integration of their work with the sciences and the efforts to invite diversity into the field. The results are similar to findings in implementation and observation of earlier completed CURE studies.

Through the CUREs, the STEM students were able to engage in original research regarding the COVID-19 anthropause and rebounding effects on water quality. Distinct from usual laboratory and research classes, students had autonomy in selecting the region of interest for their projects and had to investigate region-specific trends for themselves. There are several published and ongoing studies on the impacts of the COVID-19 anthropause on the environment. Having the students engage in this CURE and create a database of their findings may allow for the collection of preliminary results for future investigation. The scientific data provided by these CUREs has been evaluated to be reliable and of sufficient quality for research use, especially when compared to data collected by a non-experimental (i.e. not in a CURE) group [31], which supports an ideology for the increased inclusion of CUREs to contribute to large environmental investigations. Research groups may use such databases in confidence, and in turn, the students gain new skills through working on an original research topic that can pique their interest in similar fields.

In comparing the differences in mean responses between similar groups (i.e., female vs male participants, first-generation vs not, STEM vs non-STEM, and underrepresented minority vs not) the results were found to be not statistically significantly different for interest in a career in environmental research. The underrepresented groups, therefore, did not appear to benefit considerably more than their peers from the CUREs, but the process is still conducive to the collective advancement of scientific understanding and personal self-confidence. A recent review of the state of undergraduate research experiences states that CUREs alone don't offer the necessary mentoring to support URM students to persist in STEM [32].

This study shows the viability of GEE as a powerful teaching tool for investigating environmental change, working with remote sensing data, and learning to code in JavaScript. GEE is advantageous in that it houses many datasets and students can get access to imagery without downloading space-intensive images onto their computers. It is also accessible to any student with internet access regardless of their computer's operating system without the need to download costly software. A recent study found that using Google Earth tools can help students bolster grades and increase critical thinking skills in physical geology courses [33]. In the future, the integration of remote sensing products in teaching will be more important as online learning education continues to grow [34].

5. Conclusions

In this study, we examined the effects of remote sensing modules on confidence in students' ability to alter code, investigate environmental change, and interest in science and a career in environmental research. The study involved both STEM and non-STEM students where the STEM students engaged in a CURE on COVID-19 anthropause effects on water quality. Through the intervention, students' confidence in their ability to alter code, understand remote sensing, and ability to apply skills on environmental issues significantly increased among all student identities for both classes. There were no significant differences in students' existing interest in science and career in environmental research through the one-term study. Nonetheless, GEE proved to be an accessible tool for teaching remote sensing to a wide range of students compared to other geospatial tools. A CURE was also an excellent option for making research more accessible to advanced engineering and environmental science students, especially during the COVID-19 pandemic when opportunities were scarce. Educators in environmental sciences and engineering should consider integrating Google Earth Engine as a teaching resource in their courses and use CUREs to capitalize on students' curiosity and decrease barriers to partaking in original research.

6. References

1. Fisher, A. J. *et al.* Structure and belonging: Pathways to success for underrepresented minority and women PhD students in STEM fields. *PLoS One* **14**, e0209279 (2019).
2. Lambert, W. M. *et al.* Research culture: Career choices of underrepresented and female postdocs in the biomedical sciences. *Elife* **9**, (2020).
3. Miriti, M. N. The Elephant in the Room: Race and STEM Diversity. *Bioscience* **70**, 237–242 (2020).
4. Stockard, J., Rohlfing, C. M. & Richmond, G. L. Equity for women and underrepresented minorities in STEM: Graduate experiences and career plans in chemistry. *Proc. Natl. Acad. Sci. U. S. A.* **118**, (2021).
5. NSF. Women, Minorities, and Persons with Disabilities in Science and Engineering :

2019. *National Science Foundation* (2019).

6. Slovacek, S. P. *et al.* Minority Students Severely Underrepresented in Science, Technology Engineering and Math. *J. STEM Educ.* **12**, 5–16 (2011).

7. Hensel, N. H. & Davidson, C. N. *Course-Based Undergraduate Research: Educational Equity and High-Impact Practice*. (Stylus Publishing, 2018).

8. Qiang, Z., Obando, A. G., Chen, Y. & Ye, C. Revisiting Distance Learning Resources for Undergraduate Research and Lab Activities during COVID-19 Pandemic. *J. Chem. Educ.* **97**, 3446–3449 (2020).

9. Erickson, O. A. *et al.* 'How Do We Do This at a Distance?!' A Descriptive Study of Remote Undergraduate Research Programs during COVID-19. *CBE Life Sci. Educ.* **21**, ar1 (2022).

10. Winkelmann, K. *et al.* Improving students' inquiry skills and self-efficacy through research-inspired modules in the general chemistry laboratory. *J. Chem. Educ.* **92**, 247–255 (2015).

11. Pantoya, M., Hughes, P. C. & Hughes, J. S. A Case Study in Active Learning: Teaching Undergraduate Research in an Engineering Classroom Setting. *Eng. Educ.* **8**, 54–64 (2013).

12. Hung, W. C. *et al.* Incorporating field-based research into remote learning: An assessment of soil lead pollution in different land-use types in Los Angeles. *Environ. Res.* **216**, 114480 (2023).

13. Weaver, G. C., Russell, C. B. & Wink, D. J. Inquiry-based and research-based laboratory pedagogies in undergraduate science. *Nat. Chem. Biol. 2008 410* **4**, 577–580 (2008).

14. Brownell, S. E. *et al.* A high-enrollment course-based undergraduate research experience improves student conceptions of scientific thinking and ability to interpret data. *CBE Life Sci. Educ.* **14**, (2015).

15. Bangera, G. & Brownell, S. E. Course-Based Undergraduate Research Experiences Can Make Scientific Research More Inclusive. *https://doi.org/10.1187/cbe.14-06-0099* **13**, 602–606 (2017).

16. Genné-Bacon, E. A. & Bascom-Slack, C. A. The PARE Project: A Short Course-Based Research Project for National Surveillance of Antibiotic-Resistant Microbes in Environmental Samples. *J. Microbiol. Biol. Educ.* **19**, (2018).

17. NASEM. Integrating Discovery-Based Research into the Undergraduate Curriculum. *Report of a Convocation. Washington, DC: National Academies Press* (2015) doi:10.17226/21851.

18. Genné-Bacon, E. A., Wilks, J. & Bascom-Slack, C. Uncovering factors influencing instructors' decision process when considering implementation of a course-based research experience. *CBE Life Sci. Educ.* **19**, (2020).

19. Cooper, K. M., Soneral, P. A. G. & Brownell, S. E. Define Your Goals Before You

Design a CURE: A Call to Use Backward Design in Planning Course-Based Undergraduate Research Experiences. *J. Microbiol. Biol. Educ.* **18**, (2017).

20. Jin, G. & Bierma, T. STEM for non-STEM Majors: Enhancing Science Literacy in Large Classes. *J. Coll. Sci. Teach.* **042**, 20–26 (2013).

21. Cotner, S., Thompson, S. & Wright, R. Do Biology Majors *Really* Differ from Non–STEM Majors? *CBE—Life Sci. Educ.* **16**, ar48 (2017).

22. Farah, J. C. *et al. Bringing Computational Thinking to non-STEM Undergraduates through an Integrated Notebook Application*. *15th European Conference on Technology Enhanced Learning* http://infoscience.epfl.ch/record/278325 (2020).

23. Ray, B. B., Rogers, R. R. H. & Hocutt, M. M. Perceptions of non-STEM discipline teachers on coding as a teaching and learning tool: what are the possibilities? *https://doi.org/10.1080/21532974.2019.1646170* **36**, 19–31 (2020).

24. Hejmanowska, B. *et al.* Modern Remote Sensing and the Challenges Facing Education Systems in Terms of Its Teaching. *Edulearn15 7th Int. Conf. Educ. New Learn. Technol.* (2015).

25. Wang, J., Zhang, A. & Zhao, X. Development and application of the multi-dimensional integrated geography curricula from the perspective of regional remote sensing. *J. Geogr. High. Educ.* **44**, 350–369 (2020).

26. Redford, J., Mulvaney Hoyer, K. & Ralph, J. *First-Generation and Continuing-Generation College Students: A Comparison of High School and Postsecondary Experiences*. *Stats in Brief* vol. 90 (2017).

27. National Science Foundation. *Women, Minorities, and Persons with Disabilities in Science and Engineering - US National Science Foundation (NSF) Special Report NSF 13-304*. https://www.nsf.gov/statistics/2017/nsf17310/digest/introduction/ (2014).

28. Callejas, I. A. *et al.* Effect of COVID-19 Anthropause on Water Clarity in the Belize Coastal Lagoon. *Front. Mar. Sci.* **8**, 490 (2021).

29. Jay, J. A. & Mika, K. B. Collaborative research with K-12 students on impacts of climate change on ecosystems in an environmental engineering service-learning course. *World Trans. Eng. Technol. Educ.* **10**, 105–109 (2012).

30. Mika, K. B. *et al.* Incorporating service learning in traditionally lecture-based environmental engineering courses through researching bacterial contamination at a local beach. *Glob. J. Eng. Educ.* **14**, 155–162 (2012).

31. Marley, S. A., Siani, A. & Sims, S. Real-life research projects improve student engagement and provide reliable data for academics. *Ecol. Evol.* **12**, e9593 (2022).

32. Krim, J. S. *et al.* Models and impacts of science research experiences: A review of the literature of cures, ures, and tres. *CBE Life Sci. Educ.* **18**, (2019).

33. Monet, J. & Greene, T. Using Google Earth and Satellite Imagery to Foster Place-Based Teaching in an Introductory Physical Geology Course. *https://doi.org/10.5408/10-203.1*

60, 10–20 (2018).

34. Coleman, J. C., Hensel, N. H. & Campbell, W. E. *Undergraduate Research in Online, Virtual, and Hybrid Courses : Proactive Practices for Distant Students*. vol. First edit (2022).

7. Supplementary Materials

Likert plots

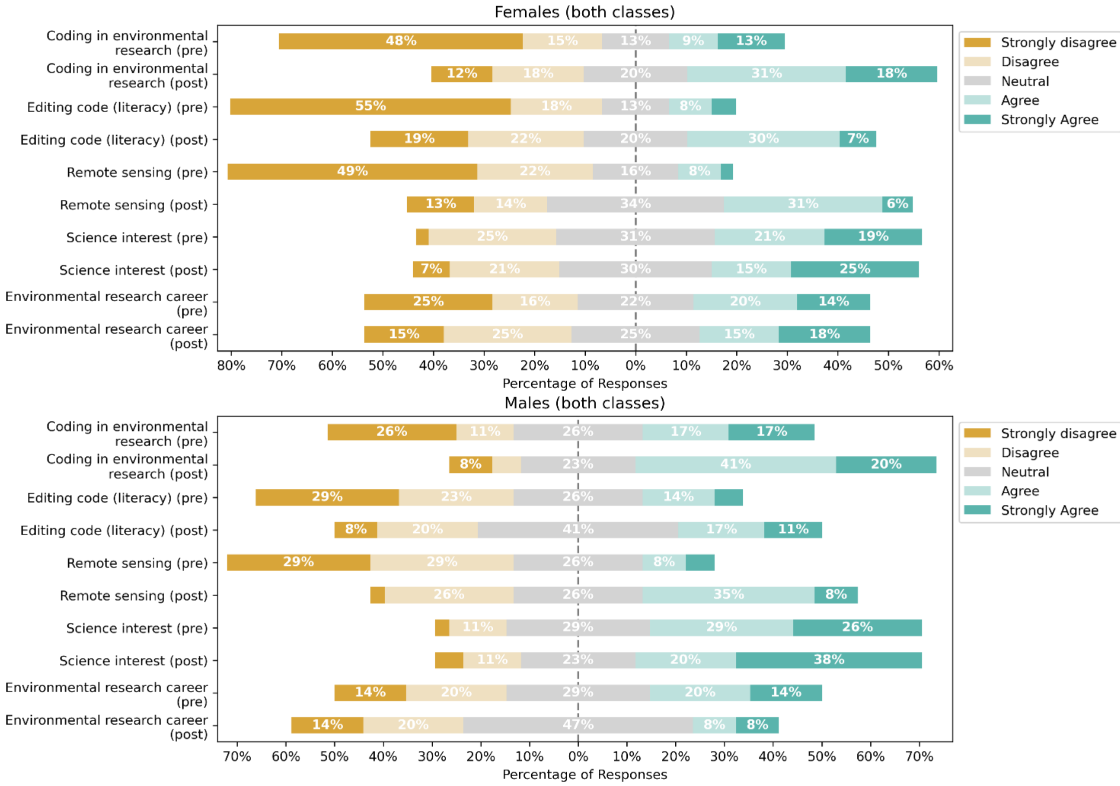

Figure 1. Likert plots for male and female students.

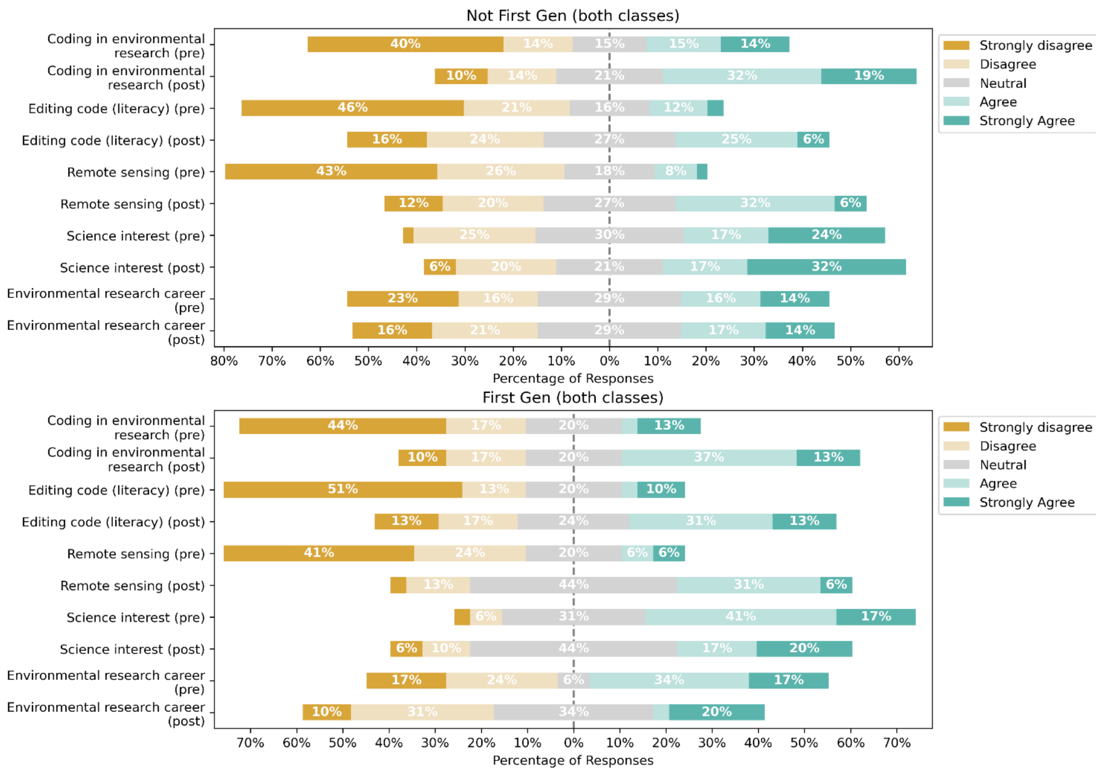

Figure 2. Likert plots for first-generation and non-first-generation students.

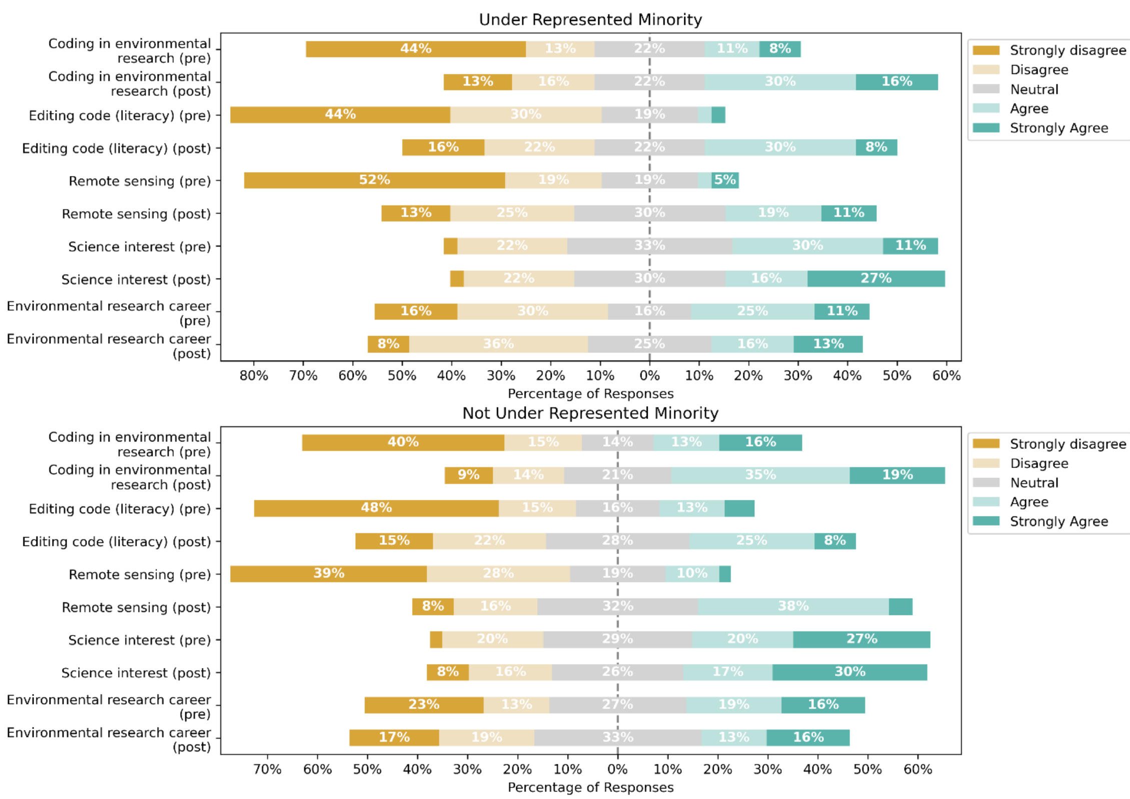

Figure 3. Likert plots for underrepresented minority (URM) students and non-URM students.

Pre and Post Surveys

Below are the pre and post surveys along with question type.

Pre-Survey

1. What is your favorite number? (Short answer)

2. What is the name of your first best friend? (Short answer)

3. What is the name of your first pet? (Short answer)

4. What gender do you identify with? (Multiple choice)

5. What is your major? (Short answer)

6. What year are you in? (Multiple choice)

7. With what group or groups do you identify? Please select any boxes that apply. (Checkboxes)

8. Are you a first-generation student (a student whose parent(s)/guardian(s) have no education experience past high school)? (Multiple choice)

9. I am confident in my ability to make small edits to code. (5-point likert)

10. I am confident in my ability to leverage current coding skills to investigate environmental change. (5-point likert)

11. I understand remote sensing for studying the environment. (5-point likert)

12. I have a strong interest in science. (5-point likert)

13. I would consider a career in environmental research. (5-point likert)

Post-Survey

1. What is your favorite number? (Short answer)

2. What is the name of your first best friend? (Short answer)

3. What is the name of your first pet? (Short answer)

4. I am confident in my ability to make small edits to code. (5-point likert)

5. I am confident in my ability to leverage current coding skills to investigate environmental change. (5-point likert)

6. I understand remote sensing for studying the environment. (5-point likert)

7. I have a strong interest in science. (5-point likert)

8. I would consider a career in environmental research. (5-point likert)

9. Has the COVID-19 pandemic impacted your search for research opportunities? (Short answer)

10. If answered yes above, how? (Short answer)